Journal Pre-proof

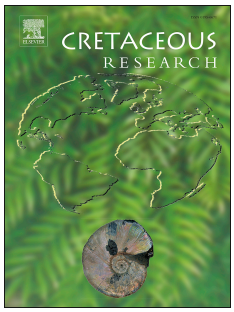

Barremian charophytes from the Maestrat Basin (Iberian Chain)

Jordi Pérez-Cano, Telm Bover-Arnal, Carles Martín-Closas

PII: S0195-6671(20)30230-5

DOI: https://doi.org/10.1016/j.cretres.2020.104544

Reference: YCRES 104544

To appear in: *Cretaceous Research*

Received Date: 17 January 2020

Revised Date: 16 May 2020

Accepted Date: 4 June 2020

Please cite this article as: Pérez-Cano, J., Bover-Arnal, T., Martín-Closas, C., Barremian charophytes from the Maestrat Basin (Iberian Chain), *Cretaceous Research*, https://doi.org/10.1016/j.cretres.2020.104544.

Barremian charophytes from the Maestrat Basin (Iberian Chain)

Jordi Pérez-Cano[1*], Telm Bover-Arnal[2,3], Carles Martín-Closas[1]

[1]Departament de Dinàmica de la Terra i de l'Oceà. Facultat de Ciències de la Terra, Institut de Recerca de la Biodiversitat (IRBio), Universitat de Barcelona-UB, 08028 Barcelona, Catalonia, Spain

[2]Departament de Mineralogia, Petrologia i Geologia Aplicada, Facultat de Ciències de la Terra, Universitat de Barcelona-UB, 08028 Barcelona, Catalonia, Spain

[3]Institut de Recerca GEOMODELS, c/ Martí Franquès s/n, 08028 Barcelona, Catalonia, Spain

**Corresponding author:* jordi_perez-cano@ub.edu

Abstract

A lower and upper Barremian 690 metre-thick succession composed of freshwater and brackish limestones, marls and clays was measured and sampled in the Maestrat Basin, Eastern Iberian Chain (Castelló, Spain). Thirty-three taxa were identified from charophyte fructifications and thalli, belonging to the three families that coexisted during the Early Cretaceous, i.e. Porocharaceae, Characeae and Clavatoraceae. Up to 25 different Clavatoraceae utricles were identified. This high species richness of clavatoraceans has not been observed elsewhere and sheds light on the role of Iberia, and particularly the Maestrat Basin, as a diversity hotspot for this family during the Barremian. Several of them have been taxonomically revisited, as regards both utricles and thalli. The *Echinochara lazarii* utricle is reinterpreted as showing bilateral rather

than triradial symmetry. Anagenetic evolution within *Clavator calcitrapus* has been documented and has enabled us to distinguish between two varieties linked by intermediate morphotypes of biostratigraphic and palaeobiogeographic interest. The taxon *Clavator grovesii* var. *jiuquanensis* is reported for the first time in the Iberian Chain and in Spain. The structure of *Charaxis spicatus* is revisited and a new type of cortication is defined, called the double triplostichous cortication, which is unknown in either fossil or extant charophytes. This thallus is found in anatomical connection with *Echinochara lazarii* utricles, enabling a whole-plant reconstruction of the *Echinochara* plant. Lastly, new characters were found in *Munieria grambastii* thalli that confirm the membership of genus *Munieria* to the clavatoracean charophytes, particularly the calcification pattern of the internodal cell, which recalls that of clavatoroid utricles.

Keywords: Charophyta, Taxonomy, Evolution, Lacustrine, Mesogea, Spain,

1. Introduction

Knowledge of Early Cretaceous charophytes steadily increased in the 20th Century thanks to the study of specimens from different basins in Europe (e.g. Harris, 1939, Grambast, 1974), China (e.g. Z. Wang and Lu, 1982) and America (e.g. Peck, 1957, Musacchio, 1971). A significant amount of information on Early Cretaceous charophytes has been obtained from the Iberian Chain and particularly from the Maestrat Basin, where many of the type localities of the species from that age have been defined (Grambast, 1966a, b, 1967, 1968, 1969, 1970; Martín-Closas and Grambast-Fessard, 1986; Martín-Closas 2000). Indeed, the Maestrat Basin records one of the most expanded Lower Cretaceous freshwater to brackish successions in Europe characterized

by the presence of rich and diverse charophyte assemblages belonging to the families Porocharaceae, Characeae and Clavatoraceae. Of these families, the Clavatoraceae is the most abundant and species-rich. Its fossil record extends worldwide between the Late Jurassic and the end of the Cretaceous (Grambast, 1974; Feist and Grambast-Fessard in Feist et al., 2005), locally reaching the base of the Paleocene (Vicente et al., 2019). The high evolutionary rate of their fructifications (utricles) renders this family a useful biostratigraphic tool mainly for Lower Cretaceous non-marine settings (e.g. Grambast, 1968, 1974; Z. Wang and Lu, 1982; Schudack, 1993; Feist et al., 1995; Riveline et al., 1996), and several biozone stratotypes have been defined as well in the Maestrat Basin (Grambast, 1974; Riveline et al., 1996).

The present study provides an updated taxonomy of the Barremian charophyte flora from the Maestrat basin, in a continuous and expanded sedimentary succession that includes several stratigraphic units, one of which was previously overlooked from the viewpoint of its charophyte fossil record. The results have generated better knowledge of the symmetry and structure of the utricles and thalli from several clavatoracean species, which until now have been poorly understood. In some cases, the results have provided new biostratigraphic data that are useful to improve the Barremian biozonation. Together, these data portray the Iberian Chain and Iberia in general as one of the areas of greatest charophyte diversity during the Early Cretaceous worldwide.

2. Geological Setting

The Maestrat Basin is located in the north-eastern Iberian Peninsula (Fig. 1A), in the so-called Linking Zone between the Iberian Chain and the Catalan Coastal Chain (Guimerà, 2018). During the Late Jurassic-Early Cretaceous, the Iberian Plate

underwent two discrete episodes of continental rifting related to the opening of the Atlantic Ocean, the Alpine Tethys and the Bay of Biscay (Salas and Casas, 1993; Tugend et al., 2015; Salas et al. in Martín-Chivelet et al., 2019). These successive rifting episodes and the activity of listric faults favoured the compartmentalization of areas with high and low subsidence (Fig. 1B), defining several sub-basins (Salas et al. in Martín-Chivelet et al., 2019). The sedimentary successions deposited form more than 1500 m-thick deposits and record a wide variety of sedimentary environments from freshwater to open marine settings (Canérot et al., 1982; Salas et al., 2001). During the late Eocene–early Miocene there was an inversion of the basin related to the Alpine orogeny (Salas et al., 2001; Guimerà, 2018).

----------Please insert Figure 1 near here----------

The studied succession crops out in the northern margin of the Maestrat Basin, within the Morella sub-basin, close to the Herbers fault (Figs. 1B–C). The Barremian sedimentary record overlies the lacustrine Herbers Formation of Hauterivian age (Salas, 1987; Martín-Closas and Salas, 1994; Salas et al., 2001). Basinwards, the Herbers Formation changes to the marine Llàcova Formation (Salas, 1987; Salas et al., 2001). In the northern Maestrat Basin, the base of the Barremian is usually marked by a thick laterite and related bauxite deposits developed on top of a karstified surface (Combes, 1969). Above, the succession is constituted by five lithostratigraphic units that record an evolution from freshwater to marine settings during the Barremian (Fig. 2), which corresponded to the highest Early Cretaceous rifting activity in the Maestrat Basin (Salas et al. in Martín-Chivelet et al., 2019). The oldest Barremian unit corresponds to

the freshwater, charophyte-rich lacustrine marls and limestones of the Cantaperdius Formation. In the northern margin of the Morella sub-basin, the Cantaperdius Formation reaches a thickness of up to 400 meters (Fig. 2). Laterally and upwards, this unit changes to the shallow marine marls and limestones of the Artoles Formation. This latter is 700-meters-thick in the center of the Morella sub-basin, while in the marginal areas it becomes thinner and only reaches approximately 200 meters of thickness. The overlying Morella, Cervera del Maestrat and Xert formations have been dated as upper Barremian by Bover-Arnal et al. (2016) according to both strontium-isotope stratigraphy and ammonite biostratigraphy. The Morella Formation is built up by a succession of grey and red clays, interbedded with cross-stratified sandstones interpreted as being deposited in tidal plain or mudflat environments (Gámez et al., 2003). This formation includes abundant dinosaur and charophyte remains and corresponds to the youngest non-marine record of the Barremian in the area. The Cervera del Maestrat Formation is a transitional unit laterally equivalent to the Morella Formation and is built up of tidally-influenced coastal deposits (Salas, 1987; Bover-Arnal et al., 2016). The uppermost Barremian corresponds to a fully marine siliciclastic and carbonate succession that belongs to the Xert Formation (Salas, 1987; Canérot et al., 1982). The limestones of the Xert Formation are commonly rich in *Palorbitolina lenticularis* Blumenbach as reported by Bover-Arnal et al. (2010, 2016). The early Aptian succession is represented by the ammonoid-rich basin marls of the Forcall Formation (e.g. Moreno-Bedmar et al., 2009, 2010; García et al., 2014) and the overlying shallow-water carbonates with rudists and corals of the Villarroya de los Pinares Formation (e.g. Bover-Arnal et al., 2009).

----------Please insert Figure 2 near here----------

3. Materials and methods

This study of the charophyte flora was conducted in the Herbers-Mas de Petxí section, which is a continuous, expanded and well-exposed Barremian succession located on the northern margin of the Maestrat Basin (base 40º42'39''N, 0º0'36''W; top 40º42'34''N, 0º0'30''E; Figs. 1, 3–4). The analysed charophyte remains occur in the lacustrine Cantaperdius Formation, in the lower part of the shallow marine Artoles Formation and in the mudflat and floodplain clays and lacustrine limestones of the Morella Formation (Figs. 2–4).

----------Please insert Figure 3 and 3 (continuation) near here----------

----------Please insert Figure 4 near here----------

Around 3 kg of rock was sampled in each marly interval. In the laboratory, each sample was disaggregated with a solution of water, sodium carbonate (Na_2CO_3) and hydrogen peroxide (H_2O_2). After several days the samples were sieved using meshes of 1, 0.5 and 0.2 mm aperture. Once each sample size had dried, the charophyte thalli and fructifications, as well as the associated ostracod carapaces, foraminifera and molluscan shells were hand-picked under a Wild M5A binocular microscope with magnifications of x12, x25 and x50. Utricle and gyronite measurements and photographs were obtained using Motic Images Plus 2.0 software. About 100 gyrogonites were measured for characean and porocharacean species (Appendix A), 5–10 utricles for clavatoraceans and 50 gyrogonites for *Echinochara lazarii* (Martín-Closas, 2000) comb. nov.

(Appendix B). The abundance of charophyte fructifications for each sample is found in Appendixes C and D. Selected utricles, gyrogonites and thalli were studied and photographed with a Quanta 200 scanning electron microscope (SEM) housed in the Scientific and Technological Centres of the UB (CCiTUB). The figured specimens have been deposited at the *Museu de Geologia del Seminari Conciliar de Barcelona* (MGSCB) with the numbers MGSCB 85579–85660 and 85677. The hand-picked material is stored in the Department of Earth and Ocean Dynamics at the University of Barcelona. The systematic study of charophytes followed the systematics of Martín-Closas (1989, 1996) and Schudack (1993). In this regard, the use of the variety instead of the subspecies has been preferred to characterise the anagenetic change within gradualistic lineages of clavatoracean fructifications, following Martín-Closas (1996).

Thin sections were used to study the microfacies of limestone beds. For each limestone sample, two thin sections (one parallel and a second perpendicular to the stratification) of *ca*. 30 μm were prepared. This methodology provides more comprehensive observations of the charophyte thalli and fructifications beyond the two-dimensional limit of a cross-section. Thirty-two non-marine limestone beds of the Cantaperdius and Morella Formation were sampled and thus, sixty-four representative thin sections were manufactured. Thin sections were observed by using a Motic BA 310 petrographic microscope. The thin sections with figured specimens have been deposited at the *Museu de Geologia del Seminari Conciliar de Barcelona* (MGSCB) with the numbers MGSCB 85661–85676.

4. Results (Systematic palaeobotany)

Charophyte fructifications

Division Charophyta Migula 1897

Class Charophyceae Smith, 1938

Order Charales Lindley 1836

Family "Porocharaceae" Grambast, 1962 emend. Schudack, 1993

Porochara maestratica (Martín-Closas et Grambast-Fessard, 1986) Schudack, 1989

Figure 5A–C

1986 *Musacchiella maestratica* nov. sp. – Martín-Closas and Grambast-Fessard p. 6-8, Pl II, fig.1–6; Pl. II, fig. 1–3.

1989 *Porochara maestratica* (Martín-Closas and Grambast-Fessard, 1986) nov. comb. – Schudack, p. 413, Pl. 1, fig. 1–3.

Material: 100 gyrogonites from sample H61 (Fig. 4) and smaller populations in other samples from the section (Figs. 3–4 and Appendixes C–D).

Description: The gyrogonites of this species are medium sized, measuring 452–633 μm high and 391–598 μm wide (Appendix A). Their shape varies from subglobular to ellipsoidal, with an isopolarity index (ISI= height x100/ width) of 90–122. The apex is rounded or flattened with a large apical pore (36–145 μm across) pentagonal in shape. The base is rounded with a small (30–50μm) pentagonal basal pore. The basal plate is multipartite and cannot be seen from external view. Spiral cells present 6–11 convolutions in lateral view.

Distribution: Besides its occurrence in Herbers, this species has previously been reported from the upper Barremian of Coll de Querol, its type locality (Martín-Closas and Grambast-Fessard, 1986). Outside the Iberian Peninsula, it has been probably reported from thin sections in the Subalpine Chains (Mojon, 1988). However, this occurrence would need to be verified with tridimensional specimens.

Family Characeae (Richard ex C. Agardh, 1824) emend. Martín-Closas et Schudack, 1991

Genus *Aclistochara* Peck, 1937

Aclistochara sp.

Figure 5D–F

Material: 56 poorly preserved gyrogonites, probably reworked, in sample H37 (Fig. 3 and Appendix C).

Description: Small-sized gyrogonites measuring of 388–449 μm high and 287–437 μm wide. The ISI varies between 82 and 131 (Appendix A). Laterally, the gyrogonites show 8–12 convolutions. The base tapers, ending in short and broad column. At the apex, the spiral cells turn down into a shallow apical depression, converging in its central area to close the apex forming a small prominent cap. The basal plate was not been observed but is documented to be multipartite in this genus (Schudack, 1993).

Genus *Mesochara* Grambast, 1962

aff. *Mesochara harrisii* (Mädler, 1952) Shaïkin, 1967

Figure 5G–I

1952 *Tolypella harrisii* Mädler, p. 31–32, Pl. B, Figs. 31–35.

1967 *Mesochara harrisii* (Mädler) nov. comb.; Shaïkin, p. 47.

Material: 100 gyrogonites from sample H39 (Fig. 3) and small populations in other samples from the section (Figs. 3–4 and Appendixes C–D).

Description: The gyrogonites are small, measuring of 211–458 μm high and 182–303 μm wide, with an ISI (isopolarity index) spanning 88–147, mostly 110–130 (Appendix A). Apex rounded or slightly pointed, showing the junction of apical cells without any periapical modification. Base rounded showing a small, pentagonal basal pore.

Remarks: Similar characean populations observed in the Iberian Barremian record have been attributed either to *Mesochara harrisii* by Martín-Closas (1989, 2000), Martín-Closas et al. (2009) and Vicente and Martín-Closas (2013), or to aff. *Tolypella grambastii* Feist et Brouwers 1990 by Martín-Closas et al. (2018), depending on the basal plate, which is unicellular in genus *Mesochara* and multipartite in genus *Tolypella*. No basal plate was visible in the material studied, rendering determination of these gyrogonites challenging.

Distribution: This species has been extensively described in the Maestrat Basin, Cameros Basin (Martín-Closas, 2000) and in the South-Western Iberian Chain (Vicente and Martín-Closas, 2013). Outside of the Iberian Peninsula, this species has been identified in the Berriasian record of the Aquitaine Basin (Benoit et al., 2017) and in NW German basins (Mädler, 1952; Schudack, 1993). It occurs in the Barremian of the

Subalpine Chain and Jura Basin (Martín-Closas, et al. 2009) and has also been described in the Early Cretaceous of eastern European basins (Shaikin, 1967), China (S. Wang, 1965), Japan (Kubota, 2005) and the United States (Peck, 1957).

----------Please insert Figure 5 near here----------

Family Clavatoraceae Pia, 1927

Subfamily Atopocharoidae (Grambast, 1968) emend. Martín-Closas ex Schudack, 1993

Genus *Echinochara* (Peck, 1957) emend. nov. Pérez-Cano, Bover-Arnal et Martín-Closas

Original diagnosis (Peck, 1957): "Clavatoraceae with six cortical tubes budding from each end of the nodal cells and extending as tapering dextral coils around the central tube, interfingering with the cortical tubes from adjoining nodes. Individual cortical cells short, of uniform length and, at their distal ends giving rise to long spines that extend over and almost completely cover the next cortical cell. Branchlets massive, stubby, bearing oogonia in whorls of six, the oogonia enclosed in thick utricles. Utricle cells originate below base of oogonia as short stubby units that repeatedly branch and resemble spines on cortical cells. Oogonia normal for family."

Emended diagnosis (Schudack, 1993): "Clavatoroideae with utricles which consist of two series of bracts. The internal bracts (3 or 6) are trifurcately ramified whereas the external bracts (also 3 or 6) are more variable. Utricle without nodular

256 layer. Uncalcified oogonium with numerous thin whorls in a side view, summit
257 stretched into a long neck."

258 New emended diagnosis: Utricle formed by two superposed series of bract-cells.
259 Inner series with one, three or six bract-cells trifurcated once. Outer series with one,
260 three or six bract-cells that may be trifurcated repeatedly. Oospore not calcified,
261 ellipsoidal, bottle-shaped, with apical and basal necks, and more than 10 convolutions
262 visible in lateral view.

263

264 *Echinochara lazarii* (Martín-Closas, 2000) nov. comb. Mojon ex Pérez-Cano,
265 Bover-Arnal et Martín-Closas

266 Figures 6–8

267 *Basionym*: *Echinochara peckii* var. *lazarii* Martín-Closas – Martín-Closas (2000,
268 p. 70–76, Pl. 6, Figs. 1–8; Pl. 7, Figs. 1–6); holotype number 66792 Museu Geològic
269 del Seminari Conciliar de Barcelona (Pl. 7, Fig. 1).

270 Material: 150–200 fructifications in each of the samples H124B, H128A, H128B,
271 H88 and H94 (Fig. 4). Other smaller populations with ca. 70 utricles each (Figs. 3–4,
272 Appendixes A–B).

273 Original diagnosis: "Utricle of *Echinochara peckii* with the external whorl formed
274 by three radially-symmetric units of seven vertical bract-cells, directly articulated to the
275 utricle base. The two small central cells which are present in the first and second
276 trifurcation of each unit in the nominal variety *Echinochara peckii* var. *pecki* have
277 disappeared" (Martín-Closas, 2000).

Emended diagnosis: Atopocharoidean fructification with bilateral symmetry. Utricle constituted by two superimposed series of bract-cells occurring only in the abaxial area. Inner series formed by one short bract-cell trifurcating apically into three long bract-cells that hold the fructification on its abaxial side. The outer series covers the inner series, partially interdigitating with the cells of the latter apically. Outer series formed by seven vertical bract-cells: three central cells organized in a fan, and two lateral cells at each side of the central set. Lateral bract-cells in the outer series are directly attached to the basal node.

Description: The *Echinochara lazarii* fructification includes the uncalcified oospore and the utricle, the latter covering the oospore only on its outer or abaxial part. The oospore is known from (1) external casts or impressions on the internal utricle wall (Fig. 6A–B, 6G) and (2) calcitic internal casts preserved either dispersed in the sediment or attached to the utricle wall (Figs. 6C–D, 6M, 7A–C). The oospore measures 450–650 μm high and 200–300 μm wide and the ISI varies between 130 and 200 (Appendix B), which would correspond to a prolate to perprolate oospore with short apical and basal necks (Figs. 6B–C, 6M, 7A). The number of convolutions visible on the casts varies between 14 and 16.

----------Please insert Figure 6 near here----------

The utricle includes two superimposed series of bract-cells, known from their impressions on the external utricle wall (Fig. 6E). The inner series is formed by a single forked unit per oospore, located abaxially and composed of three long, slightly curved bract-cells (470–800 μm long) attached to a short basal cell (Fig. 6D–F, 6K), 48–105

302 μm in diameter (Appendix B). This basal bract is often preserved as a well-calcified
303 tube directly attached to the basal node of the fructification (Fig. 6D–E). The outer
304 series is also formed by a single unit of bract-cells, which covers completely the inner
305 series but may interdigitate with it in the apical part, as observed in the external view of
306 some three-tridimensional fossils (Fig. 6E) or in thin sections (Fig. 7B–C). This outer
307 series is formed by 7 long, vertical or slightly curved bract-cells, three of which are
308 organized in a central fan, flanked on each side by two lateral bract-cells. The four
309 lateral cells are directly attached to the base of the utricle, while the central set of three
310 cells form a trifurcation borne upon the lateral cells and without connection to the
311 utricle base (Fig. 6H–J, Fig. 8).

312 Fertile whorls are made up of six tightly packed utricles stacked with overlying
313 and underlying fertile whorls in compact layers (Figs. 6C, 6F–G, 6J–M, 7–8). Up to
314 three stacked fertile whorls (more commonly two) were observed (Fig. 6C, M). Bract-
315 cells of the outer series of a whorl can be extremely long and may completely cover the
316 overlying fertile whorl, rendering individualization of adjacent fertile whorls difficult
317 from the outside. Structures with the same external morphology as described herein for
318 a fertile whorl of *E. lazarii* were attributed to non-fertile whorls by Martín-Closas
319 (2000, Pl. 6, figs. 5–8), because fructifications were not observed. However, the
320 vegetative structure of this species, which was observed to be anatomically attached to
321 the fructifications has a different organization, as described below under the taxonomic
322 heading of *Charaxis spicatus*.

323

324 ----------Please insert Figure 7 near here----------

325

Remarks: The new data presented here show that the utricle of *E. lazarii* is formed by only one inner and one outer units of bracts, instead of three as formerly thought (Martín-Closas, 2000). The two units are superposed in the abaxial part of the gyrogonite. Therefore, the utricle symmetry of *E. lazarii* is bilateral rather than triradiate as proposed for *E. peckii* by Schudack (1993) and for *E. peckii* var. *lazarii* by Martín-Closas (2000). This difference suggests that *E. peckii* and *E. lazarii* are indeed two different species, without intermediates, undermining the hypothesis of Martín-Closas (2000) that both species could be related by a continuum of utricle variation in an anagenetic lineage. Besides this fundamental difference regarding the utricle symmetry, the utricle structure of *E. lazarii* is a simplification of the structure described for *E. peckii* because there is (1) a reduction in the number of trifurcations in the outer utricle series from three to two and (2) a reduction in the length of the basal bract-cell bearing the trifurcation of the inner bract-cells.

The new utricle structure described for *E. lazarii* utricles gives rise to an emended diagnosis of genus *Echinochara* and to a new combination for the basionym *E. peckii* var. *lazarii* Martín-Closas 2000. The new species combination presented here was previously proposed by Mojon (2003); however, this author failed to comply with the rules of the International Code of Nomenclature for Algae, Fungi and Plants (ICNAFP), at that time the ICBN (International Code for Botanical Nomenclature), since no reference was given to the basionym. This resulted in a non-validly published new combination, which is proposed here again, according to article 41.5 of the ICNAPF (Turland et al., 2018).

----------Please insert Figure 8 near here----------

Distribution: In the Iberian Chain, this species has been described in the Barremian Blesa Formation (Oliete Sub-basin; Fig. 1B). It also occurs in the Terradets pass, South-central Catalan Pyrenees (Martín-Closas, 2000). Outside the Iberian Peninsula, this species was identified it in the Barremian of the Subalpine Chain and Jura Mountains (Martín-Closas et al., 2009) and in the lower Aptian of Tunisia (Trabelsi et al., 2016).

Genus *Globator* Grambast, 1966a

Globator maillardii (Saporta, 1891) Grambast, 1966a, emend. Martín-Closas ex Schudack, 1993

Globator maillardii var. *trochiliscoides* (Grambast, 1966a) nov. comb. Martín-Closas, 1996

Figure 9A–C

1966a *Globator trochiliscoides* n. sp. – Grambast, p. 1932, Figs. 1–3, 7.

1993 *Globator maillardi trochiliscoides* (Grambast, 1966a) Martín-Closas, 1989 – Schudack, p. 101, Pl. 14, Figs. 17–20.

1996 *Globator maillardi* var. *trochiliscoides* (Grambast, 1966a) Martín-Closas nov. comb. – Martín-Closas, p. 269.

Material: 328 utricles from sample H27 (Fig. 3). Smaller populations occur in other samples (Figs. 3–4 and Appendixes C–D).

371 Description: The utricle is large, 453–975 μm high and 542–800 μm wide
372 (Appendix B), globular to sub-spherical, occasionally fusiform, bottle-shaped, and with
373 a short apical neck. The impression of the non-calcified oospore can be observed on the
374 internal wall of the utricle. The utricle itself is organized in a single layer with three
375 symmetry units, each formed by five filiform cells that coil clockwise from the base to
376 the apex and are directly attached to the basal pore. In lateral view, between 10 and 14
377 convolutions are visible.

378 Distribution: This species has been widely described mainly from the Barremian
379 throughout the Iberian Peninsula, especially in the Iberian Chain (Martín-Closas, 2000)
380 and in the Algarve (Portugal) by Rey and Ramalho (1973-1974). Outside the Iberian
381 Peninsula, this species has been reported from the Subalpine Chain and the Jura
382 Mountains (Mojon, 1988; Martín-Closas et al., 2009). The same variety has also been
383 described in the Middle Atlas by Feist in Andreu et al. (1988) and in the High Atlas
384 (Haddoumi et al., 2019). Trabelsi et al. (2016) have described this species in the lower
385 Aptian of the Central Tunisian Atlas. Avram et al. (1993) also reported it from the
386 Dobrogean basin (Romania). The species, including all its varieties, has never been
387 found outside the peri-Tethyan palaeogeographic domain.

388

389 *Globator maillardii* var. *biutricularis* Vicente et Martín-Closas, 2013

390 Figure 9D–F

391 2013 *Globator maillardii* var. *biutricularis* nov. var. – Vicente and Martín-Closas,
392 p. 232, Fig. 4.

Material. 114 utricles from sample H27 (Fig. 3) and smaller populations mainly from other samples from the Cantaperdius and Morella formations (Figs. 3–4 and Appendixes C–D).

Description: The utricles are globular, measuring 830–963 μm high and 709–885 μm wide (Appendix B), and typically show an apical neck and an inflated ring around the basal pore. According to Vicente and Martín-Closas (2013), the utricle has two layers. The internal layer is equivalent to that of *Globator maillardi* var. *trochiliscoides* whereas the external layer is only visible in the lower part of the basal ring. However recent personal observations suggest that these two layers were a calcification artefact and that the utricle is in fact single-layered. The basal ring was produced by a consistent lack of calcification around the base of the utricle (Fig. 9D).

Distribution: In the Iberian Peninsula this variety of *Globator maillardi* was previously known only from its type locality, La Huérguina (south-western Iberian Chain), described by Vicente and Martín-Closas (2013). Outside the Iberian Peninsula, it occurs in the lower Aptian of the Central Tunisian Atlas (Trabelsi et al., 2016).

----------Please insert Figure 9 near here----------

Genus *Atopochara* Peck, 1938

Atopochara trivolvis (Peck, 1938) emend. Martín-Closas, 1996

Atopochara trivolvis var. *triquetra* (Grambast, 1968) Martín-Closas, 1996

Figure 9G–I

1968 *Atopochara trivolvis* subsp. *triquetra* subsp. nov. – Grambast, p. 9, Fl. 3, fig. 14A–C.

1996 *Atopochara trivolvis* var. *triquetra* (Grambast 1968) Martín-Closas nov. comb. – Martín-Closas, p. 272, Fig. 8.

Material: 500 utricles from sample H26 (Fig. 3). Other large populations were found in the section (Figs. 3–4 and Appendixes C–D).

Description: The utricle is usually 494–783 μm high and 465–839 μm wide (Appendix B), sometimes smaller (400 μm), is bi-tetrahedral in shape and shows a triradiate symmetry formed by three identical bract-cell units. Each symmetry unit is formed at the base by three equally large bract-cells that are directly attached to the basal pore. The two left basal cells bear a second trifurcation with two long, helicoidal cells on the left and one short, rounded cell on the right. The third bract cell unit bifurcates into two small diamond-shaped cells that flank a central cell displaying the impression of one antheridial shield. Three morphotypes have been defined by Martín-Closas and Grambast-Fessard (1986). The 'primitive morphotype', mostly found in the lower part of the Cantaperdius Formation, displays gaps between the branches and occasionally shows the three basal cells of each symmetry unit attached to a short basal bract that connects directly with the basal pore. The "typical morphotype" corresponds to the description provided above and is mostly found in the Cantaperdius and Artoles formations. The "advanced morphotype" has a more rounded shape in apical view and the antheridial impressions are smaller. The latter is recorded in the Morella Formation.

Distribution: In the Iberian Peninsula this taxon has been widely described in the Iberian Chain, the Pyrenees and in the Lusitanian and Algarve Basins (Martín-Closas, 2000, and references therein). Outside the Iberian Peninsula this variety is distributed

439 worldwide, with the exception of North America and Australia (Martín-Closas and Q.
440 Wang, 2008, and references therein).

441

442 *Atopochara trivolvis* var. *trivolvis* (Peck, 1938)

443 Figure 9J–L

444 1938 *Atopochara trivolvis* n. sp. – Peck, p. 173-176, Fig. 1; Pl. 28, figs. 5–12.

445 1968 *Atopochara trivolvis* subsp. *trivolvis* – Grambast, p. 8, Pl. 3, fig. 16.

446 1996 *Atopochara trivolvis* var. *trivolvis* – Martín-Closas, p. 113–116 Pl. 9, figs. 9–
447 10.

448 Material: 45 utricles from sample H94 and 30 utricles from the sample H95 (Fig.
449 4 and Appendix D).

450 Description: This utricle is usually around 783–840 μm high and 681–774 μm
451 wide (Appendix B), rounded in shape and shows a triradiate symmetry formed by three
452 identical bract-cell units. Each symmetry unit basically has the same structure as
453 described for *A. trivolvis* var. *triquetra* (advanced morphotype). However, the long cells
454 of each unit show more spirals and are more closely packed than in var. *triquetra*.

455 Distribution: This is the first report of this variety from the upper Barremian of the
456 Iberian Chain, where it has traditionally been associated with the Aptian and Albian
457 stages. Canérot (1974) described this species from the Aptian record of the Oliete sub-
458 basin (Fig. 1B), while Martín-Closas (1988) has described it from the lower Albian
459 Escucha Formation. Outside the Iberian Chain, it has also been reported from the lower
460 Aptian of the Algarve (Rey and Ramalho, 1973-74; Grambast-Fessard, 1980a) and the
461 Lusitanian Basin (Pereira and Cabral, 2005). Outside the Iberian Peninsula, the species

462 has a worldwide distribution in Aptian–Albian records. During the Aptian, this species
463 became cosmopolitan (Martín-Closas and Q. Wang, 2008, and references therein).

464

465 Subfamily Clavatoroidae (Grambast, 1969) emend. Martín-Closas ex Schudack,
466 1993

467 Genus *Clavator* (Reid et Groves, 1916) emend. Martín-Closas ex Schudack, 1993

468 *Clavator grovesii* (Harris, 1939) emend. Schudack, 1993

469 *Clavator grovesii* var. *jiuquanensis* (S. Wang, 1965) nov. comb. Grambast, 1970
470 emend. Martín-Closas, 1996

471 Figure 10A–C

472 1965 *Perimneste jiuquanensis* sp. nov. – S. Wang, p. 467, Pl. 1.

473 1970 *Clypeator jiuquanensis* (S. Wang) nov. comb – Grambast, p. 1965, Fig. D;
474 Pl. 3, figs. 1-5.

475 1973 *Clypeator europaeus* – Mädler in Neagu et Georgescu-Donos, p. 178, Pl. I,
476 fig. 7-8; Pl. II, figs. 1–9.

477 1996 *Clavator grovesii* var. *jiuquanensis* (S. Wang, 1965) Grambast, 1970 emend.
478 Martín-Closas – Martín-Closas, p. 278, Fig. 12.

479 Material: 10 utricles from sample H96 and less abundant populations in other
480 samples, all from the Morella Formation (Fig. 4 and Appendix D).

481 Description: The fructification is 446 μm high and 385–431 μm wide (Appendix
482 B) and is formed by a calcified clavatoroid gyrogonite covered by a utricle with bilateral
483 symmetry. The utricle is formed of two layers. The internal layer is nodular, while the

484 external layer contains the impressions of the phylloid and three bract-cells, including
485 an abaxial bract-cell, opposite the phylloid and two lateral bract-cells. Each of these
486 lateral bracts bears ten elongated radial cells at the tip, forming a very protruding shield
487 at each side of the utricle. These cells cover the utricle surface completely. This variety
488 is distinguished from closely related ones by the equal development of the elongated
489 radial cells, with the lower ones reaching the basal pore.

490 Distribution: In the Iberian Peninsula this variety of *C. grovesii* has been
491 described by Grambast-Fessard (1980b) in the Algarve Basin (Portugal) and here it is
492 reported for the first time in the Iberian Chain. Otherwise, it has a subcosmopolitan
493 distribution in Eurasia (Martín-Closas, 2015), reaching as far East as Gansu province in
494 China (Z. Wang and Lu, 1982) and the Korean Peninsula (Choi, 1989).

495

496 *Clavator harrisii* (Peck, 1941) emend. Martín-Closas, 1996

497 *Clavator harrisii* var. *dongjingensis* (Hu et Zeng, 1981) Martín-Closas, 2000

498 Figure 10D–F

499 1981 *Flabellochara dongjingensis* nov. sp. – Hu et Zeng, p. 147-148, Pl. 2, figs.
500 20-23.

501 2000 *Clavator harrisii* var. *dongjingensis* (Hu et Zeng, 1981) nov. comb. –
502 Martín-Closas, p. 148, Pl. 15, fig. 1.

503 Material: 20 utricles from sample H–38 and other small populations (up to 15
504 utricles) in the lower part of the Cantaperdius Formation (Fig. 3 and Appendix C).

505 Description: The fructification measures 604–718 μm high and 586–677 μm wide
506 (Appendix B) and is formed by an internal clavatoroid gyrogonite covered by the

utricle. The utricle is formed by an internal nodular layer and an external structured layer that displays bilateral symmetry. This layer is formed by two opposing fans of bract-cells and a large abaxial bract opposite the phylloid. The lateral fans are composed of 6 arched cells borne by a bract-cell directly connected to the basal pore, and two shorter, broadly triangular cells laterally tightened at the base of this bract. These triangular cells do not occur in the nominal variety.

Remarks: This variety is characteristic of the Valanginian and Hauterivian (Martín-Closas, 2000), but has been reported in the basal Barremian by Martín-Closas and Peybernès (1987). In the early Barremian it forms mixed populations with the dominant *C. harrisii* var. *harrisii* and is occasionally associated with *C. harrisii* var. *reyi*.

Distribution: This variety has been reported from a number of Valanginian and Hauterivian localities of the Iberian Chain, such as in the Catalan Coastal Chain and eastern Iberian Chain (Martín-Closas, 2000). It has also been reported in the Pyrenees by Martín-Closas (2000) and in the Prebetic Chain by García-Cortés et al. (1995). Outside the Iberian Peninsula this variety is widely distributed in Eurasia, from the Iberian Peninsula to China (Martín-Closas, 2015, and references therein).

Clavator harrisii var. harrisii (Peck, 1941) Martín-Closas, 1996

Figure 10G–H

1941 *Clavator harrisii* nov. sp. – Peck, p. 292-294, Pl. 42, figs. 25-37.

1959 *Flabellochara harrisii* (Peck) nov. comb. – Grambast, p. 559.

1996 *Clavator harrisii* var. *harrisii* (Peck, 1941) – Martín-Closas, p. 278–279.

Material: 107 utricles from sample H39 (Fig. 3) and smaller populations from numerous samples from throughout the entire section (Figs. 3–4 and Appendixes C–D).

Description: The fructification measures 601–703 μm high and 471–528 μm wide (Appendix B) and it is formed by an internal clavatoroid gyrogonite covered by the utricle. The utricle is formed by an internal nodular layer and an external structured layer that displays bilateral symmetry. This layer is formed by two opposing fans of bract-cells and a large abaxial bract, opposite the phylloid. The lateral fans are composed of 6–8 arched cells that do not completely cover the internal layer and are borne by a large central cell, directly connected to the basal pore of the utricle. Two long digitated cells fringe each lateral fan and are also connected to the utricle base.

Distribution: In Spain this variety is widely distributed in the Barremian records of the Maestrat Basin, the Serranía de Cuenca, the Basque-Cantabrian Basin and the Prebetic Chain (Martín-Closas, 2000, and references therein). Rey and Ramalho (1973-74) have also reported this variety in the Lusitanian Basin, Portugal. Otherwise, this species, and particularly this variety, presents a cosmopolitan biogeographic range in the Barremian and Aptian (Martín-Closas, 2015). It is found in northern Africa (Trabelsi et al. 2016; Haddoumi et al., 2019), North America (Peck, 1941; Soulié-Märsche, 1994), South America (Mussacchio, 1989) and China (Z. Wang and Lu, 1982).

----------Please insert Figure 10 near here----------

Clavator harrisii var. *reyi* (Grambast-Fessard, 1980a) Martín-Closas, 1996

Figure 10I

553 1980a *Stellatochara reyi* n. sp. – Grambast-Fessard, p. 42-44, Pl. 3, figs. 6–9.

554 1996 *Clavator harrisii* var. *reyi* (Grambast-Fessard, 1980) nov. comb. – Martín-
555 Closas p. 279.

556 2005 *Luzochara reyi* nov. comb. – Pereira and Cabral, p. 173-178, Pl. 1, figs. 1–6.

557 Material: 100 utricles from sample H76 (Fig. 4) and minor populations in
558 numerous samples along the section (Figs. 3–4 and Appendixes C–D).

559 Description: The fructification measures 512–568 μm high and 403–419 μm wide
560 (Appendix B). In contrast to the previous variety, only small portions of the gyrogonite
561 are covered by the external utricle layer allowing the nodular layer to crop out and form
562 most of the utricle surface. In the populations studied, some gyrogonites were even
563 devoid of nodules and only the clavatoroid gyrogonite was visible, showing convex
564 cells separated by characteristic undulated sutures and a wide apical neck with a rose-
565 shaped apical pore.

566 Remarks: This type of fructification has often been misinterpreted as belonging to
567 the porocharaceans (e.g. Grambast-Fessard, 1980a) or as a different clavatoroidean
568 genus (Pereira and Cabral, 2005). However, the occasional occurrence of the outer
569 utricle layer with the structure of *C. harrisi* and the particular calcification of the spiral
570 cells in empty tubes around the apical pore of the clavatoroid gyrogonite
571 ("Ringstruktur" according to Schudack, 1993) justify its ascription to *C. harrisii*.

572 Distribution: In the Iberian Peninsula this variety often occurs in association with
573 the previously described variety. Thus, in the Maestrat Basin, it occurs in the Morella,
574 Aliaga, Penyagolosa and Oliete sub-basins (Martín-Closas, 2000). It has also been
575 described in the Serranía de Cuenca (South-Western Iberian Chain) by Martín-Closas,
576 (2000) and Vicente and Martín-Closas (2013). Grambast-Fessard (1980a) reported this

variety in the Algarve Basin, while Pereira and Cabral (2005) found it in the Lusitanian Basin (Portugal). Outside the Iberian Peninsula this variety has been reported in Tunisia (Trabelsi et al., 2016).

Clavator calcitrapus (Grambast, 1969) Martín-Closas ex Schudack, 1993

Clavator calcitrapus var. *jiangluoensis* (Z. Wang et Z.W. Li in Z. Wang et Lu 1982) nov. comb. Pérez-Cano, Bover-Arnal et Martín-Closas

Figure 10J–L

Basionym: *Triclypella jiangluoensis* Z. Wang et Z. W. Li in Z. Wang and Lu (1982), p. 99, Pl. 3 fig. 6a–f. holotype number PB 8733, Nanjing Institute of Geology and Palaeontology, Chinese Academy of Science.

Synonym: 1989 *Triclypella patagonica* nov. sp. – Musacchio, p. 840, Pl. 2, figs. 1–2.

Material: 20 utricles from the sample H38; 10 utricles from the sample H40 (Fig. 3 and Appendix C)

Description: The fructification measures 417–558 μm high and 457–532 μm wide (Appendix B) and is formed by a clavatoroid gyrogonite and a bilayered utricle. The inner layer of the utricle corresponds to a nodular layer that covers the gyrogonite and is coated by three inner bracts, 120º apart from each other. Each bract bears a whorl of small radial cells in a terminal position that cover the entire utricle surface, forming three radial shields, each constituted by 10–14 polygonal cells. The cells of each shield are connected to those of the adjacent shields with a zigzag suture that runs from the apical part until the equator of the utricle. The apical view of the utricle shows a

hexagonal outline (Fig. 10J) and a slightly triradiated symmetry. However, at the posterior part of the fructification two of the shields are separated by a vertical furrow corresponding to the phylloid, indicating that the real symmetry of the utricle is bilateral, rather than triradial.

Distribution: In the Iberian Peninsula, *Clavator calcitrapus* var. *jiangluoensis* (generally named *C. calcitrapus*) has been reported in the Barremian record of several localities of the Eastern Iberian Chain, such as Herbers and Galve, while in the Cameros Basin it has been reported from Ciria and Mambrillas (Martín-Closas and Grambast-Fessard, 1986; Schudack, 1987; Martín-Closas, 2000). This taxon has been described also in Southern England (English Wealden Facies) by Feist et al. (1995), who dated its occurrence from the latest Hauterivian to the early Barremian. A similar latest Hauterivian–early Barremian age was proposed by Z. Wang and Lu (1982) for this taxon in its type locality, Huixian (Gansu Province, China) and in South America, Argentina (*Triclypella patagonica*), by Musacchio (1989, 2000).

Clavator calcitrapus var. *calcitrapus* (Grambast, 1969) Martín-Closas ex Schudack, 1993

Figure 10M–O

1969 *Triclypella calcitrapa* n. gen. n. sp. – Grambast, p. 881, Pl. 1, figs. 1–7.

1989 *Clavator calcitrapus* (Grambast, 1969) nov. comb. – Martín-Closas p. 278–280, Fig. II-46; Pl. 7, Figs. 10–12 (unpublished).

1993 *Clavator calcitrapus* (Grambast 1969) Martín-Closas 1989 – Schudack, p. 82–82, Pig. 37; Pl. 10, figs. 15-18.

623 Material: 30 utricles from sample H51 (Fig. 3) and a smaller population from H50
624 (Fig. 3 and Appendix C).

625 Description: The nominal variety is larger than the one described previously. The
626 fructification measures 568–674 μm high and 550–735 μm wide (Appendix B). This
627 variety is also formed by a clavatoroid utricle covered by a nodular layer and three main
628 bracts 120º apart from each other. The tip of these main bracts bears a whorl of 10 to 14
629 thinner and polygonal bract-cells that cover the entire utricle surface and interdigitate
630 with similar cells of adjacent whorls, as in the previous variety. The main difference
631 with respect to the previous variety resides in the greater length of the inner bracts,
632 rendering the three shields more prominent and horn-like with a more triangular apical
633 view. As a result, the thin cells born at the tip of these bracts are also longer (Fig. 10M).

634 Remarks: The type locality of this species was established in Herbers by
635 Grambast (1969); however, the type layer was not precisely defined. The marl yielding
636 sample H51 at 338 m from the laterite at the base of Cantaperdius Formation, Herbers
637 section (Fig. 3) is proposed here as an alternative type layer.

638 Distribution: This variety has only been described in Herbers by Grambast (1969)
639 and in the present work, suggesting that it might be an Iberian endemism.

640

641 Genus *Ascidiella* (Grambast, 1966b) emend. Martín-Closas ex Schudack, 1993

642 *Ascidiella stellata* (Martín-Closas et Grambast-Fessard, 1986) nov. comb. Martín-
643 Closas ex Schudack, 1993

644 *Ascidiella stellata* var. *stellata* (Martín-Closas and Grambast-Fessard, 1986)
645 comb. nov. Martín-Closas ex Schudack 1993

Figure 11A–D

1986 *Embergerella stellata* nov. sp. – Martín-Closas and Grambast-Fessard, p. 31–33, Pl. 7, Figs. 7–9.

1989 *Ascidiella stellata* (Martín-Closas et Grambast-Fessard, 1986) nov. comb. – Martín-Closas, p. 281-283, Fig II-47; Pl. 8, figs.4–8.

1993 *Ascidiella stellata* (Martín-Closas et Grambast-Fessard 1986) Martín-Closas 1989 – Schudack, p. 84, Pl. 11, figs. 5–8.

Material: 50 utricles from sample H7 (Fig. 3) and other smaller populations throughout the Cantaperdius Formation (Fig. 3 and Appendix C).

Description: This fructification measures 457–625 μm high and 358–429 μm wide (Appendix B) and has an ellipsoidal shape. The clavatoroid gyrogonite is covered by a utricle formed by an internal nodular layer and an external structured layer. The external layer is built up of a calcified phylloid portion with 1–2 nodes and three long bract-cells attached to the basal node. Two of these bract-cells are lateral to the phylloid while the third lies in an abaxial position. Other smaller bracts are intercalated with the longer ones in the basal half of the utricle. All bract-cells bear a terminal rosette with 6 petal-shaped cells. Similar rosettes are also attached directly to the phylloid nodes. The angle of the gyrogonite axis in relation to the phylloid is acute.

Distribution: This variety of *Ascidiella stellata* occurs widely in the Valanginian to Barremian record of the Iberian Chain. In the Maestrat Basin, this taxon has been found in the Morella and Galve sub-basins (Martín-Closas and Grambast-Fessard 1986; Schudack, 1989; Martín-Closas, 2000). This species has also been found in the Cap del Terme section of the Catalan Coastal Chain (Martín-Closas, 2000) and has been

described in the Valanginian-Hauterivian of the Aguilón sub-Basin by Soria et al. (1995). So far, this species is exclusive to the Iberian Peninsula.

Ascidiella stellata var. *lata* Martín-Closas, 1996

Figure 11E–G

1996 *Ascidiella stellata* var. *lata* Martín-Closas nov. var. – Martín-Closas, p. 282–283, Fig. 14.4–14.8.

Material: 40 utricles from sample H44 (Fig. 3) and other small populations in the upper part of the Cantaperdius Formation (Fig. 3 and Appendix C).

Description: The utricle is very similar to the nominal variety. The main differences are: (1) the portion of the phylloid attached to the utricle is larger than in *A. stellata* s.s., completely calcified, and bears short bracts with petal-shaped rosettes, and (2) the angle between the phylloid and the axis of the gyrogonite is almost 90º.

Distribution: This variety has only been identified in the upper Barremian of its type locality, in the Blesa Formation (Oliete sub-basin) by Martín-Closas (1996; 2000) and the Cantaperdius Formation in Herbers (present work). In the upper Barremian of the High Atlas (Morocco), Haddoumi et al. (2019) have reported *A. stellata* from the Upper Barremian of the High Atlas (Morocco). However, the illustrations published do not correspond to this species.

----------Please insert Figure 11 near here----------

691 *Ascidiella triquetra* (Grambast, 1969) Martín-Closas, 1996

692 Figure 11H–J

693 1969 *Embergerella triquetra* n. gen. n. sp – Grambast, p. 879–881, Pl. 3, figs. 15–
694 21.

695 1996 *Ascidiella triquetra* (Grambast, 1969) nov. comb. – Martín-Closas, p. 283,
696 Figs. 13B, 15.

697 Material: 147 utricles from sample H27 (Fig. 3), and other smaller populations in
698 several samples from the Cantaperdius Formation (Fig. 3 and Appendix C).

699 Description: The fructification measures 452–927 μm high and 535–805 μm wide
700 (Appendix B) and is formed by a calcified clavatoroid gyrogonite and a utricle with an
701 internal nodular layer and an external structured layer. The external layer is composed
702 of a complete phylloid portion and two lateral internal bract-cells. These three elements
703 provide 3 axes, 120º apart, that diverge from the base until the apex of the utricle,
704 resulting in a fructification shape similar to a tetragon, but with bilateral symmetry. In
705 the apex, a large rose-shaped pore corresponds to the gyrogonite apical pore. The two
706 lateral bracts and the phylloid portion have a compound rosette at their tip, formed by a
707 first very small whorl of petal-shaped bracts and a second whorl of longer filamentous
708 bracts that cover most of the utricle surface. Smaller bract-cells with an identical
709 structure may occur at the base of the utricle.

710 Distribution: This species has been widely identified in the Maestrat Basin
711 (Martín-Closas and Grambast-Fessard, 1986; Martín-Closas, 2000). The only other
712 occurrence in the Iberian Peninsula has been reported in Terradets (Pyrenees) by
713 Martín-Closas and López-Morón (1996). Outside the Iberian Peninsula this species has

714 only been identified reworked in Berland (Chartreuse Massif, sub-Alpine chain) by
715 Martín-Closas et al. (2009).

716

717 *Ascidiella cruciata* (Grambast, 1969) Martín-Closas ex Schudack, 1993

718 Figure 11K–M

719 1969 *Embergerella cruciata* n. sp. – Grambast, p. 879, 881, Pl. 2 figs. 8–14

720 1993 *Ascidiella* (*Embergerella*) *cruciata* (Grambast 1969) Martín-Closas 1989 –
721 Schudack, p. 84–85, Pl. 11, figs. 9–14.

722 1996 *Ascidiella cruciata* (Grambast, 1969) Martín-Closas ex Schudack, 1993–
723 Martín-Closas, p. 283, Figs. 13C, 15.

724 Material: 10 utricles in samples H128B, H94, H95 and H96 (Fig. 4 and Appendix
725 D).

726 Description: Clavatoroid fructification measuring 515–730 μm high and 531–854
727 μm wide (Appendix B), formed by a calcified gyrogonite and a utricle with an internal
728 nodular layer and an external structured layer. The utricle shape is an inverted square
729 pyramid. The external utricle layer has a structure similar to *A. triquetra* but with three
730 bracts instead of two, one in anterior position, opposite the phylloid, and two lateral
731 bracts, all bearing composite rosettes at the tips, like *A. triquetra*. In apical view these
732 three bracts and the phylloid occur at the vertexes of a cross-like outline, hence the
733 name of the species.

734 Distribution: Besides the upper Barremian of Herbers, this species has also been
735 identified in the neighbouring locality of El Parrisal near Beseit (Morella sub-basin) by
736 Martín-Closas and Grambast-Fessard (1986). In the El Perelló sub-basin it occurs in the

upper Barremian of Sant Carles de la Ràpita (Grambast, 1974; Martín -Closas, 2000). This species has also been found in Alcalá de la Vega, which corresponds to its type locality (Grambast, 1969) and Aliaga (Martín-Closas, 2000), both in the Aliaga Sub-Basin. The species is particularly abundant in the upper Barremian of the Serranía de Cuenca in the south-western Iberian Chain (Schudack, 1989; Vicente and Martín-Closas, 2013). In the Iberian Peninsula, this species has been reported from the upper Barremian of the Algarve Basin by Rey and Ramalho (1973–74). Outside Iberia, *A. cruciata* has so far been reported from the Aptian of Hungary by Rasky (1945: p. 53, Pl. III figs. 24–26), who attributed it to a charophyte thallus, and in the Cenomanian of France (Feist, 1981).

Genus *Hemiclavator* Z. Wang and Lu, 1982

Hemiclavator adnatus (Martín-Closas et Grambast-Fessard, 1986) Schudack, 1989

Figure 12A–C

1974 *Clavator adnatus* (*nomen nudum*) – Grambast, Fig 8.

1986 *Nodosoclavator adnatus* nov. sp. – Martín-Closas and Grambast-Fessard, p. 10–13, Figs. 2–4, Pl. 2, figs 7–11.

1989 *Hemiclavator adnatus* (Martín-Closas et Grambast-Fessard) n. comb. – Schudack, p. 418, Pl. 2, figs. 14-16.

Material: 15 utricles from sample H12 and smaller populations (<10 utricles) in samples H27 and H29a (Fig. 3 and Appendix C).

759 Description: Bottle-shaped clavatoroid fructification measuring 622–850 μm high
760 and 499–535 μm wide (Appendix B), formed by a calcified gyrogonite and a utricle
761 with an internal nodular layer and an external structured layer limited to the adaxial
762 side. The utricle external layer is formed by the phylloid mark in posterior or adaxial
763 position, bearing one or two fans of usually 6 short triangular cells, 3 at each side,
764 attached to two adjacent superposed nodes. When the phylloid portion is completely
765 calcified, it is usually sufficiently long and curved to flank the gyrogonite base.
766 Fructifications and the phylloids bearing them are attached to a node in whorls of six
767 showing the utricle anterior or abaxial face oriented to the internode (Martín-Closas,
768 1996).

769 Distribution: This species is widely represented in the Iberian Peninsula from the
770 Valanginian to the early Barremian (Martín-Closas, 2000). In the Maestrat Basin,
771 *Hemiclavator adnatus* has been found in the Morella, Aliaga-Penyagolosa, Aguilón and
772 Galve sub-basins (Canérot, 1974; Martín-Closas and Grambast-Fessard, 1986;
773 Schudack, 1989; Soria et al., 1995; Martín-Closas, 2000). In the Cameros Basin it
774 occurs in the localities of Hortezuelos (Martín-Closas and Alonso-Millán, 1998),
775 Peñacoba and Fitero (Schudack, 1987), with a Valanginian–Hauterivian age. Martín-
776 Closas and Peybernès (1987) have documented this species in the Basque-Bearnian
777 Pyrenees. In the Betic Chain, García-Cortés et al. (1995) reported this species from the
778 Valanginian–Hauterivian of Sierra del Pozo (Jaén) and Martín-Closas (2000) from the
779 early Barremian of Alzira (València).

780

781 *Hemiclavator neimongolensis* Z. Wang and Lu, 1982

782 *Hemiclavator neimongolensis* var. *posticecaptus* (Martín-Closas et Grambast-
783 Fessard, 1986) Martín-Closas, 1996

784 Figure 12D–F

785 1986 *Pseudoglobator posticecaptus* nov. sp. – Martín-Closas and Grambast-
786 Fessard, p. 13–17, Fig. 3 Pl. 2 fig 7–11.

787 1996 *Hemiclavator neimongolensis* var. *posticecaptus* (Martín-Closas et
788 Grambast-Fessard, 1986) Martín-Closas, 1996 – Martín-Closas, p. 286, Fig.16.

789 Material: 100 utricles from sample H12 (Fig. 3 and Appendix C).

790 Description: Bottle-shaped clavatoroid fructification measuring 618–911 μm high
791 and 506–581 μm wide (Appendix B), formed by a calcified gyrogonite and a utricle
792 with an internal nodular layer and an external structured layer. The adaxial part of the
793 external utricle layer is equivalent to that described for *H. adnatus*. However, in the
794 anterior or abaxial part, it shows 4–9 long, filiform to digitated cells, which split radially
795 from the base and may reach the apical region of the utricle.

796 Distribution: This species is well-represented in the Valanginian to lower
797 Barremian of the Maestrat Basin at Herbers, Coll de Querol, El Mangraner, Jaganta,
798 Seno and Villores (Martín-Closas, 2000). Outside the Iberian Peninsula, this variety has
799 been reported from the lower Barremian of Pas du Frou (Chartreuse, France) by Martín-
800 Closas et al. (2009). Mojon et al. (2009) have identified this species from the Lower
801 Barremian of Aït Attab (Morocco), without supplying, however, any illustration.
802 Another possible occurrence of this species is in the Pre-Dobrogean Basin (Romania),
803 as reported by Avram et al. (1993, Fig. 11f–g).

804

----------Please insert Figure 12 near here----------

Hemiclavator neimongolensis var. *neimongolensis* Z. Wang et Lu, 1982

Figures 12G–I

1982 *Hemiclavator neimongolensis* Z. Wang and Lu gen. nov. sp. nov. – Z. Wang and Lu, p. 99, 102; Pl. 4, figs. 1–5.

Material: 120 utricles from sample H39 (Fig. 3) and other small populations from the upper part of the Cantaperdius Formation (Fig. 3 and Appendix C) and in the Morella Formation (Fig. 4 and Appendix D).

Description: The fructification measures 427–888 μm high and 415–592 μm wide (Appendix B), and is formed by a clavatoroid gyrogonite and a utricle with an internal nodular layer and an external structured layer. The utricle of this variety is more globular, and the apical neck is shorter than in var. *posticecaptus*. However, the main difference with this variety resides in the posterior or adaxial side of the utricle, which generally shows only one fan of up to 7 radial and filiform bract-cells borne at the tip of the phylloid. Some specimens show additional small fans of triangular cells at the base of the phylloid, similar to those of *H. neimongolensis* var. *posticecaptus*.

Distribution: In the Maestrat Basin, this species occurs in the Morella, Oliete and Aguilón sub-basins (Martín-Closas, 2000). In the Catalan Pyrenees it has also been found in the Terradets Pass section, Montsec thrust sheet (Martín-Closas, 2000). Elsewhere, this variety is widely represented in the northern Tethyan domain including European and Asian basins (Martín-Closas, 2015). It has been documented in Chartreuse (France) by Martín-Closas et al. (2009), in the Dobrogean Basin (Romania)

by Neagu and Georgescu-Donos (1973) and in the Neimongol Province, or Inner Mongolia (China), which is also the site of the type locality (Z. Wang and Lu, 1982).

Genus *Pseudoglobator* Grambast, 1969

Pseudoglobator paucibracteatus Martín-Closas et Grambast-Fessard, 1986

Figure 12J–K

1986 *Pseudoglobator paucibracteatus* n. sp. – Martín-Closas and Grambast-Fessard, p. 17–19, Pl. 5, fig 1–4.

Material: 12 well preserved utricles from sample H94 (Fig. 4) and other small populations from the Artoles and Morella formations (Fig. 4 and Appendix D).

Description: Globular to bottle-shaped clavatoroid fructification measuring 625–673 μm high and 483–557 μm wide (Appendix B). The gyrogonite is covered by a utricle, comprising an internal nodular layer and an external structured layer. The external layer is formed by 4–8 short and wide, finger-shaped to petal-shaped bracts attached to the basal node, which can reach the apical neck.

Distribution: In the Iberian Peninsula this species has only been identified in the El Parrisal section of the Morella sub-basin (Martín-Closas and Grambast-Fessard, 1986). Outside the Iberian Peninsula *P. paucibracteatus* has been identified in the Chartreuse Massif, France by Mojon (1988) and Martín-Closas et al. (2009). These latter authors have also reported this species in Montanges (Jura Mountains) and Berland (Subalpine Chains). Another possible occurrence of this species has been reported in the Pre-Dobrogean Basin, Romania (Avram et al. 1993, Fig. 12m).

Charophyte thalli

Genus *Charaxis* Harris, 1939

Charaxis spicatus Martín-Closas et Diéguez 1998 emend. Pérez-Cano, Bover-Arnal et Martín-Closas

Figures 13A–H, 14–15

1998 *Charaxis spicatus* n. sp. – Martín-Closas and Diéguez, p. 1138–1140, Pl. 1, fig. 5; Pl. 2, figs. 1–9.

2000 *Charaxis spicatus* – Martín-Closas, p. 179–180, Pl. 19, Figs. 1–7.

Material: Dozens of thin-sections in samples H77-79; H90 and H90b (Fig. 4).

Original diagnosis (Martín-Closas and Diéguez, 1998): 'Thallus of *Charaxis* with nodes formed by six nodal cells bearing up to 18 ecorticate branchlets which are longer than internodes above, completely covering them. Internodes several milimeters long and *c*. 1 mm wide formed by an internodal cell coated by first six then 18 cortical cells. Gyrogonites ellipsoidal (400–530 μm x 260–290 μm), showing *c*. 16–18 circumvolutions and probably apical and basal necks'.

Emended diagnosis: Thallus of *Charaxis*, with nodes formed by six globular nodal cells, each of them bearing 3 ecorticate brachlets, longer than the following internodes and covering them. Internodes several milimeters long and up to 1 mm wide, constituted by 18 primary cortical cells of different size and structure. Six primary cortical cells are long and large and extend downwards in the internode reaching at least its central part. Six more pairs of shorter and thinner primary cells separate the six larger primary cells near the node. At a distance from the nodal cell, each of the 6 large primary cells develops a small cortical node, emitting four secondary cortical cells, two larger

874 secondaries grow distally, while two thinner secondary cortical cells bend upwards
875 covering the larger primary cortical cell.

876 Description: Thallus corticated. Nodes are formed by six globular cells with an
877 apical protrusion from which three branchlets emerge upwards, resulting in 18
878 extremely long branchlets per whorl, which tightly cover the overlying internodes in
879 young, apical parts of the plant (Fig. 13A).

880

881 ----------Please insert Figure 13 near here----------

882

883 The internodes are constituted by one large internodal cell (250–450μm in
884 diameter), that is surrounded by a complex cortical structure. Three primary cortical
885 cells emerge from each nodal cell, including one long cell 85–150 μm in diameter,
886 flanked by two smaller ones, measuring 60–85 μm in diameter. Each long primary
887 cortical cell distally expands and forms a 'cortical node' (Fig. 13B, D, G), from which
888 two pairs of secondary cells emerge, one pair of larger cells, measuring 45–60 μm,
889 grows downwards (i.e. distally), flanking the primary cortical cell, while the other pair,
890 formed by very thin cells, measuring 25–30 μm in diameter, bends upwards (i.e.
891 proximally) covering the primary cortical cell that emitted them (Fig. 13B, C, E, F).

892 As a result of this complex cortical structure, three types of transversal thin
893 sections can be recognized along the same internode: (1) Internodal thin sections located
894 close to the node, show 6 large primary cortical cells, separated each other by one pair
895 of smaller primary cortical cells. Each large primary cortical cell is covered by an
896 additional pair of very small cells that corresponds to the pair of secondaries growing
897 upwards (Fig. 13F). This type of thin sections may recall somewhat the triplostichous

898 anisostichous cortication of extant *Chara* but differs from it by being produced by
899 primary cells and in the very small pairs of secondary cells covering the larger
900 primaries. (2) Internodal thin sections located at the level of 'cortical nodes' show parts
901 of the branching of secondaries growing either proximally or distally (Fig. 13E, G).
902 These two types of sections are very useful to determine *Charaxis spicatus* in thin
903 sections. (3) Internodal thin sections corresponding to distal parts of the internode, i.e.
904 below the 'cortical node', show a normal triplostichous isostichous cortication formed by
905 18 cells (Fig. 13H).

906 The term 'double triplostichous cortication' is proposed here for this complex new
907 type of cortication (Fig. 14). It differs from the usual triplostichous cortication of extant
908 *Chara* in that a double pair of secondary cortical cells is emitted from the primary
909 cortical cells, at the same point (here called a 'cortical node'), one pair growing upwards
910 and the other downwards.

911

912 ----------Please insert Figure 14 near here----------

913

914 Remarks: The new diagnosis provided here modifies the characterization of the
915 species by Martín-Closas and Diéguez (1998) and Martín-Closas (2000), who did not
916 fully understand the complex cortication of this species. Indeed, the cortication of
917 *Charaxis spicatus* is much more complex than any cortication described so far in
918 charophytes and corresponds to an unknown Bauplan in this group of plants.

919 Furthermore, this vegetative structure has been found anatomically connected to
920 utricles of *Echinochara lazarii* in a limestone bed in the Morella Formation (Fig. 15),
921 which provides evidence of the relationship between both taxa and has permitted whole-

plant reconstruction of the *Echinochara* plant. Therefore, the fertile structures of this thallus have been ommited from the emended diagnosis, reserving the name *Charaxis spicatus* solely for the thallus.

----------Please insert Figure 15 near here----------

Distribution: This taxon was only known from its type locality at the Las Hoyas palaeontological site near Cuenca (Southwestern Iberian Chain, Spain). Unpublished data of our own show that *C. spicatus* also occurs in Barremian beds of the Garraf Massif (Catalan Coastal Chain) and the Terradets Pass section (Montsec thrust sheet, Pyrenees). In Morocco, Haddoumi et al. (2019, Fig. 13F) have ascribed a triplostichous thallus similar to transversal sections of the upper part of the internode of *C. spicatus* to dasycladales. A similar thallus, described in the lower Barremian of Neuquén (Argentina) by Musacchio (1971, Fig. 4 and Pl. 1, fig. 8) as *Diectochara andica* Musacchio, may correspond to the same species. However, the original material should be revised to confirm this possibility.

Charaxis sp.

Figure 13I–J

Description: Portions of thalli with strong similarities to the corticated thalli of present-day *Chara*. Two types of transversal sections are known, which clearly differ from *Charaxis spicatus*. The first type shows a cortication formed by 12 cells of equal size, i.e. corresponding to an isostichous cortication (Fig. 13I), while the second type is

anisostichous, showing an alternation of 12 larger and smaller cortical cells in transversal sections, suggesting that it corresponds to a diplostichous thallus (Fig. 13J).

Remarks: The insufficient connection between the two types of cortication described under this heading hinders verification of whether they belong to the same thallus or not.

Occurrence: In the studied section, isostichous thalli occur in limestones of both the Cantaperdius and Morella formations. Both types may be associated in limestones of the Morella Formation.

Genus *Munieria* Deecke, 1883 emend Granier in Granier et al. 2015

Munieria grambastii Bystrický, 1976

Figure 16A–G, 17A–K

1976 *Munieria grambastii* n. sp. – Bystrický (1976), p. 48–54, Pl. I, Figs. 1–14; Pl. II, figs. 1–16; Pl. IV, fig. 2.

Description: Thallus corticated. Nodes are formed by 6–10 large nodal cells of variable in morphology, frequently barrel-shaped or tronco-conical (Fig. 16B, C; Fig. 17A). These nodal cells are well calcified and flank a short internodal cell. Nodal cells show a distal opening, which is attributed to the attachment gap left by the uncalcified branchlets. They are covered on the outside by the proximal calcified part of the cortical cells that emerge from them (Fig. 16A).

----------Please insert Figure 16 near here----------

Internodes cylindrical, measuring 290–390 μm across, formed by a large internodal cell measuring 72–202 μm in diameter and covered by up to 26 smaller isostichous primary cortical cells measuring 20–30 μm in diameter. About 10 cortical cells emerge from each nodal cell. Four to five of these cortical cells grow upwards and downwards, respectively, from each nodal cell and interdigitate at the internode centre with the cortical cells from the adjacent node, forming a zigzag line. Calcification of the internode is limited to the intercellular area between the internodal cell and the cortical cells, with the result that the cortical cells are only visible as concave furrows on the outer surface of the fossil thallus (Fig 16F). In thin sections these cortical cells appear as a crenulated outline on the surface of the internode (Figs. 17B–H). The calcified space between the internodal cell and the cortical cells is variable in thickness, generally massive and recrystallised in sparry calcite. In some exceptionally well-preserved specimens the calcified internodal wall shows concentrical lamination formed by very thin laminas, 0.75–3.00 μm thick (Figs. 16D–E, 17B–F, I). The empty space corresponding to the internodal cell is very variable in diameter representing 20–66% the total diameter of the internode (Appendix E) and generally sited in its central part (Figs. 17B–E), but sometimes eccentrically (Figs. 17F–G). In longitudinal thin sections of internodes, the diameter of the internodal cell increases towards the nodes, keeping the shape of the complete internode cylindrical (Fig. 17K and Appendix E). Transversal thin sections of the internodes with smaller internodal cells show a larger number of concentric laminas (Fig. 17B–D), which may indicate that the calcification of the internodes was centripetal, from the outer parts of the internode to the central areas. According to these observations, sections with a larger internodal cell and a thinner calcification would correspond to younger specimens or the earlier ontogenetic stages of

992 the plant, whereas those sections with smaller diameter of the internodal cell and a
993 thicker clacification would represent mature specimens of the late ontogenetic stages.

994 Remarks: Since Deecke (1883) described first this type of thallus, the taxonomy
995 of *M. baconica* and its related species has been problematic (Pia, 1920; Feist et al.,
996 2003). Here genus *Munieria* Deecke is understood as a charophyte thallus with the
997 diagnosis emended by Granier in Granier et al. (2015, p. 207) and four species are
998 recognized:

999 1) The type species of the genus, *Munieria baconica* Deecke 1883, is a robust
1000 thallus about 500–1100 μm across. The type material corresponds to the apical tips of
1001 thalli or branchlets, with a tapering shape and poorly developed internodes. The number
1002 of nodal cells varies between 12 and 18 (Deecke, 1883; Feist et al., 2003) and show
1003 elongated, petal-like morphologies. The internodes are cylindrical and show about 36–
1004 72 cortical cells, which are all primary and slightly ondulated.

1005 2) *Munieria grambastii* is considered here as a different organ-species than *M.*
1006 *baconica*. It exhibits a cyclindrical thallus, 265–507 μm across in the type material, i.e.,
1007 significantly thinner than that of *M. baconica*. Cortical cells are straight and occur in
1008 numbers of 28–60 in the type material. The number of nodal cells varies between 7 and
1009 12 and their morphology is very variable even in the same node, changing from globose
1010 to elongate. The subspecies *M. grambastii* subsp. *sarda* Cherchi, Gušić, Schmidt et
1011 Schroeder, 1981 differs from *M. grambastii* s.s. by its longer internodes. Since the
1012 length of internodes increases from the apical, germinative part of the plant towards the
1013 basal, mature internodes (Fig. 17K and Appendix E), *M. grambastii* subsp. *sarda* should
1014 be considered merely an ontogenetic morphotype of *M. grambastii* s.s. However, such a
1015 morphotype has no the evolutionary or biogeographic meaning required for the rank of

subspecies, and a new combination is proposed here, relegating this subspecies to the rank of forma:

Munieria grambastii forma *sarda* (Chierchi et al., 1981) nov. comb. Pérez-Cano, Bover-Arnal et Martín-Closas

Basionym: *Munieria grambastii* subsp. *sarda* (Cherchi, Gušić, Schmidt et Schroeder, 1981) – Cherchi et al. (1981), p. 141–146, Figs. 2–3; Pls. 1–2. Holotype: slide PF-A-1, Geological and Palaeontological Institute of the University Frankfurt a. M. (Germany), collection of R. Schroeder.

3) *Munieria parvula* (Carozzi, 1946), formerly *Clypeina parvula*, has been accomodated recently within genus *Munieria* by Granier et al. (2015) and may be equivalent to *M. grambastii*, as proposed by these authors. However, the data available from the type material lack significant detail to be sure about this equivalence, including the features of nodes and the detail of the cortication. It is kept provisionally apart from the latter species and regarded as a poorly known thallus within genus *Munieria*.

----------Please insert Figure 17 near here----------

4) *Munieria martinclosasi* (Granier et al., 2015) nov. comb. Pérez-Cano, Bover-Arnal et Martín-Closas

Basionym: *Charaxis martinclosasi* Granier et al. – Granier et al., 2015 p. 209–210, Pl. 4, Figs. E–I; Pl. 5, Figs. E, G–I, Pl. 6, Figs. A–F. Holotype is hosted at the Museum of Natural History of the Lebaneese University with MHNUL numbers, Holotype Pl. 5, Fig H.

1983 *Munieria tesense* n.sp. (*nomen nudum*) – Császár and Bodrogi, Pl. VI, figs. 1–4; Pl. VII, figs. 1–2; Pl. VII, figs. 1–2; Pl. XIV, figs. 1–2.

2008 *Salpingella* sp. – Veltz, Fig. 108b–c; Fig. 113g; Fig. 114g, i, j.

2015 *Charaxis martinclosasi* n.sp. – Granier et al., p. 209–210, Pl. 4, figs. E–I; Pl. 5, figs. E, G–I, Pl. 6, figs. A–F.

2020 *Charaxis martinclosasi* – Maksoud et al., Fig. 3S.

This species is distinguished from other species of *Munieria* by the shape of internodes, which corresponds to a hyperboloid of revolution. Internodes are up to 750 μm wide and covered by about 50 straight primary cortical cells. Nodes bear 8–10 nodal cells (Granier et al., 2015 and J. Sanjuan pers. comm., 2020) of variable-morphology, most commoly elongated.

M. martinclosasi was originally accommodated within genus *Charaxis*, based on the relatively high internodal cell width in comparison to the total internode diameter (Granier et al., 2015). However, this character is highly variable within genus *Munieria* (Appendix E) and bears no relationship to the definition of genus *Charaxis*. Instead it depends on the calcification degree of the internodal cell.

Genus *Munieria* was synonymized with genus *Charaxis* by Martín-Closas (2000). Although the general structure of both genera is similar, there are a number of characters that would justify keeping them separate. Thus, in *Munieria* the the internode is concentrically calcified, as it is observed in several specimens from thin section or obtained from sieved material (Figs. 16D–E; 17B–F, I). Furthermore, this calcification is regularly restricted to the intercellular space between the internodal cells and the cortical cells, the branchlets are never calcified. The nodal cells are completely calcified except at the point where they were attached to branchlets. In constrast, the calcification

of the *Charaxis* thallus is strictly an outer encrustation, generally on the cortical cells, sometimes including the nodes (not the nodal cells) and branchlets.

The species *Munieria tesense* Császár and Bodrogi (1983) is considered here as a non-valid synomym (nomen nudum) of *M. martinclosasi*, since it lacks the definition of a holotype. The proposed synonymy is based on the hyperboloidal morphology of the internodes, characteristic of *M. martinclosasi* (e.g., Császár and Bodrogi 1983, Pl. VIII, fig. 1). These authors also figured small portions of thalli with poorly developed internodes (Császár and Bodrogi 1983, Pl. VI, figs. 1–3), which probably belong to the apical parts of the same plant.

Genus *Clavatoraxis* Martín-Closas et Diéguez, 1998

Clavatoraxis sp.

Figures 16H, 18A–B, E, 19A

Description: Portions of corticated charophyte thalli that display spine-cell rosettes on the cortical cells. Occasionally, they have been found in anatomic connection with *Hemiclavator adnatus* and *H. neimongolensis* var. *posticecaptus* (Fig. 12E). In the thin sections surveyed, they are frequently associated with clavatoroid utricles (Fig. 18E).

----------Please insert Figure 18 near here----------

Genus *Favargerella* (Mojon, 1996) emend. Martín-Closas, 1998

Favargerella aquavivae Martín-Closas et Salas, 1998

Figures 16I–J, 18C–D, 19B

1996 *Favargerella stellata* (Martín-Closas and Grambast-Fessard 1986) nov. comb. – Mojon, p. 77–78, Pl. 3, fig. 2.

1998 *Favargerella aquavivae* sp. nov. – Martín-Closas and Salas, p. 106.

Description: Portions of ecorticate charophyte thalli, probably corresponding to branchlets, bearing a number of superposed whorls of 5–6 short phylloids, each with a terminal whorl of six petal-shaped cells. A pore occurs in the centre of the whorl, corresponding to the section of the bearing phylloid. *Favargerella aquavivae* is frequently associated in the same beds with utricles of genus *Ascidiella* and is considered to represent portions of its thallus.

Remarks: The swollen whorls of small branchlets bearing petal-shaped cells of genus *Favargerella* clearly differ from the spine-cell rosettes of genus *Clavatoraxis*. The latter are not whorls of branchlets, but hemispheres formed by a number or rod-shaped cells, directly borne on cortical cells of the main axis or on the surface of ecorticate phylloids (Fig. 19B).

Distribution: *Favargerella aquavivae* is abundant in marls of the Cantaperdius Formation (Maestrat Basin) where it is associated with *Ascidiella stellata* and *A. triquetra* (Martín-Closas, 2000). Outside Iberia, nodes and internodes of the genus *Favargerella* (probably *F. aquavivae*) have been recently reported from the upper Hauterivian – Barremian of the Aquitaine Basin by Granier and Clavel (2019, Fig. 4k and 4m), who described them as “charophyte stems”.

----------Please insert Figure 19 near here----------

5. Discussion

5.1. High Barremian clavatoracean biodiversity in the Maestrat Basin

The charophyte flora described from the Barremian record of the Herbers-Mas de Petxí section comprises 28 taxa belonging to fructifications of the three different families that coexisted during the Cretaceous: the Porocharaceae, the Characeae and the Clavatoraceae. Twenty-five out of these taxa (species or varieties) belong to the Clavatoraceae, including the first report of *Clavator grovesii* var. *jiuquanensis* in the Iberian Chain. However, three species previously reported from Barremian localities in the Iberian Chain, i.e. *Nodosoclavator bradleyi*, *Clavator grovesii* var. *combei* and *Ascidiella iberica* (Grambast, 1966b; Martín-Closas, 2000, Vicente and Martín-Closas, 2013), were not found in the studied samples, but they do appear in other Iberian Chain basins, including the Maestrat Basin.

Of the four large basins into which the Iberian Chain was subdivided by Salas et al. (2001), two other basins besides the Maestrat Basin are also significant as regards the Barremian clavatoracean biodiversity, the South-Western Iberian Basin (Serranía de Cuenca) and the Cameros Basin. In the former, the assemblages of Barremian clavatoracean fructifications include 7 species or varieties, *Globator maillardii* var. *trochilicoides* and var. *biutricularis, Atopochara trivolvis* var. *triquetra*, *Clavator grovesii* var. *combei*, *Clavator harrisii* var. *reyi*, *Ascidiella cruciata* and *Ascidiella iberica* (Vicente and Martín-Closas, 2013). These assemblages are enriched with *Echinochara lazarii*, as the utricles of this species are now known to be those borne by the thallus *Charaxis spicatus*, whose type locality is sited in this basin (Martín-Closas

and Diéguez, 1998). Meanwhile, the Cameros Basin includes up to 5 Barremian clavatoracean taxa, *Atopochara trivolvis* var. *triquetra*, *Clavator harrisii*, *C. calcitrapus*, *Hemiclavator adnatus* and *Ascidiella iberica* (Schudack, 1987; Martín-Closas and Alonso-Millán, 1998).

Other areas where Barremian clavatoraceans have been documented in the Iberian Peninsula are the Pyrenees, the Betic Ranges, the Lusitanian Basin and the Algarve Basin. The Barremian Pyrenean assemblages, mainly belonging to the Montsec thrust sheet (Catalan Pyrenees) and the Arzacq-Mauléon Basin (Bearnian Pyrenees), are formed by 8 species or varieties belonging to the Clavatoraceae, *Echinochara lazarii*, *Atopochara trivolvis* var. *triquetra*, *A. trivolvis* var. *trivolvis*, *Clavator harrisii* var. *dongjingensis* and var. *harrisii*, *Ascidiella triquetra*, *Hemiclavator adnatus* and *Hemiclavator neimongolensis* var. *neimongolensis* (Martín-Closas and Peybernès, 1987; Martín-Closas, 2000). In the Prebetic zone of the Betic Chain, the Barremian clavatoracean assemblages are scarce and are composed of 5 species *Atopochara trivolvis* var. *triquetra*, *Globator maillardii* var. *trochiliscoides, Clavator hariisii* var. *harrisii, Hemiclavator adnatus* and *Pseudoglobator fourcadei* (Grambast, 1969; García-Cortés et al. 1995; Martín-Closas, 2000). The Portuguese Algarve Basin contains up to 8 Barremian–Aptian clavatoraceans (Rey and Ramalho, 1973–74; Grambast-Fessard, 1980a, b; 1986), including *Atopochara trivolvis* var. *triquetra*, *Globator maillardi* var. *trochiliscoides, Clavator grovesii* var. *jiuquanensis*, *Clavator harrisii* var. *harrisii* and var. *reyi, Ascidiella cruciata, Ascidiella reticulata* var. *irregularis* (Grambast-Fessard 1986) Martín-Closas 1996. In the Barremian–Aptian Lusitanian Basin, Pereira and Cabral (2005) reported *Atopochara trivolvis triquetra* and var. *trivolvis, Clavator harrisii* var. *harrisii* and var. *reyi* and *Ascidiella* sp.

Outside Iberia, Barremian clavatoracean assemblages are also relatively diverse on other palaeo-islands from the Tethyan Cretaceous Archipelago. In the Wealden in southern England, latest Hauterivian–early Barremian assemblages are formed by *Atopochara trivolvis* var. *triquetra*, *Clavator grovesii* var. *combei*, *Clavator calcitrapus* and *Ascidiella iberica* (Feist et al., 1995). In the Subalpine Chains and Jura Mountains (France and Switzerland) the Barremian clavatoracean biodiversity is relatively higher but still less than in the Maestrat basin. It includes *Echinochara lazarii*, *Globator maillardi* var. *trochiliscoides*, *Atopochara trivolvis* var. *triquetra*, *Clavator grovesii* var. *combei* and var. *jiuquanensis, Hemiclavator neimongolensis* var. *posticecaptus* and var. *neimongolensis*, *Ascidiella triquetra* and *Pseudoglobator paucibracteatus* (e.g., Mojon, 1988; Martín-Closas et al., 2009). In Hungary, Barremian–Aptian clavatoracean assemblages are formed by *Atopochara trivolvis* var. *triquetra* and var. *trivolvis*, and *Ascidiella cruciata* (Rasky, 1945). In the Easternmost European Basins (Dobrogean and Caspian Basins) the Barremian clavatoracean record is relatively limited and formed by *Globator maillardi* var. *trochiliscoides*, *Atopochara trivolvis* var. *triquetra*, *Clavator grovesii* var. *jiuquanensis* and *Hemiclavator neimongolenis* (Neagu and Georgescu-Donos, 1973; Shaikin et al., 1992; Avram et al., 1993). The occurrence of the genus *Pseudoglobator* in this area is inconclusive from the illustrations provided by Avram et al. (1993).

In the southern margin of the Tethyan Cretaceous Archipelago, the Barremian clavatoracean floras from Tunisia are formed by *Echinochara lazarii*, *Globator maillardi* var. *trochiliscoides* and var. *biutricularis*, *Atopochara trivolvis* var. *triquetra* and var. *trivolvis*, *Clavator harrisii* var. *harrisii* and var. *reyi* and *Ascidiella iberica* (Andreu et al. 1988; Feist et al., 1999; Trabelsi et al., 2016; Haddoumi et al. 2019). In eastern Africa and the Middle East (Somalia, Israel and Lebanon), the clavatoracean

flora is not as diverse but is dominated by two species that are rare outside this region, *Clavator ampullaceus* (Grambast et Lorch, 1968) Martín-Closas, 1996, and *Ascidiella reticulata* (Grambast et Lorch, 1968) Martín-Closas, 1996, as well as *Atopochara trivolvis triquetra* (Grambast and Lorch, 1968; Luger and Schudack, 2001; Granier et al., 2015). Outside the Cretaceous Tethyan Archipelago only six Barremian clavatoraceans have been reported and were considered as cosmopolitan or subcosmopolitan by Martín-Closas and Q. Wang (2008) and Martín-Closas (2015): *A. trivolvis* var. *triquetra* and var. *trivolvis, Clavator grovesii* var. *jiuquanensis, Clavator harrisii* var. *harrisii, Clavator calcitrapus* and *Hemiclavator neimongolensis* var. *neimongolensis*.

5.2. Biostratigraphic characterization of the Morella Formation based on charophytes

The charophyte assemblages described in this study encompass two Barremian charophyte biozones (Figs. 3–4) the Atopochara trivolvis var. triquetra biozone and the Ascidiella cruciata–Pseudoglobator paucibracteatus biozone (Riveline et al., 1996 modified by Martín-Closas et al., 2009). The charophyte record from the Cantaperdius Formation was already known to belong to the lower Barremian, based on the association of *Atopochara trivolvis* var. *triquetra*, *Globator maillardi* var. *trochiliscoides*, *Clavator harrisii* var. *harrisii* and var. *reyi*, *Ascidiella stellata* var. *stellata* and var. *lata*, *A. triquetra*, *Hemiclavator adnatus* and *H. neimongolensis* var. *posticecaptus* and var. *neimongolensis* (Martín-Closas, 1989, 2000; Martín-Closas and Salas, 1994). The charophyte assemblages from the Morella Formation are described for the first time here and characterised as late Barremian in age with the occurrence of *H. neimongolensis* s.s., *A. cruciata* and *P. paucibracteatus* that correspond to the A.

cruciata–P. paucibracteatus biozone of Martín-Closas et al. (2009). This age coincides with the data on ammonite biostratigraphy and geochronological ages derived from strontium isotopes (García et al., 2014; Bover-Arnal et al., 2016), as well as with the palynological biostratigraphic results (Villanueva-Amadoz et al., 2014) obtained from different sections of the Morella Formation in the Maestrat Basin.

5.3. A new evolutionary lineage for the Clavatoraceae

A number of evolutionary lineages of clavatoraceans were defined by Grambast (1974), who understood them as a continuous chronostratigraphic succession of species. Later, Martín-Closas (1989, 1996) described new lineages and redefined them in terms of the evolutionary species concept of Wiley (1981), corresponding to anagenetic change within species, a view that was followed by Schudack (1993). The data obtained from the study of the clavatoracean floras from the Herbers-Mas de Petxí section leads to the description of a new lineage composed of at least two successive anagenetic varieties within the species *Clavator calcitrapus*. The primitive variety, *C. calcitrapus* var. *jiangluoensis* is small and short-bracted with the three shields barely protruding, whereas the younger variety, *C. calcitrapus* var. *calcitrapus*, corresponds to the morphology of the holotype described by Grambast (1969) and has very prominent shields. Intermediate morphotypes have been identified between these two extremes. These two varieties show that the evolutionary trend of *C. calcitrapus* is marked by a progressive increase in length of bract-cell length, producing more prominent shields and larger fructifications over time (Fig. 20).

----------Please insert Figure 20 near here----------

1229 The short biostratigraphic range of *Clavator calcitrapus* combined with its
1230 cosmopolitan palaeobiogeographic distribution render the new anagenetic lineage
1231 potentially useful for biostratigraphic correlation at the intercontinental scale. The
1232 primitive variety, *Clavator calcitrapus* var. *jiangluoensis*, occurred over a large
1233 biogeographic area, including Iberia (Martín-Closas and Grambast-Fessard, 1986;
1234 Schudack, 1993; Martín-Closas, 2000), southern England (Feist et al., 1995), China (Z.
1235 Wang and Lu, 1982) and South America (Musacchio, 1971, 1989, 2000). In contrast, the
1236 more derived anagenetic variety has only been described so far from its type locality in
1237 Herbers (Grambast, 1969 and the present study). This palaeobiogeographic distribution
1238 suggests that this species rapidly reached its cosmopolitan distribution as suggested by
1239 Martín-Closas (2015), but its lastest occurrences were quite suddenly relegated to
1240 Iberia.

1241

1242 **5.4. *Echinochara lazarii–Charaxis spicatus* whole-plant reconstruction**

1243 The abundant and well-preserved utricles of *Echinochara lazarii* analyzed here
1244 permit a redefinition of the utricle structure of this species. The utricle exhibits a
1245 simpler structure than previously thought (Martín-Closas, 2000), with only one unit of
1246 bract-cells (instead of three) in the inner and the outer utricle series alike. The inner
1247 utricle series shows a very small basal cell that is apically trifurcated into three long
1248 cells (Figs. 6D–F, 8). This basal cell-reduction appears to be a common evolutionary
1249 trend in the subfamily Atopocharoidae, as it has previously been described for the
1250 evolutionary species *Globator maillardii* and in *Atopochara trivolvis* (Grambast, 1966a,
1251 1967, 1968, 1974; Martín-Closas, 1996). The occurrence of only one inner and outer
1252 utricle series and their superposition in the abaxial part of the fructification results in a
1253 bilateral utricle symmetry. This is a unique feature within the Atopocharoidae and may

be considered a derived character of the *E. lazarii* utricle, since *E. peckii*, which is older and more plesiomorphic, shows triradial symmetry (Schudack, 1993).

The anatomical connection found in sample H90b between *Echinochara lazarii* fructifications and the thalli known as *Charaxis spicatu*s has permitted a whole-plant reconstruction of *Echinochara* plant. This confirms that the organ-genus *Charaxis* was not a vegetative structure restricted to characeans despite its morphological similitude with extant *Chara*. The association of *C. spicatus* with clavatoraceans was previously hypothesized by Martín-Closas (2000) based on the attachment of this species to non-calcified clavatoracean-like gyrogonites with an apical neck. The data presented here not only confirm this relationship but also define it at species level with new evidence based on anatomically connected organs (Fig. 15). A similar situation but in the opposite direction (i.e. a characean species bearing *Clavatoraxis*, which is a clavatoracean-like thallus) has been documented by Villalba-Breva and Martín-Closas (2011). Taken together these results reinforce the view of Grambast (1962, 1974) that fossil charophyte taxonomy should rely on fructifications rather than vegetative characters.

A study of abundant thin sections of *Charaxis spicatus* from the Herbers-Mas de Petxí section indicated that the cortication of this species is more complex than previously reported by Martín-Closas and Diéguez (1998) and far more complex than in extant species. The term 'double triplostichous cortication' is proposed here for this previously unknown type of cortication (Fig. 14).

5.5. The taxonomy of *Munieria baconica* and its ascription to the Clavatoraceae

The taxonomy of genus *Munieria* and its ascription to the charophytes or to the dasycladales has long been a matter of long debate (e.g. Pia, 1920; Feist et al., 2003). A revision of the taxonomy of species belonging to this genus suggests that the genus probably includes four organ species that can be distinguished by the diameter of the thalli, the morphology of the nodal cells and the morphology of the internode. The specimens of the *Munieria* type of thallus found in the Barremian of the Maestrat Basin are attributed to *M. grambastii*.

Radoičić (1969) proposed an affinity between *Munieria grambastii* and the charophytes, by comparing it with the dasycladalean *Clypeina pejovici* Radoičić, 1969. Fabre-Taxy and Châtelet (1971) observed an anatomical connection between *Munieria* thalli affine to *M. grambastii* and *Clavator brachycerus* (synonym: *Septorella brachycera*) in the Late Cretaceous of Provence. Later, Martín-Closas (2000) showed that the cortication of *M. grambastii* was identical to that of other charophytes, particularly because the cortical cells issuing from adjacent nodes interdigitate in the middle of the internode, which is a structure unknown in dasycladales. Feist et al. (2003) still considered *Munieria* to be dasycladalean and questioned whether of *M. grambastii* belonged to genus *Munieria*. In recent years, additional evidence about the anatomical connection between *Munieria grambastii* and the fructifications of *Clavator brachycerus* and *C. ultimus* has been obtained from the Upper Cretaceous of the Pyrenees (Vicente et al., 2015, 2019). In addition, *Clavator ampullaceus* also shows *Munieria* thalli anatomically connected to fructifications (Grambast and Lorch, 1968, Pl. III, fig. 1b; Granier et al., 2015, Pl. 3, Fig. H), reinforcing the relationship between *Munieria* and *Clavator*.

The present study provides independent microstructural evidence to support the ascription of genus *Munieria* to the Clavatoraceae. Numerous thin sections and sieved

specimens of *M. grambastii* from the Barremian of Herbers-Mas de Petxí show that its internodal cell underwent a centripetal calcification following concentric lamination, which strongly recalls the *Ringstruktur* calcification described by Schudack (1987) in the spiral cells of clavatoroid gyrogonites. The *Ringstruktur* calcification results in the spiral cells of clavatoroid gyrogonites being concentrically calcified to form empty tubes (Fig. 21), whereas in all other charophyte families the spiral cells are filled in by calcite forming eventually a massive tube. In combination with earlier evidence (anatomical connection of *M. grambastii* to *Clavator* and the interdigitation of cortical cells in the centre of the internode), this new evidence further supports the proposal that organ genus *Munieria* belong to charophytes and it particular to Clavatoroidae.

----------Please insert Figure 21 near here----------

Vicente et al. (2019) observed that *Munieria* from the Upper Cretaceous of the Pyrenees always occurs in recrystallized form, suggesting that the original mineralogy was aragonite instead of low-magnesium calcite. However, non-recrystallized *Munieria* from the Barremian of the Maestrat preserving the original calcification pattern of internodal cells suggests that its biomineralization would include both aragonite and calcite. By way of comparison, Anadón et al. (2002) observed that both aragonite and calcite biomineralization occurs in extant charophytes and is strongly controlled by hydrological parameters (temperature, Mg/Ca content and conductivity), and may also be species-specific. In contrast, the dasycladalean calcification is mostly aragonitic, with rare calcitic exceptions (Granier, 2012) and experiments about the influence of the Mg/Ca ratio on the calcification of dasycladales suggest that the hydrological

parameters have limited influence over the dasycladalean mineralogy (Ries, 2006; Stanley et al. 2010).

6. Conclusions

Twenty-nine clavatoracean taxa (including thalli and utricles) are described from the Barremian of the Herbers-Mas de Petxí section (northern Maestrat Basin). Such clavatoracean species richness has not been previously reported from any other locality worldwide. This shows that Iberia, which represented the westernmost island of the Tethyan Cretaceous Archipelago, and particularly the Iberian Chain, was a hotspot for clavatoracean diversity worldwide.

The charophyte assemblages studied in the northern Maestrat Basin belong to two European charophyte biozones encompassing the entire Barremian. The lower Barremian clavatoracean assemblages from the Cantaperdius Formation were already known, but the results obtained provide significant new data for the biostratigraphic correlation at an intercontinental scale, with the definition of the new *Clavator calcitrapus* evolutionary lineage. The clavatoracean assemblages from the upper Barremian dinosaur-bearing Morella Formation were previously unknown. They are formed by two European biozone index species, *Ascidiella cruciata* and *Pseudoglobator paucibracteatus,* along with two subcosmopolitan species, *Clavator grovesii* var. *jiuquanensis* and *Hemiclavator neimongolensis* var. *neimongolensis*, which allow for biostratigraphical correlations with distant floras, such as those from China.

The new utricle structure of *Echinochara lazarii* challenges the present view on the evolution of genus *Echinochara*. The more derived bilateral symmetry observed in the Barremian utricle of *Echinochara lazarii* contrasts with the triradial utricle symmetry of the more plesiomorphic Kimmeridgian–Tithonian *Echinochara peckii*. The

finding of new records to fill in the relatively long gap (Berriasian–Hauterivian) in the fossil record of this genus is essential to understand the evolutionary processes that occurred between the two species.

The present study shows that the vegetative structure of the clavatoraceans is far more complex than previously known. In the case of *Charaxis spicatus*, which is the thallus of the *Echinochara* plant, the cortication corresponds to a new type, which here has been called here "double triplostichous cortication". This cortication appears to be unique to the clavatoraceans, and particularly to genus *Echinochara*, showing that this extinct family developed a high number of unique characters. In the case of *Munieria grambastii* a previously unknown calcification pattern of the internodal cell has been described. This cell biomineralized following a pattern similar to the *Ringstruktur*-calcification of clavatoroid gyrogonites, supporting the ascription of *Munieria* to the Charophyta, and specifically to the clavatoraceans (genus *Clavator*). This type of calcification again shows that this fossil family developed unique calcifying mechanisms that were different from those of the other charophyte families.

Acknowledgements

The present study is a contribution to the projects BIOGEOEVENTS (CGL2015-69805-P) of the Spanish Ministry of Economy and Competitiveness and the European Regional Development Fund (ERDF) and 2017SGR-824 of AGAUR (Catalan Research Agency). The research was also supported by predoctoral grant BES-2016-076469 from the Spanish Ministry of Economy and Competitiveness to JP-C and grant SYNTHESYS HU-TAF6533 from the European Union to CM-C. We are very grateful for productive discussions with Dr. Pere Anadón (Institut de Ciències de la Terra Jaume Almera–Spanish Research Council) and Dr. Jaume Cambra (University of Barcelona). We thank

Dr. Alejandro Gallardo (UB) for his technical support in the preparation of thin sections and Ivan Montllor for his support in the graphic presentation of the results. We are indebted to Bruno Granier (University of Brest), Josep Sanjuan (American University of Beirut) and the editor Eduardo Koutsoukos for greatly improving the manuscript during the peer review process. The English text was corrected by Dr. Christopher Evans (Fundació Bosch i Gimpera, Universitat de Barcelona).

References

Agardh, C.A., 1824. Systema Algarum. Lundae Literis Berlingianis, Lund, 1–312.

Anadón, P., Utrilla, R., Vázquez, A., 2002. Mineralogy and Sr–Mg geochemistry of charophyte carbonates: a new tool for paleolimnological research. Earth and Planetary Science Letters 197(3-4), 205–214.

Andreu, B., Canérot, J., Charrière, A., Feist, M., 1988. Mise en évidence du Wealdien (Barrémien) dans le Moyen-Atlas (région de Boulmane, Maroc). C.R. Acad. Sci. Paris Sér. II 307, 2069–2075.

Avram, E., Szasz, L., Antonescu, E., Baltres, A., Iva, M., Melinte, M., Neagu, T., Rădan, S., Tomescu, C., 1993. Cretaceous terrestrial and shallow marine deposits in northern South Dobrogea (SE Romania). Cretaceous Research 14, 265–305.

Benoit, R. A., Néraudeau, D., Martín-Closas, C., 2017. A review of the Late Jurassic–Early Cretaceous charophytes from the northern Aquitaine Basin in south-west France. Cretaceous Research 79, 199–213.

1398 Bover-Arnal, T., Salas, R., Moreno-Bedmar, J.A., Bitzer, K., 2009. Sequence
1399 stratigraphy and architecture of a late Early-Middle Aptian carbonate platform
1400 succession from the western Maestrat Basin (Iberian Chain, Spain). Sedimentary
1401 Geology 219, 280–301.

1402 Bover-Arnal, T., Moreno-Bedmar, J.A., Salas, R., Skelton, P.W., Bitzer, K. Gili,
1403 E., 2010. Sedimentary evolution of an Aptian syn-rift carbonate system (Maestrat
1404 Basin, E Spain): effects of accommodation and environmental change, Geologica
1405 Acta 8(3), 249–280.

1406 Bover-Arnal, T., Moreno-Bedmar, J.A., Frijia, G., Pascual-Cebrian, E., Salas,
1407 R., 2016. Chronostratigraphy of the Barremian–Early Albian of the Maestrat Basin
1408 (E Iberian Peninsula): integrating strontium-isotope stratigraphy and ammonoid
1409 biostratigraphy. Newsletters on Stratigraphy 49(1), 41–68.

1410 Bystrický, J., 1976. *Munieria grambasti* sp. nov. in Kalk Gerölle des Upolav-
1411 Konglomerate des Mittleren Váh-Gebietes (Klippenzone, Westkarpaten). Geologica
1412 Carpathica 27(1), 45–64.

1413 Canérot, J., 1974. Recherches géologiques aux confins des chaînes ibérique et
1414 catalane (Espagne). Ph.D. Thesis Univ.Toulouse, 517 pp.

1415 Canérot, J., Leyva, F., 1976. Mapa Geológico de España, E.1:50.000 nº 520
1416 (Peñarroya de Tanstavins). Segunda serie (MAGNA). IGME, Madrid.

1417 Canérot, J., Cugny, P., Pardo, G., Salas, R., Villena, J., 1982. Ibérica central-
1418 Maestrazgo. García, A. (Ed.), El Cretácico de España. Universidad Complutense de
1419 Madrid, 273–344.

Carozzi, A., 1946. Sur quelques Dasycladacées du Purbeckien du Jura. Comptes Rendus des Séances de la Société de Physique et d'Histoire Naturelle de Genève 63(1), 24–26.

Cherchi, A., Gušić, I., Schmidt, M., Schroeder, R., 1981. Lacustrine Middle Cretaceous with *Munieria grambasti sarda* n. ssp. (Charophyta?) of Alghero (NW Sardinia). Revue de Micropaléontologie 23, 138–150.

Combes, P.J., 1969. Recherches sur la genèse des bauxites dans le nord-est de l'Espagne, le Languedoc et l'Ariège (France). Mémoires du Centre d'Études et de Recherches Géologiques et Hydrogéologiques 3–4, 335 pp.

Császár G., Bodrogi I., 1983. Munieriák a Magyarországi Krétában [*Munieria* in the Cretaceous of Hungary]. Magyar Állami Földtani Intézet Évi Jelentése, Budapest, Évröl p. 167-212.

Deecke, W., 1883. Über einige neue Siphoneen. Neues Jahrbuch für Mineralogie. Geologie und Paläontologie 1, 1–14.

Fabre-Taxy, S., Châtelet, H., 1971. Précisions paléontologiques sur les algues *Munieria* Deecke et *Septorella* Grambast. Comptes Rendus des Séances de l'Académie des Sciences Série D 272, 3021–3023.

Feist, M., 1981. Charophytes du Crétacé moyen et données nouvelles sur l'évolution des Clavatoracées. Cretaceous Research 2(3-4), 319–330.

Feist, M., Brouwers, E.M., 1990. A new *Tolypella* from the Ocean Point dinosaur locality, North Slope, Alaska and the Late Creteceous to Paleocene nitelloid charophytes. US Geological Survey Bulletin 1990-F, 1–7.

1442 Feist, M., Génot, P., Grambast-Fessard, N., 2003. Ancient Dasycladales and
1443 Charophyta convergences and differences with special attention to *Munieria*
1444 *baconica*. Phycologia 42(2), 123–132.

1445 Feist, M., Lake, R.D., Wood, C.J., 1995. Charophyte biostratigraphy of the
1446 Purbeck and Wealden of Southern England .Palaeontology 38, 407–442.

1447 Feist, M., Charriere, A., Haddoumi, H., 1999. Découverte de charophytes
1448 aptiennes dans les couches rouges continentales du Haut-Atlas oriental (Maroc).
1449 Bulletin de la Société géologique de France 170, 611–618.

1450 Feist, M., Grambast-Fessard, N., Guerlesquin, M., Karol, K., Lu, H., Mccourt,
1451 R.M., Wang, Q., Shenzen, Z., 2005. Treatise on Invertebrate Paleontology. Part B,
1452 Protoctista 1. Volume 1: Charophyta. The Geological Society of America, Bourlde,
1453 Colorado and Lawrence, Kansas, 167 pp.

1454 Gámez, D., Paciotti, P., Colombo Piñol, F., Salas, R., 2003. La Formación
1455 Arcillas de Morella (Aptiense inferior), Cadena Ibérica oriental (España):
1456 caracterización sedimentológica. Geogaceta 34, 191–194.

1457 García, R., Moreno-Bedmar, J.A., Bover-Arnal, T., Salas, R., Latil, J.L.,
1458 Martín-Martín, J.D., Gómez-Rivas, E., Bulot, L.G., Delanoy, G., Martínez, R.,
1459 Grauges, A., 2014. Lower Cretaceous (Hauterivian-Albian) ammonite
1460 biostratigraphy in the Maestrat Basin (E Spain). Journal of Iberian Geology 40(1),
1461 99–112.

1462 García-Cortés, A., Ortiz, J.E., Mansilla, H., Torres, T., 1995. Precisiones sobre
1463 la bioestratigrafía de las Clavatoráceas del Valanginiense de la Sierra del Pozo
1464 (Provincia de Jaén, SE de España). Geogaceta 18, 121–124.

1465 Grambast, L., 1959. Tendances évolutives dans le phylum des Charophytes.
1466 C.R. Acad. Sci. Paris 249, 557–559.

1467 Grambast, L., 1962. Classification de l'embranchement des charophytes.
1468 Naturalia Monspeliensia, Série Botanique 14, 63–86.

1469 Grambast, L., 1966a. Un nouveau type structural chez les Clavatoracées, son
1470 intérêt phylogénetique et stratigraphique. C.R. Acad. Sci. Paris D 262, 1929–1932.

1471 Grambast, L., 1966b. Structure de l'utricule et phylogénie chez les
1472 Clavatoracées. C.R. Acad. Sci. Paris 262, 2207–2210.

1473 Grambast, L., 1967. La série évolutive *Perimneste-Atopochara* (Charophytes).
1474 C.R. Acad. Sci. Paris 264, 581–584.

1475 Grambast, L., 1968. Evolution of the utricle in the charophyta genera
1476 *Perimneste* Harris and *Atopochara* Peck. Journal of the Linnean Society (Botany) 61,
1477 5–11.

1478 Grambast, L., 1969. La symétrie de l'utricule chez les Clavatoracées et sa
1479 signification phylogénétique. C.R. Acad. Sci. Paris 269, 878–881.

1480 Grambast, L., 1970. Origine et évolution des *Clypeator* (Charophytes). C.R.
1481 Acad. Sci. Paris 271, 1964–1967.

1482 Grambast, L., 1974. Phylogeny of the Charophyta. Taxon 23, 463–481.

1483 Grambast, L., Lorch, J., 1968. Une flore de Charophytes du Crétacé inférieur
1484 du Proche Orient. Naturalia Monspeliensis (Série Botanique) 19, 47–56.

1485 Grambast-Fessard, N., 1980a. Quelques espèces de *Cypeator* Grambast
1486 (Clavatoraceae) et les charophytes associées du Crétacé inférieur du Portugal. Revue
1487 de Micropaléontologie 23, 37–47.

1488 Grambast-Fessard, N., 1980b. Description de deux espèces nouvelles
1489 d'*Atopochara* Peck (Clavatoraceae, Charophyta). Geobios 13, 129–135.

1490 Grambast-Fessard, N., 1986. Deux nouveaux représentats du genre *Ascidiella*
1491 (Clavatoraceae, Charophyta). Geobios 19, 255–260.

1492 Granier, B., 2012. The contribution of calcareous Green algae to the production
1493 of limestones: a review. Geodiversitas 34, 35–60.

1494 Granier, B., Clavel, B. 2019. Revised dating of the major earliest Cretaceous
1495 transgression in S Aquitaine (SW France). Cretaceous Research 99, 246-254.

1496 Granier, B., Azar, D., Maksoud, S., Gèze, R., Habchi, R., 2015. New
1497 fossiliferous sites with Barremian Charophyta in the" Grès du Liban" auct.
1498 (Lebanon), with a critical perspective regarding the nature of *Munieria* Deecke,
1499 1883. Carnets de Géologie 15(15), 199–229.

1500 Guimerà**,** J., 2018. Structure of an intraplate fold-and-thrust belt: The Iberian
1501 Chain. A synthesis. Geologica Acta 16, 427–438.

1502 Haddoumi, H., Charrière, A., Feist, M., Baidder, L., Ferrière, J., Karim, M.,
1503 Ettachfini, E. M., Mamoun, S.M., Chennouf, R., Rachdi, A., Adardor, S., 2019. A
1504 Barremian-? Aptian Tethyan precursor of the Cretaceous marine flooding of
1505 Morocco: Evidence from the red-bed series within the “Marginal Folds” of the
1506 eastern High Atlas. Cretaceous Research 95, 37–60.

1507 Harris, T.M., 1939. British Purbeck Charophyta. British Museum (Natural
1508 History). London, 1–83.

1509 Hu, J., Zeng, D., 1981. Early Cretaceous Charophytes from Hengyang Basin,
1510 Hunan. First Convention of the Micropaleontological Society of China 1979. Science
1511 Press, Beijing, 144–151. (in Chinese).

1512 Kubota, K., 2005. Charophyte gyrogonites from the Lower Cretaceous
1513 Kitadani Formation of the Tetori Group in the Takinamigawa area, Katsuyama City,
1514 Fukui Prefecture, central Japan. Paleontological Research 9(2), 203–213.

1515 Lindley, J., 1836. A natural system of Botany, second ed. Longman, London,
1516 526 pp.

1517 Luger, P., Schudack, M., 2001. On Early Cretaceous (earliest Aptian)
1518 freshwater Charophyta and Ostracoda from Northern Somalia. Neues Jahrbuch für
1519 Geologie und Paläontologie-Abhandlungen 220(2), 245–266.

1520 Mädler, K., 1952. Charophyten aus dem Nordwestdeutschen Kimmeridge,
1521 Geologisches Jahrbuch 67, 1–46.

1522 Maksoud S., Granier B., Gèze R., Alméras Y., Toland C., Dany Azar D., 2020.
1523 The Jurassic/Cretaceous boundary in Lebanon. Revision of the Salima Formation. In:
1524 Granier, B. (ed.), VSI: The transition of the Jurassic to the Cretaceous: an early
1525 XXIth century holistic approach. Cretaceous Research 107, article 104268, 8 p.

1526 Martín-Chivelet, J., López-Gómez, J., Aguado, R., Arias, C., Arribas, J.,
1527 Arribas, M.E., Aurell, M., Bádenas, B., Benito, M.I., Bover-Arnal, T., Casas-Sainz,
1528 A., Castro, J.M., Coruña, F., de Gea, G.A., Fornós, J.J., Fregenal-Martínez, M.,
1529 García-Senz, J., Garófano, D., Gelabert, B., Giménez, J., González-Acebrón, J.,

Guimerà, J., Liesa, C.L., Mas, R., Meléndez, N., Molina, J.M., Muñoz, J.A., Navarrete, R., Nebot, M., Nieto, L.M., Omodeo-Salé, S., Pedrera, A., Peropadre, C., Quijada, I.E., Quijano, M.L., Reolid, M., Robador, A., Rodríguez-López, J.P., Rodríguez-Perea, A., Rosales, I., Ruiz-Ortiz, P.A., Sàbat, F., Salas, R., Soria, A.R., Suárez-González, P., Vilas, L., 2019. The Late Jurassic–Early Cretaceous Rifting. In: Quesada, C., Oliveira, J.T. (eds.), The Geology of Iberia: A Geodynamic Approach. Volume 5: The Alpine Cycle. Springer, Heidelberg, 169–249.

Martín-Closas, C., 1988. Découverte de la plaque basale chez les Clavatoraceae (Charophyta). Implications phylogénétiques. C.R. Acad. Sci. Paris 306, II Série, 1131–1136.

Martín-Closas, C. 1989. Els caròfits del Cretaci inferior de les conques perifèriques del Bloc de l'Ebre, PhD thesis, Universitat de Barcelona. Barcelona. 608 pp.

Martín-Closas, C., 1996. A phylogenetic system of Clavatoraceae (Charophyta). Review of Palaeobotany and Palynology 94, 259–293.

Martín-Closas, C., 2000. Els caròfits del Juràssic superior i Cretaci inferior de la Península Ibèrica. Arxius de les Seccions de Ciències. Institut d'Estudis Catalans, 125, Barcelona, 304 pp.

Martín-Closas, C., 2015. Cosmopolitanism in Norhern Hemisphere Cretaceous Charophyta (Clavatoroidae). Palaeogeography, Palaeoclimatology, Palaeoecology 438, 9–23.

Martín-Closas, C., Alonso-Millán, A., 1998. Estratigrafía y bioestratigrafía (Charophyta) del Cretácico inferior en el sector occidental de la Cuenca de Cameros (Cordillera Ibérica). Revista de la Sociedad Geológica de España 11, 253–269.

1554 Martín-Closas, C., Diéguez, C., 1998: Charophytes from the Lower Cretaceous
1555 of the Iberian Ranges (Spain). Palaeontology 41, 1133–1152.

1556 Martín-Closas, C., Grambast-Fessard, N., 1986. Les charophytes du Crétacé
1557 inférieur de la région du Maestrat (Chaîne Ibérique, Catalanides, Espagne),
1558 Paléobiologie Continentale 15, 1–66.

1559 Martín-Closas, C., López-Morón, N., 1996. The lower Cretaceous charophyte
1560 flora from El Montsec (Catalonia, Spain). Fanló (Ed.), El patrimoni natural del
1561 Montsec. Institut d'Estudis Ilerdencs, Lleida, Spain, 9–19.

1562 Martín-Closas, C., Peybernés, B., 1987. Contribution à la datation de la
1563 transgression eocrétacée dans les Pyrénées Basco-Béarnaises à l'aide des
1564 charophytes. Geobios 20, 695–700.

1565 Martín-Closas, C., alas, R., 1994. Lower Cretaceous Charophytes.
1566 Biostratigraphy and evolution in the Maestrat Basin (Eastern Iberian Ranges). VIII
1567 Meeting of the European group of Charophyte Specialists Fieldtrip Guidebook,
1568 Diagonal, Barcelona, 89 pp.

1569 Martín-Closas, C., Salas, R., 1998. Lower Cretaceous charophyte biozonation
1570 in the Maestrat Basin (Iberian Ranges, Spain). A reply to P.O. Mojon. Géologie
1571 Alpine 74, 97–110.

1572 Martín-Closas, C., Schudack, M.E., 1991. Phylogenetic analysis and
1573 systematisation of post-palaeozoic charophytes. Revue de la Société Botanique de
1574 France 138, Actualités Botaniques 1, 53–71.

Martín-Closas, C., Wang, Q., 2008. Historical biogeography of the lineage *Atopochara trivolvis* Peck1941 (Cretaceous Charophyta). Palaeogeography Palaeoclimatology Palaeoecology 260, 435–451.

Martín-Closas, C., Clavel, B., Charollais, J., Conrad, M.A., 2009. Charophytes from the Barremian-lower Aptian of the Northern Subalpine Chains and Jura Mountains, France: correlation with associated marine assemblages. Cretaceous Research 30, 49–62.

Martín-Closas, C., Vicente, A., Pérez-Cano, J., Sanjuan, J., Bover-Arnal, T., 2018. On the earliest occurrence of *Tolypella* section *Tolypella* in the fossil record and the age of major clades in extant Characeae. Botany Letters 165(1), 23–33.

Migula, W., 1897. Die Characeen Deutschlands. Österreichs und der Schweiz, in: Rabenhorst, X. (Ed.), Kryptogamic Flora, vol. 5, E. Kummer, Leipzig, 765 pp.

Mojon, P.O., 1988. Les dépôts émersifs des faciès urgoniens (Hauterivien supérieur-Aptien inférieur) dans le Jura Méridional (Ain, France) et les Chaînes subalpines septentrionales (Haute-Savoie, Savoie et Isère, France). Archives des Sciences, Genève, 41, 409–417.

Mojon, P.O., 1996. Précisions sur l'intervalle Valanginien-Barrémien de la biozonation des Charophytes du Crétacé inférieur du Maestrazgo (Chaîne Ibérique Orientale, Espagne) et sur la biozonation des Charophytes de l'intervalle Jurassique supérieur-Crétacé de l'Europe occidentale. Géologie Alpine 72, 61–99.

Mojon, P.O., 2003. Précisions sur les dépôts émersifs de l'Urgonien jurassien et subalpine: réponse à Clavel et al. (2002). Revue de Paléobiologie 22(1), 457–459.

1597 Mojon, P.O., Haddoumi, H., Charrière, A., 2009. Nouvelles données sur les
1598 charophytes et ostracodes du Jurassique moyen–supérieur — Crétacé inférieur de
1599 l'Atlas marocain. Carnets de Géologie (CG2009/M03) 9(M03), 1–39.

1600 Moreno-Bedmar, J.A., Company, M., Bover-Arnal, T., Salas, R., Delanoy, G.,
1601 Martínez, R., Grauges, A., 2009. Biostratigraphic characterization by means of
1602 ammonoids of the lower Aptian Oceanic Anoxic Event (OAE1a) in the eastern
1603 Iberian Chain (Maestrat Basin, eastern Spain). Cretaceous Research 30, 864–872.

1604 Moreno-Bedmar, J.A., Company, M., Bover-Arnal, T., Salas, R., Maurrasse,
1605 F.J., Delanoy, G., Grauges, A., Martínez, R., 2010. Lower Aptian ammonite
1606 biostratigraphy in the Maestrat Basin (Eastern Iberian Chain, Eastern Spain). A
1607 Tethyan transgressive record enhanced by synrift subsidence. Geologica Acta 8, 281–
1608 299.

1609 Musacchio, E.A., 1971. Charophytas de la formación La Amarga (Cretácico
1610 inferior), Provincia de Neuquén, Argentina. Revista del Museo de La Plata. 4, 19–38.

1611 Musacchio, E.A., 1989. Biostratigraphy of non-marine Cretaceous of Argentina
1612 based on Calcareous microfossils. In: Wiedmann, J. (ed.), Cretaceous of the Western
1613 Tethys, Proceedings of the 3rd International Cretaceous Symposium, Tübingen 1987.
1614 E. Schweizerbart'sche Verlagsbuchhandlung, Stuttgart, pp. 811–850.

1615 Musacchio, E.A., 2000. Biostratigraphy and biogeography of Cretaceous
1616 Charophytes from South America. Cretaceous Research 21, 211–220.

1617 Neagu, T., Georgescu-Donos, M.O., 1973. Characeae Eocretacice die
1618 Dobrogea de Sud (Valea Akargea-Pestera). Studii si cercetari de geologie, geofiziece
1619 si geografie 18, 171–185 (in Romanian).

1620 Peck, R.E., 1937. Morrison Charophyta from Wyoming. Journal of
1621 Paleontology 11, 83–90.

1622 Peck, R.E., 1938. A new family of Charophyta from the Lower Cretaceous of
1623 Texas. Journal of Paleontology 12, 285–304.

1624 Peck, R.E., 1941. Lower Cretaceous Rocky Mountain nonmarine microfossils.
1625 Journal of Paleontology 15, 285–304.

1626 Peck, R. E., 1957. North American Charophyta. Geological Survey
1627 Professional Paper 294A, 1–44.

1628 Pereira, R.,Cabral, M.C., 2005. Charophytes from the lower Aptian of Rio de
1629 Mouro (Lisbon region, Portugal). Revista Española de Paleontología 37, 171–181.

1630 Pia J. von (1920). Die Siphoneae verticillatae vom Karbon bis zur Kreide.
1631 Abhandlungen der zoologisch-botanischen Gesellschaft in Wien, Band XI, Heft 2,
1632 263 pp.

1633 Pia, J., 1927. Charophyta, in: Hirmer, M. (Ed.), Handbuch der Paläobotanik,
1634 vol. 1. R. Oldenbourg Druck und Verlag, Munich-Berlin, 88-93.

1635 Radoičić, R., 1969. A new Lower Cretaceous Dasycladacea: *Clypeina pejovici*,
1636 and note on some Clypeinae. Geologica Romana 14, 71–84.

1637 Rásky, K., 1945. Fossile Charophyten-Früchte aus Ungarn. Verlag des
1638 Ungarischen Naturwissenschaftlichen Museums, Budapest, 61 pp.

1639 Reid, C., Groves, J., 1916. Preliminary report on the Purbeck Characeae.
1640 Proceedings of the Royal Society B 89, 252–256.

Rey, J., Ramalho, M., 1973-74. Le Crétacé inférieur de l'Algarve occidental (Portugal). Comunicaçoes dos Serviços Geologicos de Portugal 57, 155–181.

Ries, J.B., 2006. Aragonitic algae in calcite seas: efect of seawater Mg/Ca ratio on algal sediment production. Journal of Sedimentary Petrology 76, 515–523.

Riveline, J, Berger J.P., Bilan W, Feist, M., Martín-Closas, C., Schudack, M., Soulié-Märsche, I., 1996. European Mesozoic-Cenzoic Charophyte Biozonation. Bulletin Société Géologique de France 167, 453–468.

Salas, R., 1987. El Malm i el Cretaci inferior entre el Massís de Garraf i la Serra d'Espadà. Anàlisi de Conca. Ph.D. thesis. Universitat de Barcelona, Barcelona. 345 pp.

Salas, R., Casas, A., 1993. Mesozoic extensional tectonics, stratigraphy and crustal evolution during the Alpine Cycle of the astern Iberian Basin. Tectonophysics 228, 33–55.

Salas, R., Guimerà, J., Mas, R., Martín-Closas, C., Melèndez, A., Alonso, A., 2001. Evolution of the Mesozoic Central Iberian Rift System and its Cainozoic inversion (Iberian Chain). In: Ziegler, P.A., Cavazza, W., Roberston, A.H.F., Crasquin-Soleau, S. (eds.), Peri-Tethys Memoir 6: Peri-Tethyan Rift/Wrench Basins and Passive Margins. Mémoires du Muséum National d'Histoire Naturelle, Paris, pp. 145–186.

Saporta, M., 1891. Plantes jurassiques. In: Description des fossiles de la France, vol. IV, Masson Ed., Paris, 498–500.

1662 Schudack, M.E., 1987. Charophytenflora und fazielle Entwicklung der
1663 Grenzschichten mariner Jura/Wealden in den Nordwestlichen Iberischen Ketten (mit
1664 Vergleichenzu Asturien und Kantabrien). Palaeontographica Abteilung B 204, 1–108.

1665 Schudack, M.E., 1989. Charophyten floren aus den unterkretazischen
1666 Vertebraten-Fundschichten bei Galve und Uña (Östpanien). Berliner
1667 geowissenschaftliche Abhandlungen A 106, 409–443.

1668 Schudack, M.E., 1993.: Die Charophyten im Oberjura und Unterkreide
1669 Westeuropas. Mit einer phylogenetischen Analyse der Gesamtgruppe. Berl. Geowiss.
1670 Abh. (A). 8, 1–209.

1671 Shaikin, I.M., 1967. Fossil Charophyta of Upper Jurassic deposits of Dniepr-
1672 Donets depression, in: Fossi Algae of the USSR. IZDAT Nauk SSSR., 43–47. (in
1673 Russian).

1674 Shaikin, I., Kisielevsky, F., Vacula, L., 1992. Correlation of nonmarine Lower
1675 Cretaceous deposits of the South European part of the former USSR on the basis of
1676 Charophyta. Cretaceous Research 13, 331–336.

1677 Smith, G.M., 1938. Botany, vol. I, Algae and Fungi. Charophyceae. McGraw
1678 Hill 1, New York, 127 pp.

1679 Soria, A.R., Martín-Closas, C., Meléndez, A., Meléndez, M.N., Aurell, M.,
1680 1995. Estratigrafía del Cretácico Inferior continental de la Cordillera Ibérica Central.
1681 Estudios Geológicos 51, 141–152.

1682 Soulié-Märsche, I., 1994. The paleoecological implications of the charophyte
1683 flora of the Trinity Division, Junction, Texas. Journal of Paleontology 68, 1145-1157.

Stanley S.M., Ries J.B., Hardie L.A., 2010. Increasing production of calcite and slower growth for the major sediment-producing alga *Halimeda* as the Mg/Ca ratio of seawater is lowered to a "calcite sea" level. Journal of Sedimentary Research 80, 6–16.

Trabelsi, K., Soussi, M., Touir, J., Houla, J., Abbes, C., Martin-Closas, C., 2016. Charophyte biostratigraphy of the non-marine Lower Cretaceous in the Central Tunisian Atlas (North Africa): Palaeobiogeographic implications. Cretaceous Research 67, 66–83.

Tugend, J., Manatschal, G., Kusznir, N. J., 2015. Spatial and temporal evolution of hyperextended rift systems: Implication for the nature, kinematics, and timing of the Iberian-European plate boundary. Geology 43(1), 15–18.

Turland, NJ., Wiersema, J.H., Barrie, F.R., Greuter, W., Hawksworth, D.L., Herendeen, P.S., Knapp, S., Kusber, W.H., Li, D.Z., Marhold, K., May, T.W., McNeill, J., Monro, A.M., Prado, J., Price, M.J. Smith, G F. (eds.) 2018: International Code of Nomenclature for algae, fungi, and plants (Shenzhen Code) adopted by the Nineteenth International Botanical Congress Shenzhen, China, July 2017. Regnum Vegetabile 159. Glashütten: Koeltz Botanical Books.

Veltz, I., 2008. Le passage Jurassique-Crétacé au Liban. PhD Thesis. Université de Reims Champagne Ardenne, 279 pp.

Vicente, A., Martín-Closas, C., 2013. Lower Cretaceous charophytes from the Serranía de Cuenca, Iberian chain: Taxonomy, biostratigraphy and palaeoecology. Cretaceous Research 40, 227–242.

Vicente, A., Martín-Closas, C., Arz, J. A., Oms, O., 2015. Maastrichtian– basal Paleocene charophyte biozonation and its calibration to the Global Polarity Time Scale in the southern Pyrenees (Catalonia, Spain). Cretaceous Research 52, 268–285.

Vicente, A., Csiki-Sava, Z., Martín-Closas, C., 2019. European charophyte evolution across the Cretaceous–Palaeogene boundary. Palaeogeography, Palaeoclimatology, Palaeoecology 533, 109228.

Villalba-Breva, S., Martín-Closas, C., 2011. A characean thallus with attached gyrogonites and associated fossil charophytes from the Maastrichtian of the Eastern Pyrenees (Catalonia, Spain). Journal of Phycology 47, 131–143.

Villanueva-Amadoz, U., Santisteban, C., Santos-Cubedo, A., 2014. Age determination of the Arcillas de Morella Formation (Maestrazgo Basin, Spain). Historical Biology 27, 389–397.

Wang, S., 1965. Mesozoic and Tertiary Charophyta from Jinquan basin of Kansu province. Acta Palaeontologica Sinica 13, 485–499.

Wang, Z., Lu, H.N., 1982. Classification and evolution of Clavatoraceae with notes on its distribution in China. Bulletin Nanjing Institute of Geology and Paleontology. Academia Sinica 4, 77–104 (in Chinese).

Wiley, E.O., 1981. Phylogenetics. John Wiley and Sons, New York, 439 pp.

Figure captions

Figure 1. A) Location of the Maestrat Basin. Scale bar = 300 km. B) Tectonic map of the study area showing the internal compartmentalisation of the Maestrat and Garraf basins into subbasins (modified from Salas et al. in Martín-Chivelet et al., 2019). The numbers of the legend indicate the thickness of the rifting deposits. CB: Cedramán Sub-basin; GB: Galve Sub-basin; LPB: Las Parras Sub-basin; MB: Morella sub-basin; Mt: El Montmell Sub-basin; OB: Oliete Sub-basin; OrB: Orpesa Sub-basin; PB: Penyagolosa Sub-basin; SB: Salzedella Sub-basin; SgB: Sitges Sub-basin; VB: El Vendrell Sub-basin. Scale bar = 50 km. C) Geological sketch of the Herbers area and location of the sampled section (geological map modified from Canérot and Leyva, 1976). Scale bar = 500 m.

Figure 2. Lithostratigraphic framework of the uppermost Jurassic-Lower Cretaceous record of the Morella sub-basin (lithostratigraphy from Salas et al., 2001; Bover-Arnal et al., 2016).

Figure 3. Stratigraphic section of the lower part of the Herbers-Mas de Petxí section with location of samples and distribution of charophyte species. Samples in bold correspond to studied thin sections. Charophyte biozonation according to Riveline et al. (1996) and Martín-Closas et al. (2009).

Figure 3 (continuation). Legend for Figures 3 and 4.

Figure 4. Stratigraphic section of the upper part of the Herbers-Mas de Petxí section with location of samples and distribution of charophyte species. Samples in bold correspond to studied thin sections. Charophyte biozonation according to Riveline et al. (1996) and Martín-Closas et al. (2009). See Fig 3B for legend

Figure 5. Porocharacean and characean gyrogonites. A–C) *Porochara maestratica* (sample H8). A) Lateral view (specimen no. 85579 MGSCB), B) Apical view (specimen no. 85580 MGSCB), C) Basal view (specimen no. 85581 MGSCB). D–F) *Aclistochara sp*. (sample H37). D) Lateral view (specimen no. 85582MGSCB), E) Apical view (specimen no. 85583MGSCB), F) Basal view (specimen no. 85584 MGSCB). G–I) aff. *Mesochara harrisii* (sample H39). G) Lateral view (specimen no. 85585 MGSCB), H) Apical view (specimen no. 85586 MGSCB), I) Basal view (specimen no. 85587 MGSCB). Scale bar = 200 μm.

Figure 6. *Echinochara lazarii* (Martín-Closas, 2000) nov. comb. utricles A–B) external cast of the gyrogonite. A) Sample H94 (specimen no. 85588 MGSCB) and B) Sample H95 (specimen no. 85589 MGSCB), C) Internal cast of gyrogonite attached to the utricle. The arrow indicates the apical neck of gyrogonite (Sample H95, specimen no. 85590 MGSCB), D) Inner series of utricle (specimen no. Sample H128b MGSCB). Arrow indicates the small rounded basal cell of the inner utricle series (specimen no. 85591 MGSCB), E) Inner series of utricle (Sample H94). Thin arrows indicate cells belonging to the outer utricle series. Wide arrow indicates the basal cell of the inner utricle series (specimen no. 85592 MGSCB), F) Two neighbouring utricles of the same fertile whorl, showing inner utricle series (Sample H94; specimen no. 85593 MGSCB), G) Two external casts of neighbouring gyrogonites from the same fertile whorl (Sample H53; specimen no. 85594 MGSCB), H) Outer utricle series with concave cell calcification (Sample H88; specimen no. 85595 MGSCB), I) Outer utricle series with completely calcified bracts (Sample H128a; specimen no. 85596 MGSCB), J) Complete fertile whorl showing outer utricle series (Sample H41; specimen no. 85597 MGSCB), K) Complete fertile whorl showing inner utricle series (Sample H94; specimen no. 85598 MGSCB), L) Two superimposed fertile whorls (Sample H41; specimen no.

85599 MGSCB), M) Two internal gyrogonite casts of two superposed fertile whorls (Sample H88; specimen no. 85600 MGSCB), N) Outer series with partially calcified bracts (sample H88; specimen no. 85601 MGSCB). Scale bar = 500 μm.

Figure 7. Thin sections of *Echinochara lazarii* (Martín-Closas, 2000) nov. comb. utricles and gyrogonites. A) Longitudinal section of two utricles.The external cast of gyrogonites shows prolate gyrogonites with basal and apical necks (sample H90; thin section no. 85675 MGSCB), B) Transversal section of fertile whorl showing superimposition of inner and outer utricle series, the inner series is represented by the larger cells (sample H90; thin section no. 85674 MGSCB), C) Transversal section of a complete fertile whorl, showing 6 utricles (sample H90; thin section no. 85675 MGSCB). Scale bar = 250 μm.

Figure 8. Reconstruction of the whole fertile whorl of *Echinochara lazarii*. Outer utricle series (shadowed) opened to show the inner utricle series.

Figure 9. Atopocharoid utricles. A–C) *Globator maillardii* var. *trochiliscoides* (sample H27). A) Lateral view (specimen no. 85602 MGSCB), B) Apical view (specimen no. 85603 MGSCB), C) Basal view (specimen no. 85604 MGSCB). D–F) *Globator maillardii* var. *biutricularis* (sample H44), D) Lateral view (specimen no. 85605 MGSCB), E) Apical view (specimen no. 85606 MGSCB), F) Basal view (specimen no. 85607 MGSCB). G–I) *Atopochara trivolvis* var. *triquetra* (sample H51). G) Lateral view (specimen no. 85608 MGSCB), H) Apical view (specimen no. 85609 MGSCB), I) Basal view (specimen no. 85610 MGSCB). J–L) *Atopochara trivolvis* var. *trivolvis* (sample H94). J) Lateral view (specimen no. 85611 MGSCB), K) Apical view (specimen no. 85612 MGSCB), L) Basal view (specimen no. 85613 MGSCB). Scale bar = 500 μm.

Figure 10. *Clavator* utricles. A–C) *Clavator grovesii* var. *jiuquanensis*. A) Lateral view (sample H95; specimen no. 85614 MGSCB), B) Abaxial view (sample H95; specimen no. 85615 MGSCB), C) Adaxial view (sample H88; specimen no. 85616 MGSCB). D–F) *Clavator harrisii* var. *dongjingensis* (sample H38). D) Lateral view (specimen no. 85617 MGSCB), E) Abaxial view (specimen no. 85618 MGSCB), F) Adaxial view (specimen no. 85619 MGSCB). G–H) *Clavator harrisii* var. *harrisii* (sample H–38). G) lateral view (specimen no. 85620 MGSCB), H) Abaxial view (specimen no. 85621 MGSCB). I) *Clavator harrisii* var. *reyi* (sample H76; specimen no. 85622 MGSCB). J–L*) Clavator calcitrapus* var. *jiangluoensis* (Z. Wang et Li in Z. Wang and Lu, 1982) comb. nov. (sample H38). J) Apical view (specimen no. 85623 MGSCB), K) Lateral view (specimen no. 85624 MGSCB), L) Adaxial view (specimen no. 85625 MGSCB). M–O) *Clavator calcitrapus* var. *calcitrapus* (sample H51). M) Apical view (specimen no. 85626 MGSCB), N) Adaxial view (specimen no. 85627 MGSCB), O) Lateral view (specimen no. 85628 MGSCB). Scale bar = 500 μm.

Figure 11. *Ascidiella* utricles. A–D) *Ascidiella stellata* var. *stellata* (sample H6). A) Lateral view (specimen no. 85677), B) Lateral view (specimen no. 85629 MGSCB), C) Apical view (specimen no. 85630 MGSCB), D) Abaxial view (specimen no. 85631 MGSCB). E–G) *Ascidiella stellata* var. *lata* (sample H44), E) lateral view (specimen no. 85632 MGSCB), F) Apical view (specimen no. 85633 MGSCB), G) Abaxial view (specimen no. 85634 MGSCB). H–J) *Ascidiella triquetra* (sample H27). H) Oblique-abaxial view (specimen no. 85635 MGSCB), I) Lateral view (specimen no. 85636 MGSCB), J) Apical view (specimen no. 85637 MGSCB). K–M) *Ascidiella cruciata* (sample H94). K) Abaxial view (specimen no. 85638 MGSCB), L) Apical view (specimen no. 85639 MGSCB), M) Basal view (specimen no. 85640 MGSCB). The

1821 apical neck is indicated by the wide arrow, while the phylloid portion is indicated by the
1822 thin arrow. Scale bar = 500 μm.

1823 Figure 12. *Hemiclavator* and *Pseudoglobator* utricles. A–C) *Hemiclavator*
1824 *adnatus*. A) Adaxial view (sample H12; specimen no. 85641 MGSCB), B) Lateral view
1825 (sample H12; specimen no. 85642 MGSCB), C) Abaxial view (sample H27; specimen
1826 85643 MGSCB). D–F) *Hemiclavator neimongolensis* var. *posticecaptus* (sample H12).
1827 D) Adaxial view (specimen no. 85644 MGSCB), E) Lateral view (specimen no. 85645
1828 MGSCB), F) Abaxial view (specimen no. 85646 MGSCB). G–I) *Hemiclavator*
1829 *neimongolensis* var. *neimongolensis*. G) Adaxial view (sample H–39; specimen no.
1830 85647 MGSCB), H) Lateral view (sample H39; specimen 85648 MGSCB), I) Abaxial
1831 view (sample H51; specimen no. 85649 MGSCB). J–L) *Pseudoglobator*
1832 *paucibracteatus*. J) Lateral view (Sample H96; specimen no. 85650 MGSCB), K) Basal
1833 view (Sample H96; specimen no. 85650 MGSCB). Scale bar = 500 μm.

1834 Figure 13. Thin sections of *Charaxis* thalli. A–H) *Charaxis spicatus* (Martín-
1835 Closas and Diéguez) emend. A) Longitudinal-oblique section of the apical part of
1836 thallus, showing the long and still closed whorls of phylloids (Sample H90; thin section
1837 no. 85674 MGSCB), B) Longitudinal section of a mature part of the thallus. The
1838 primary cortical cells split into two secondary cortical cells, the larger growing distally
1839 and the smaller (arrow head) growing proximally (Sample H90; thin section no. 85675
1840 MGSCB), C) Longitudinal section of the mature thallus where the primary cortical cell
1841 bifurcates into two secondary cortical cells growing distally. Arrow head indicates a
1842 small secondary cortical cell growing proximally (sample H90b; thin section no. 85676
1843 MGSCB), D) Tangential section of a mature part of the thallus. Two types of primary
1844 cortical cells emerge from a node, smaller and the larger respectively. The latter form a
1845 cortical node in the middle part of the internode, where three cells emerge distally

(sample H90b; thin section no. 85676 MGSCB), E) Oblique section of the internode showing the emission of two types of secondary cortical cells in opposite directions, characteristic of *C. spicatus* (sample H90; thin section no. 85674 MGSCB), F) Transverse section through the upper part of the internode (sample H90; thin section no. 85675) showing the six large primary cortical cells (lp) separated by the smaller primary cortical cells growing distally (sp) and covered by the smaller secondary cortical cells growing proximally (pgs), G) Transversal-oblique section throughout the internode (sample H90; thin section no. 85674 MGSCB). showing the cortical node (cn) where a primary cortical cell splits in two types of secondary cells, proximally-growing secondary cells (pgs) and and distally-growing secondary cells (dgs), H) Transversal section throughout the distal part of the internode showing triplostichous isostichous cortication (sample H90; thin section no. 85676 MGSCB). I–J) Transversal sections of *Charaxis* sp. internodes showing isostichous cortication (I) and a diplostichous cortication (J) (Sample H77; thin section no. 85672 MGSCB). Scale bar A–J = 250 μm.

Figure 14. Reconstruction of the *Charaxis spicatus* structure. Abreviations: br: branchlets; nc: nodal cells, pgs: proximally-growing secondary cells, dgs: distally-growing secondary cells, lp: long primary cell, sp: short primary cell, cn: cortical node.

Figure 15. Whole *Echinochara* plant including vegetative remains (*Charaxis spicatus*) and fructifications (*Echinochara* utricles). A) *Charaxis spicatus* anatomically connected to fertile whorls of *Echinochara* (sample H90b; thin section no. 85676 MGSCB), B) Detail of Fig. 15A, showing a fertile whorl, each branchlet with two superposed fructifications, one in longitudinal section (l) and one in transversal section (t) with gyrogonites (g) covered distally by the *Echinochara* utricle (u), C) Detail of Fig. 15A showing a fertile whorl. A fertile branchlet bears two superposed fructifications showing gyrogonites (g) covered distally by the *Echinochara* utricle (u),

1871 D) Detail of A. showing the characteristic *Charaxis spicatus* cortication, with
1872 bifurcation of primary cortical cells. Scale bar = 500 μm.

1873 Figure 16. Other thalli attributed to clavatoraceans. A–G) *Munieria grambastii*
1874 thalli. A) External view of node. Each opening corresponds to the calcification gap
1875 between a nodal cell and its branchlet. The growth of primary cortical cells occurs both
1876 distally and proximally from the nodal cells (Sample H51; specimen no. 85652
1877 MGSCB), B) Node formed by 8 ellipsoidal nodal cells around a thin internodal cell
1878 (sample H7; specimen no. 85653 MGSCB), C) Node showing polymorphism of nodal
1879 cells (sample H51; specimen no. 85654 MGSCB), D) Section of internode with well-
1880 preserved concentrical calcification of the internodal cell (sample H6; specimen no.
1881 85655 MGSCB), E) Detail of previous specimen showing lamination. Scale bar = 20
1882 μm., F) External view of the internode showing the interdigitation of cortical cells rising
1883 from adjacent nodes in a zigzag line (sample H5; specimen no. 85656 MGSCB), G)
1884 Node and adjacent, poorly calcified internodes with only internodal cells preserved
1885 (sample H5; specimen no. 85657 MGSCB), H) Thallus of *Clavatoraxis* sp. showing
1886 spine-cell rosettes (sample H8; specimen no. 85658 MGSCB). I–K) Thalli of
1887 *Favargerella aquavivae*. I) Mature part of thallus with three superposed nodes (sample
1888 H7; specimen no. 85659 MGSCB), J) Apical part of thallus with rounded tip (sample
1889 H6; specimen no. 85660 MGSCB). Scale bar A–D, F–J = 200 μm.

1890 Figure 17. Thin sections of *Munieria grambastii* thalli. A) Node with 8 elongated
1891 nodal cells (sample H47b; thin section no. 85671 MGSCB), B–H) Transversal sections
1892 of internodes showing intercellular calcification between internodal cell and cortical
1893 cells; B) Transversal section with poorly calcified internodal cell (sample H5c; thin
1894 section no. 85664 MGSCB), C) Transversal section with medium calcified internodal
1895 cell (sample H2b; thin section no. 85661 MGSCB), D) Transversal section with highly

calcified internodal cell representing <25% of the total diameter of the internode (sample H5c; thin section no. 85663 MGSCB), E) Transversal section with well-calcified internodal cells showing highly ondulated laminas (sample H5c; thin section no. 85663 MGSCB), F) Transversal section with slightly eccentric internodal cell (sample H5c; thin section no. 85664 MGSCB), G) Completely recrystallized section of internode (sample H10d; thin section no. 85667 MGSCB), H) Partially recrystallized section of the internode still showing some lamination (sample H2b; thin section no. 85661 MGSCB), I) Longitudinal section through a node and adjacent internodes with some lamination, partly disolved (sample H5c; thin section no. 85664 MGSCB), J) Longitudinal section of a node (n) and adjacent internodes, preserving some lamination of the internodal cell (sample H5b; thin section no. 85662 MGSCB), K) Longitudinal section through apical part of thallus showing internodes separated by 4 nodes (sample H10f; thin section no. 85668 MGSCB). The length of the internodes increases from 136 μm in the apical part to 487 μm in the basal part (Appendix E). Scale bar in A–K = 100 μm.

Figure 18. Thin sections of *Clavatoraxis* sp. and *Favargerella* sp. thalli and clavatoroid utricles. A) Transversal section of a *Clavatoraxis* sp. thallus showing six branchlets belonging to the same node covered by spine-cell rosettes (sample H20c; thin section no. 85669 MGSCB), B) Longitudinal section of a *Clavatoraxis* sp. branchlet (sample H77-79; thin section no. 85673 MGSCB). C) Transversal section of *Favargerella* sp. node (sample H10d; thin section no. 85666 MGSCB), D) Longitudinal section of *Favargerella* sp. branchlet (sample H7b; thin section no. 85665 MGSCB). E) Clavatoroid utricle attached to a *Clavatoraxis* sp. branchlet (sample H20c; thin section no. 85670 MGSCB). F) Clavatoroid utricle attached to a *Favargerella* sp. branchlet (sample H20c; thin section no. 85670 MGSCB). Scale bar = 200 μm.

Figure 19. Comparison between *Clavatoraxis* and *Favargerella* thalli. In *Clavatoraxis*, spine cell-rosettes occur on cortical cells (A), while in *Favargerella* each nodal cell bears a whorl composed of six petal-like cells (B). Scale bar = 100 μm.

Figure 20. Anagenetic lineage of *Clavator calcitrapus* formed by three gradually changing morphotypes.

Figure 21. Concentric calcification of the *Munieria* internode compared to the *Ringstruktur*-calcification of a clavatoroid gyrogonite A) Early stage of *Munieria* calcification. B) Early stage of clavatoroid gyrogonite calcification. C) Complete development of the calcification in a *Munieria* internodal cell. D) Complete *Ringstruktur* calcification of clavatoroid gyrogonite. Scale bar A and C = 100 μm; Scale bar B and D = 250 μm.

Highlights

The most diverse clavatoracean flora (25 species) is described from the Iberian Chain

A new gradualistic evolutionary lineage is shown for *Clavator calcitrapus*

The whole plant *Echinochara* is reconstructed based on attached utricles and thalli

Double triplostichous cortication, a new type of charophyte cortication is defined

Internodal calcification of *Munieria* pinpoints its ascription to the Clavatoraceae

Author statement

Jordi Pérez-Cano: Conceptualization, Methodology, Investigation, Data Curation, Formal analysis, Roles/Writing original draft; Validation.

Telm Bover-Arnal: Conceptualization, Methodology, Formal analysis, Roles/Writing-review and editing, Supervision, Validation, Funding acquisition, Project administration.

Carles Martín-Closas: Conceptualization, Methodology, Formal analysis, Roles/Writing-review and editing, Supervision, Validation, Funding acquisition, Project administration.

Declaration of interests

☒ The authors declare that they have no known competing financial interests or personal relationships that could have appeared to influence the work reported in this paper.

☐The authors declare the following financial interests/personal relationships which may be considered as potential competing interests:

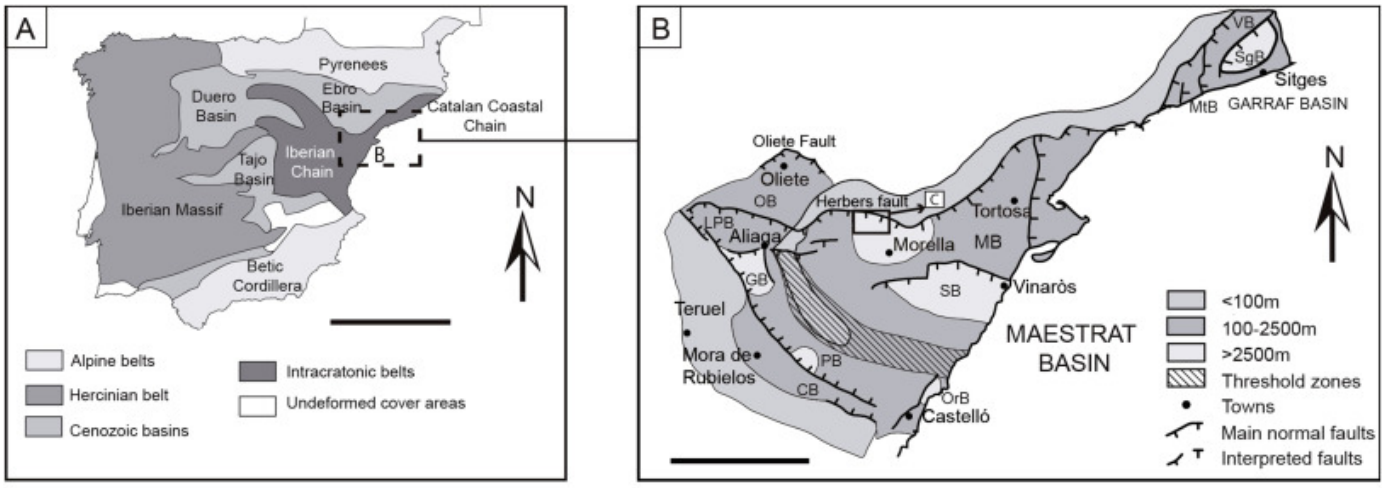
A
Pyrenees
Ebro Basin
Duero Basin
Catalan Coastal Chain
Tajo Basin
Iberian Chain
B
Iberian Massif
Betic Cordillera
N
Alpine belts
Hercinian belt
Cenozoic basins
Intracratonic belts
Undeformed cover areas
B
VB
SgB
Sitges
MtB
GARRAF BASIN
Oliete Fault
Oliete
OB
Herbers fault
C
Tortosa
LPB
Aliaga
Morella
MB
GB
SB
Vinaròs
Teruel
MAESTRAT BASIN
Mora de Rubielos
PB
CB
OrB
Castelló
N
<100m
100-2500m
>2500m
Threshold zones
Towns
Main normal faults
Interpreted faults

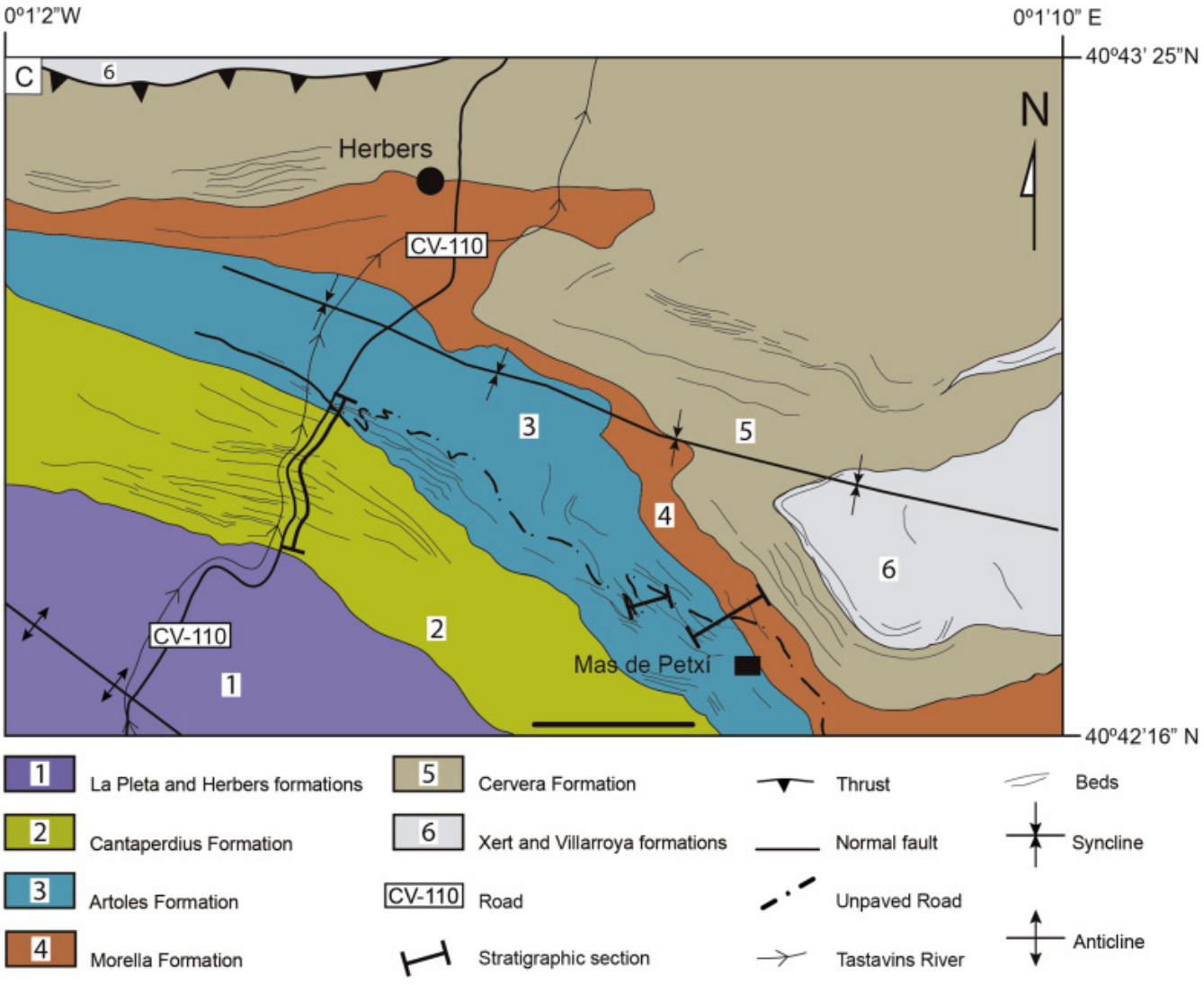
0º1'2"W
0º1'10" E
40º43' 25"N
C
6
N
Herbers
CV-110
3
5
4
6
2
CV-110
1
Mas de Petxí
40º42'16" N
1 La Pleta and Herbers formations
2 Cantaperdius Formation
3 Artoles Formation
4 Morella Formation
5 Cervera Formation
6 Xert and Villarroya formations
CV-110 Road
Stratigraphic section
Thrust
Normal fault
Unpaved Road
Tastavins River
Beds
Syncline
Anticline

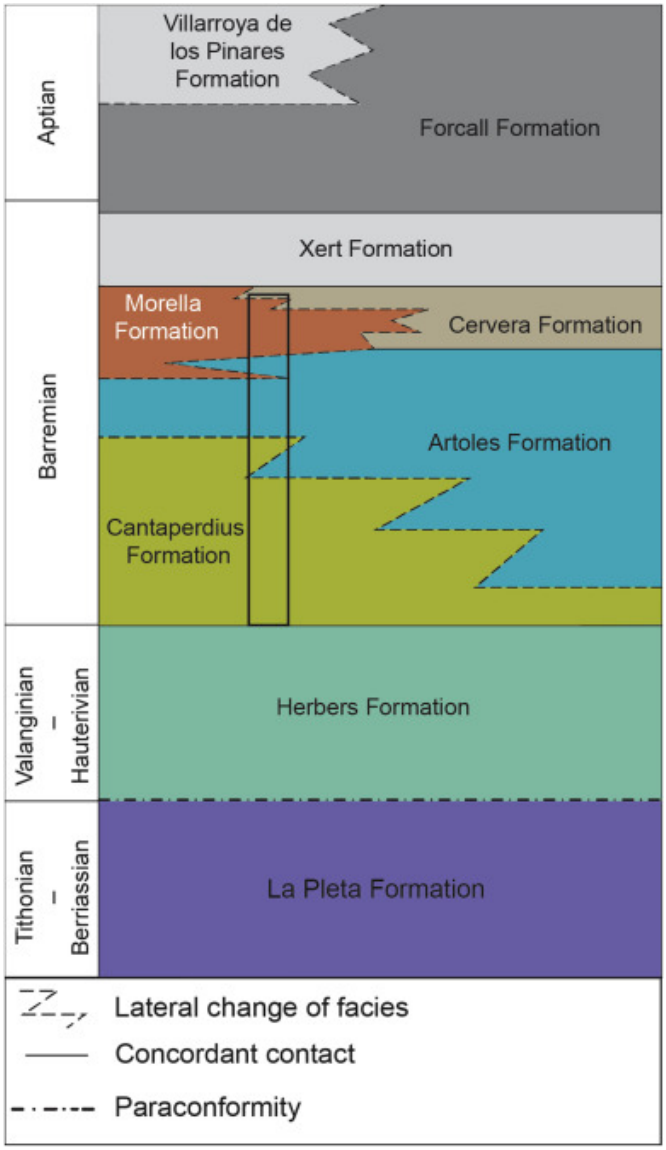
Aptian
Barremian
Valanginian – Hauterivian
Tithonian – Berriassian
Villarroya de los Pinares Formation
Forcall Formation
Xert Formation
Morella Formation
Cervera Formation
Artoles Formation
Cantaperdius Formation
Herbers Formation
La Pleta Formation
Lateral change of facies
Concordant contact
Paraconformity

A
Lithostratigraphy
Samples
Lithology
Texture
Fossil Components
P. maestratica
aff. Mesochara harrisii
E. lazarii
G. mallardii var. trochiliscoides
G. mallardii var. biutricularis
A. trivolvis var. ancora
A. trivolvis var. triquetra
C. harrisii var. dongjingensis
C. harrisii var. harrisii
C. harrisii var. reyi
C. calcitrapus var. jiangluoensis
C. calcitrapus var. calcitrapus
A. stellata var. stellata
A. stellata var. lata
A. triquetra
H. adnatus
H. neimongolensis var. posticecaptus
H. neimongolensis var. neimongolensis
Charophyte biozones
370
350
300
250
200
150
100
50
0m
Artoles Fm.
Cantaperdius Formation
H57
H56
H55
H54
H52–H53
H51
H49–H50
H48
H47b
H46–H47
H42–H45
H41
H38–H40
H37
H36b
H36
H35b
H35
H34
H33
H32
H31b
H30–H31
H29b
H25–H29a
H23–H24
H22
H21
H20b–H20c
H20
H19
H16–H18
H11–H15
H10b–H10f
H8–H10
H7b–H7c
H7
H6e
H6d
H6c
H6b
H6
H5e
H5d
H5c
H5b
H3–H5
H2
H1
Fe
F
ml md wk pk gr
Herbers Fm.
Atopochara trivolvis var. triquetra (early Barremian)
Globator maillardi var. steinhauseri biozone

B

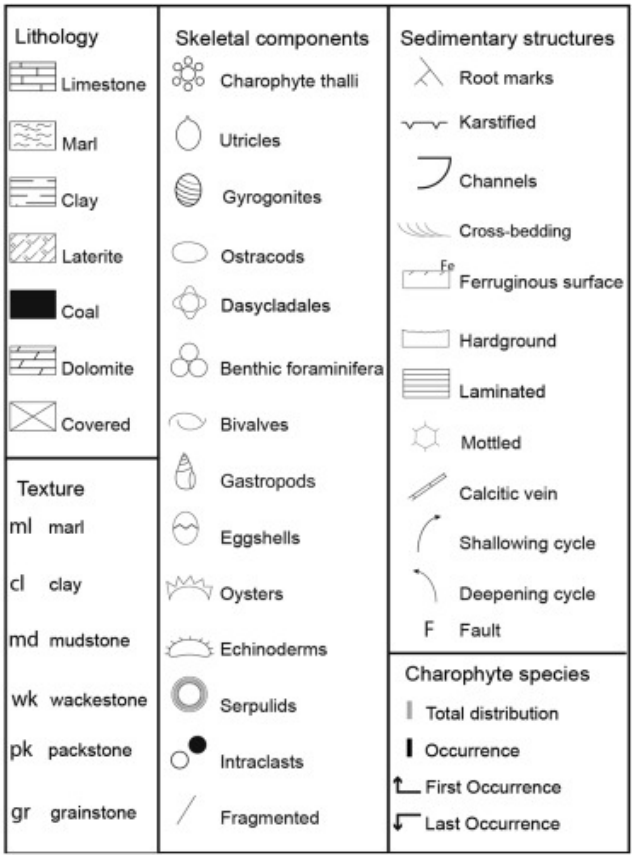
Lithology
Limestone
Marl
Clay
Laterite
Coal
Dolomite
Covered
Texture
ml marl
cl clay
md mudstone
wk wackestone
pk packstone
gr grainstone
Skeletal components
Charophyte thalli
Utricles
Gyrogonites
Ostracods
Dasycladales
Benthic foraminifera
Bivalves
Gastropods
Eggshells
Oysters
Echinoderms
Serpulids
Intraclasts
Fragmented
Sedimentary structures
Root marks
Karstified
Channels
Cross-bedding
Fe
Ferruginous surface
Hardground
Laminated
Mottled
Calcitic vein
Shallowing cycle
Deepening cycle
F Fault
Charophyte species
Total distribution
Occurrence
First Occurrence
Last Occurrence

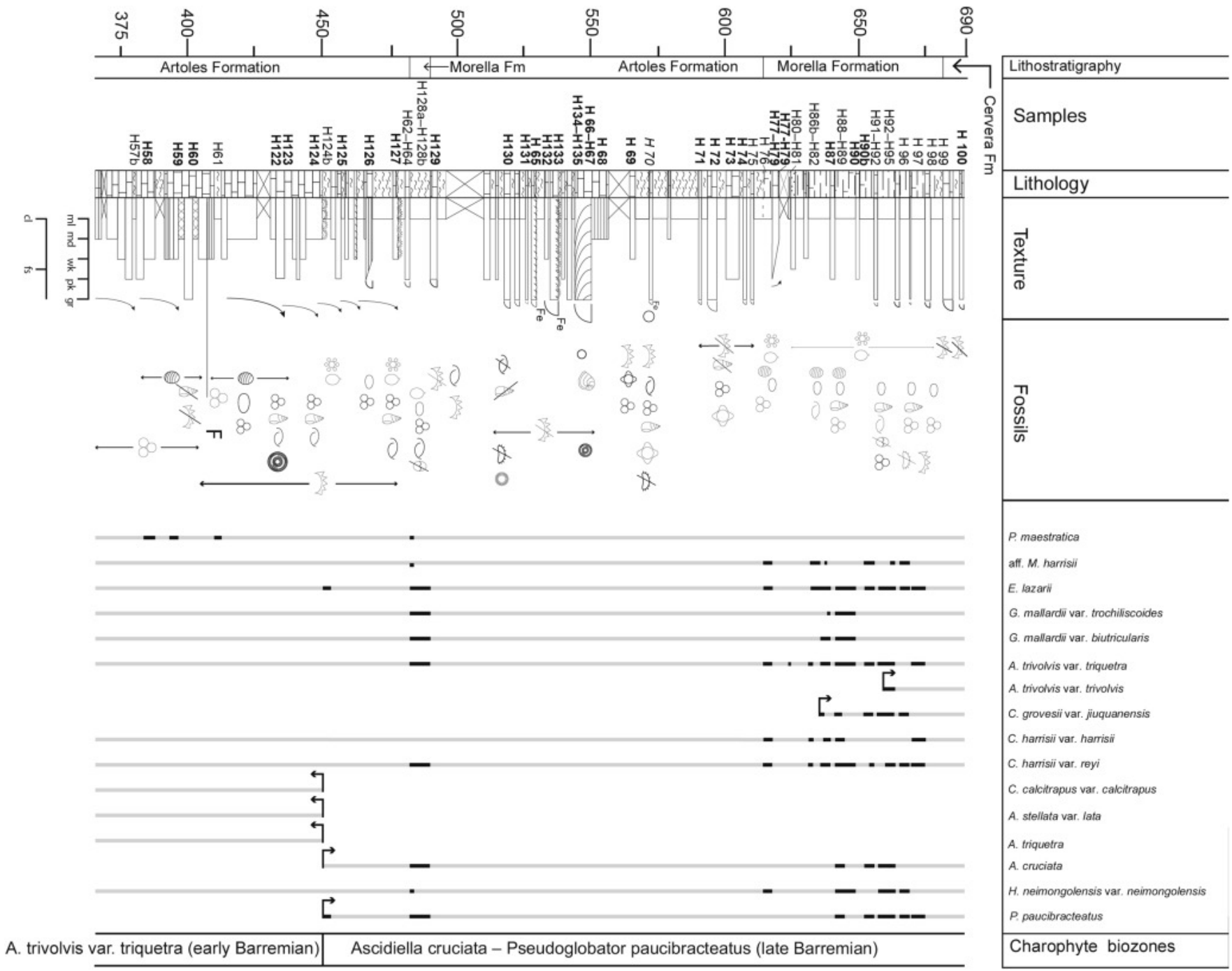
375
400
450
500
550
600
650
690
Artoles Formation
Morella Fm
Artoles Formation
Morella Formation
Cervera Fm
H58
H57b
H59
H60
H61
H123
H122
H124
H124b
H125
H126
H127
H128a–H128b
H62–H64
H129
H130
H131
H65
H132
H133
H134–H135
H 66–H67
H 68
H 69
H 70
H 71
H 72
H 73
H 74
H 75
H 76
H77–H79
H 77
H80–H81
H86b–H82
H87
H88–H89
H90b
H90
H91–H92
H92–H95
H 96
H 97
H 98
H 99
H 100
cl
fs
ml
md
wk
pk
gr
F
Fe
Fe
Fe
Lithostratigraphy
Samples
Lithology
Texture
Fossils
P. maestratica
aff. M. harrisii
E. lazarii
G. mallardii var. trochiliscoides
G. mallardii var. biutricularis
A. trivolvis var. triquetra
A. trivolvis var. trivolvis
C. grovesii var. jiuquanensis
C. harrisii var. harrisii
C. harrisii var. reyi
C. calcitrapus var. calcitrapus
A. stellata var. lata
A. triquetra
A. cruciata
H. neimongolensis var. neimongolensis
P. paucibracteatus
A. trivolvis var. triquetra (early Barremian)
Ascidiella cruciata – Pseudoglobator paucibracteatus (late Barremian)
Charophyte biozones

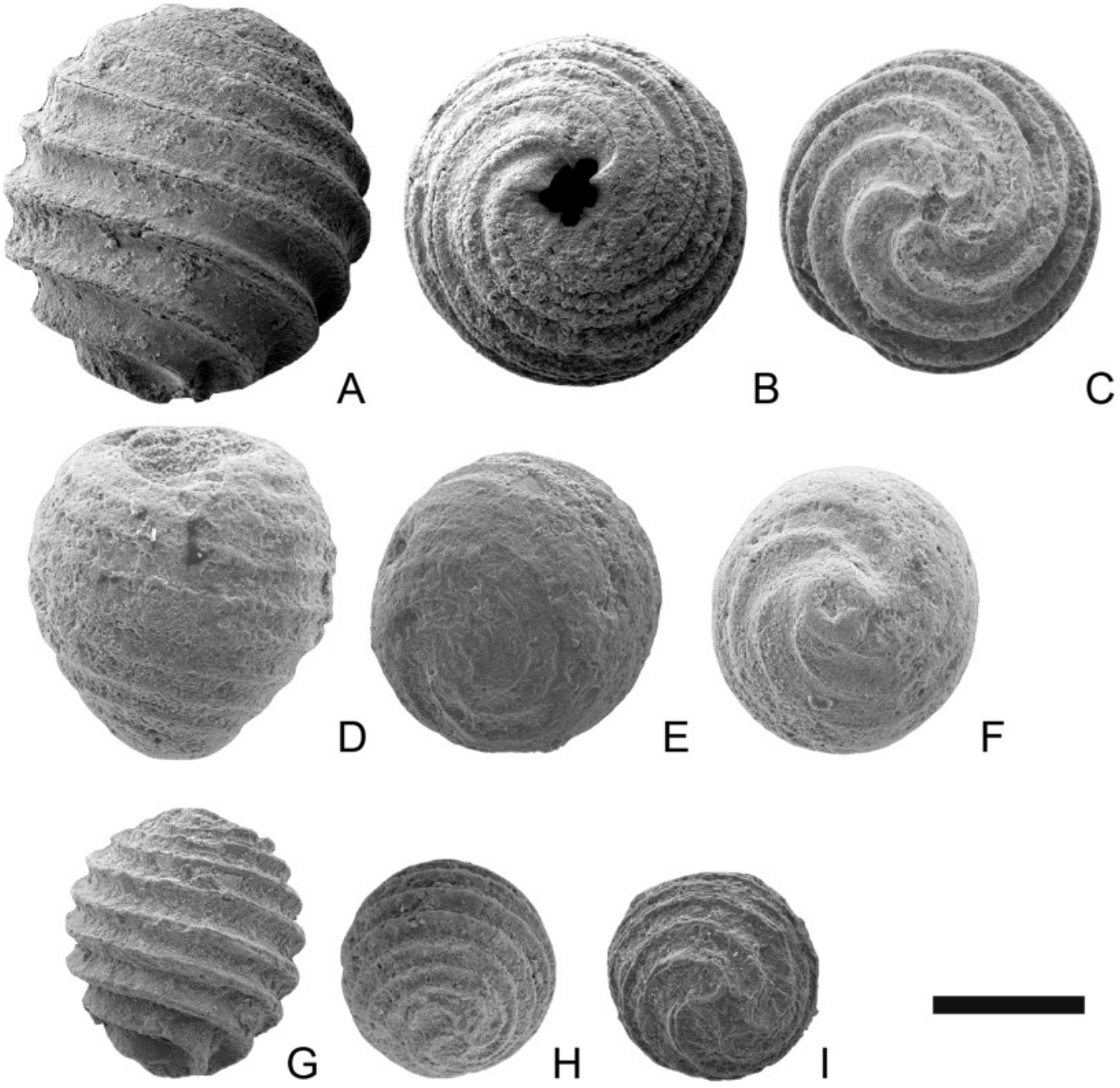
A
B
C
D
E
F
G
H
I

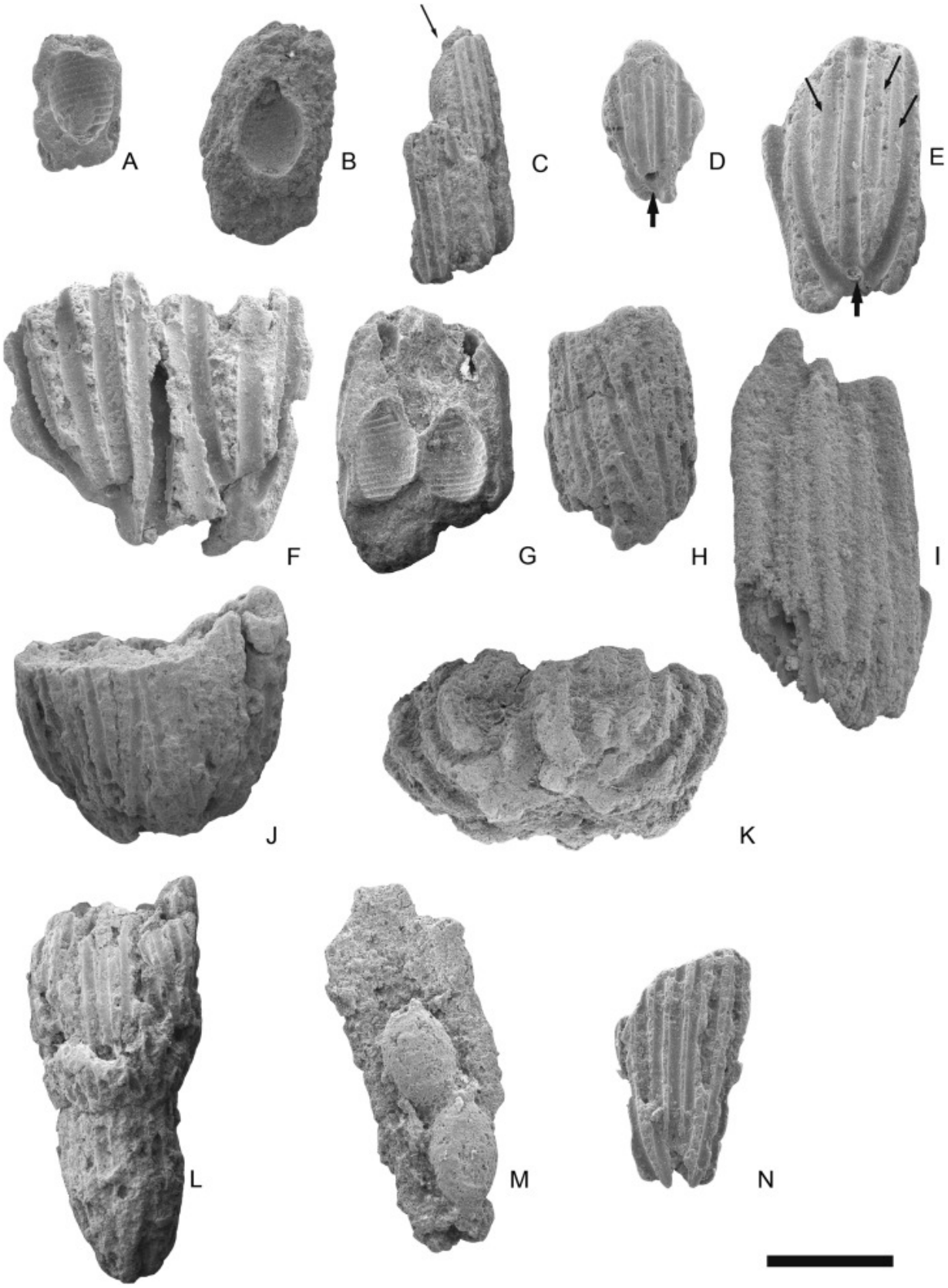
A
B
C
D
E
F
G
H
I
J
K
L
M
N

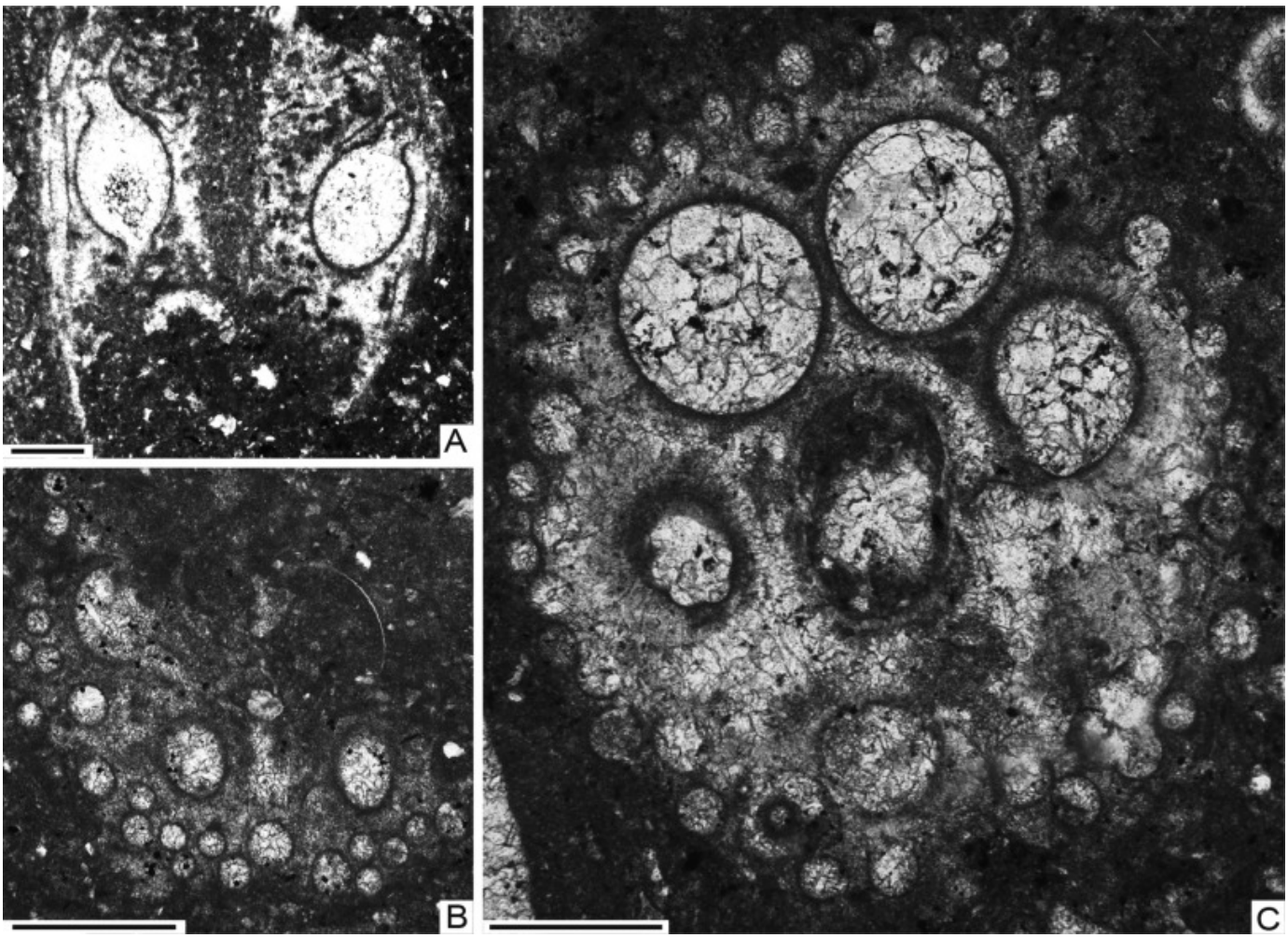
A
B
C

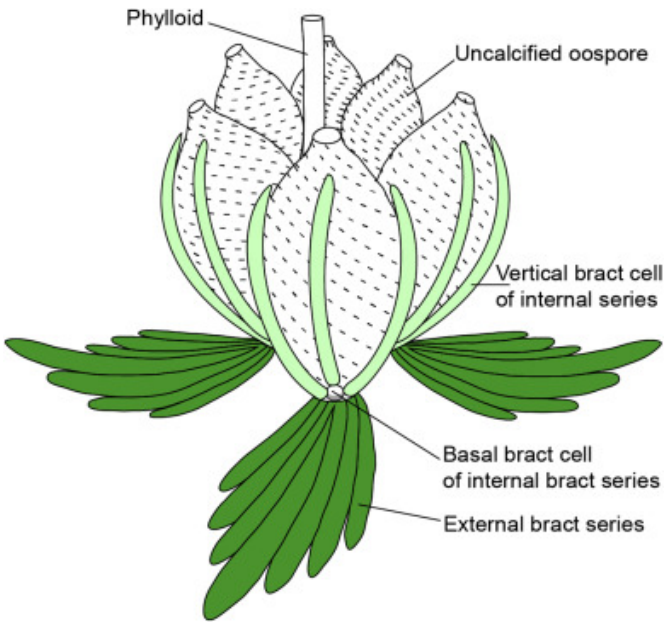
Phylloid
Uncalcified oospore
Vertical bract cell
of internal series
Basal bract cell
of internal bract series
External bract series

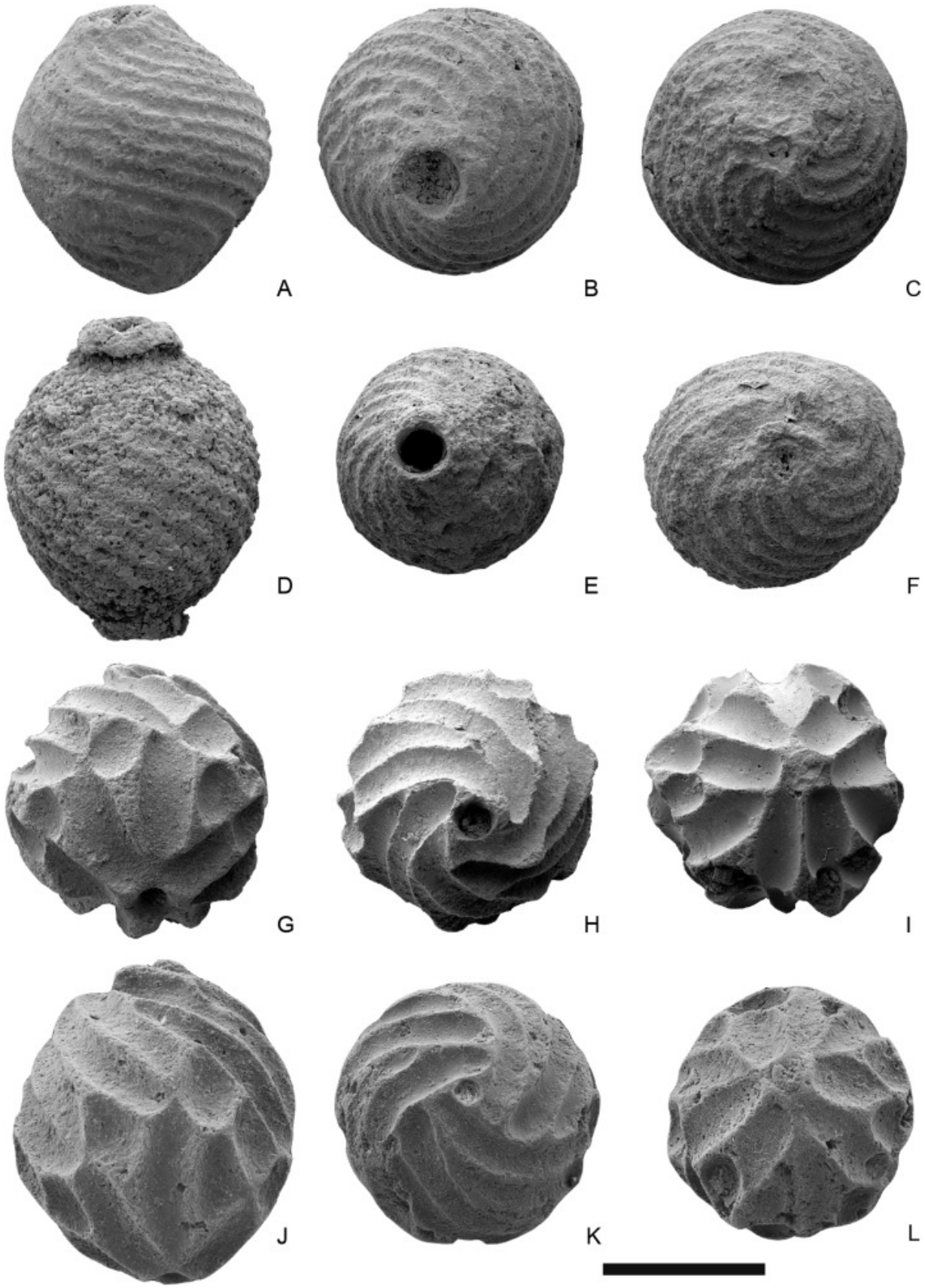
A
B
C
D
E
F
G
H
I
J
K
L

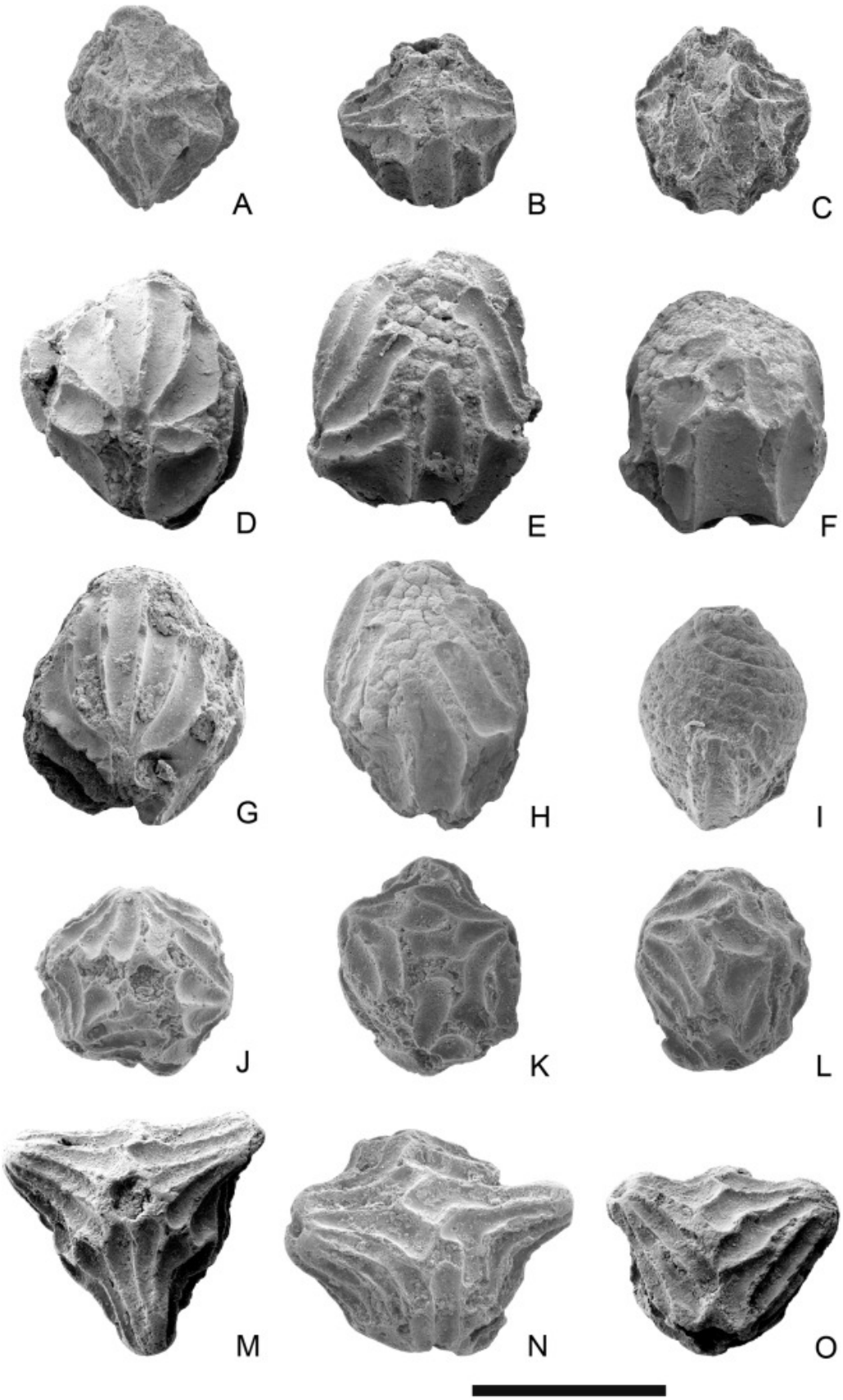
A
B
C
D
E
F
G
H
I
J
K
L
M
N
O

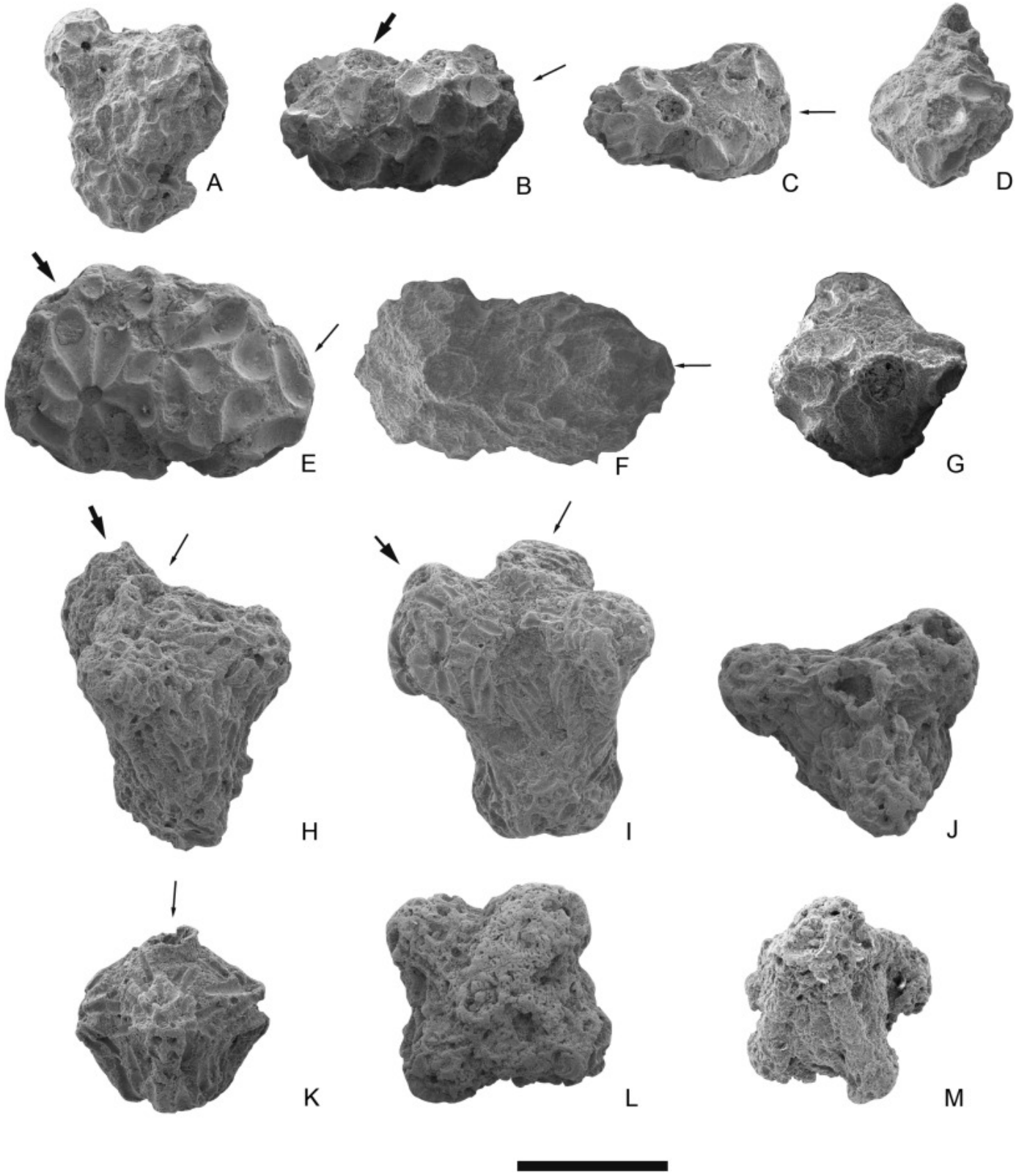
A
B
C
D
E
F
G
H
I
J
K
L
M

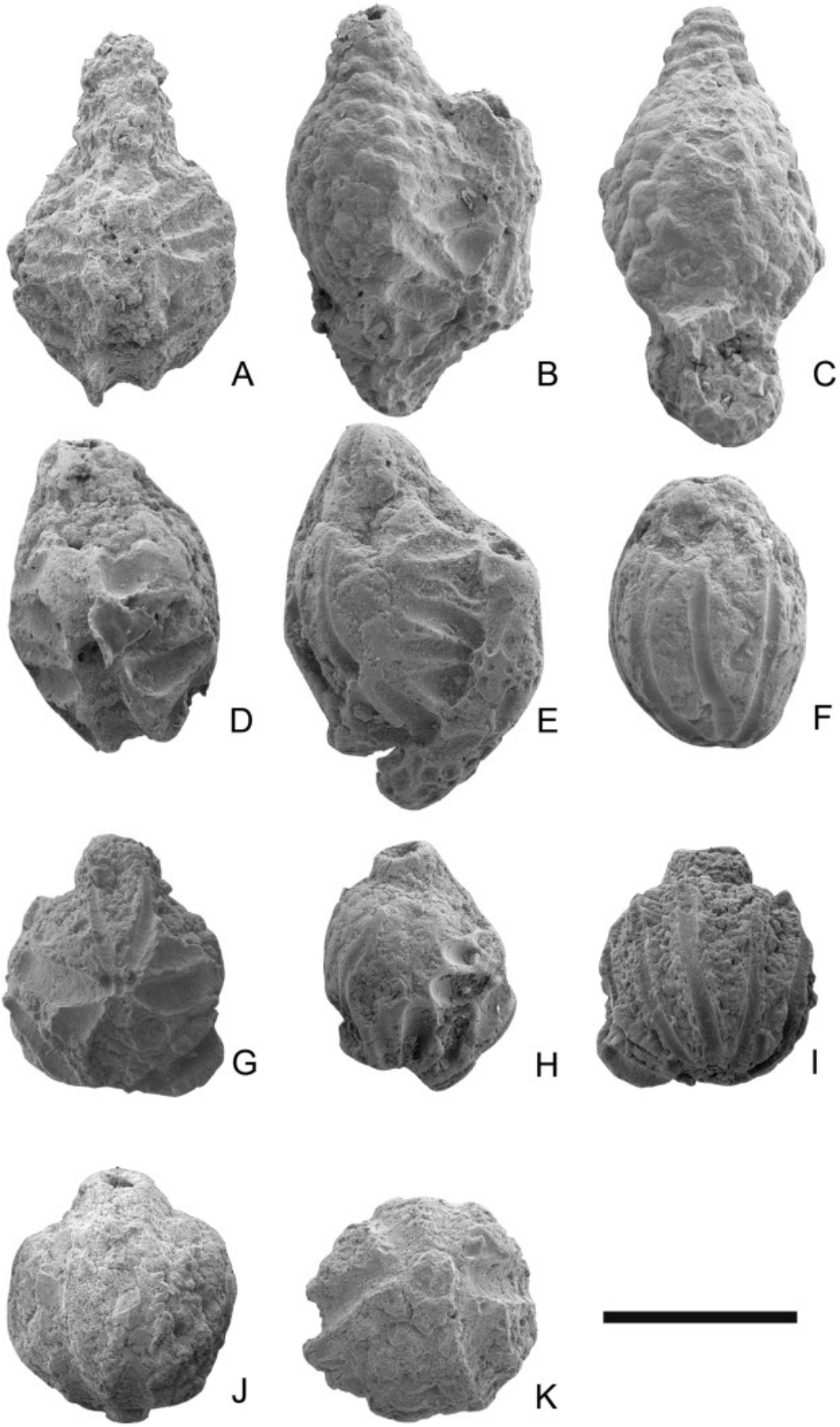
A
B
C
D
E
F
G
H
I
J
K

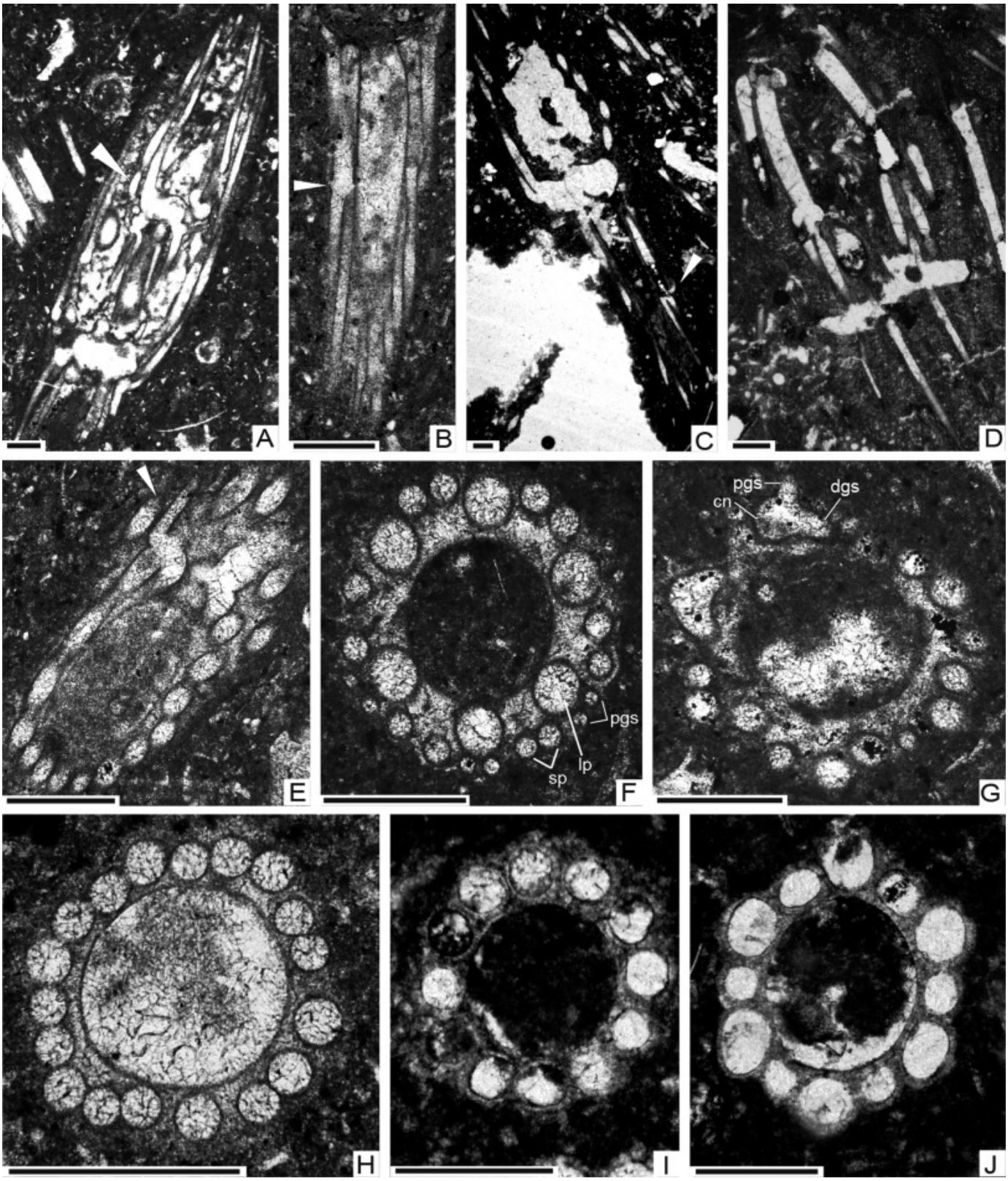
A
B
C
D
E
pgs
lp
sp
F
pgs
cn
dgs
G
H
I
J

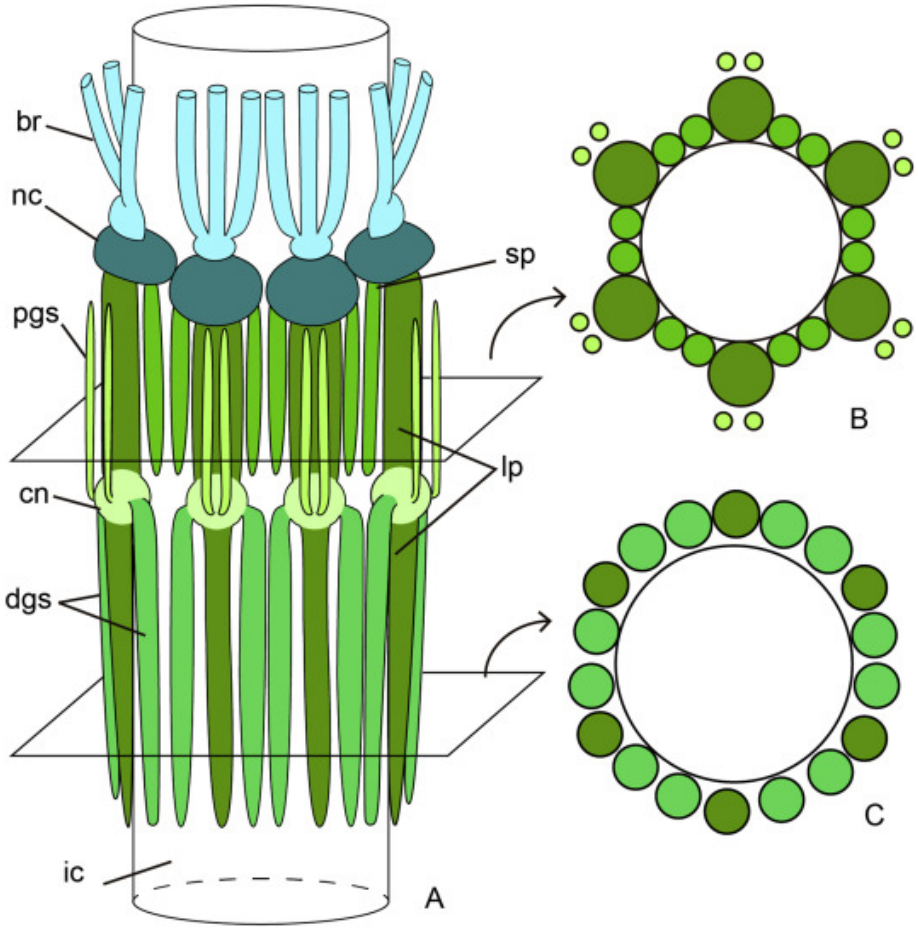
br
nc
sp
pgs
lp
cn
dgs
ic
A
B
C

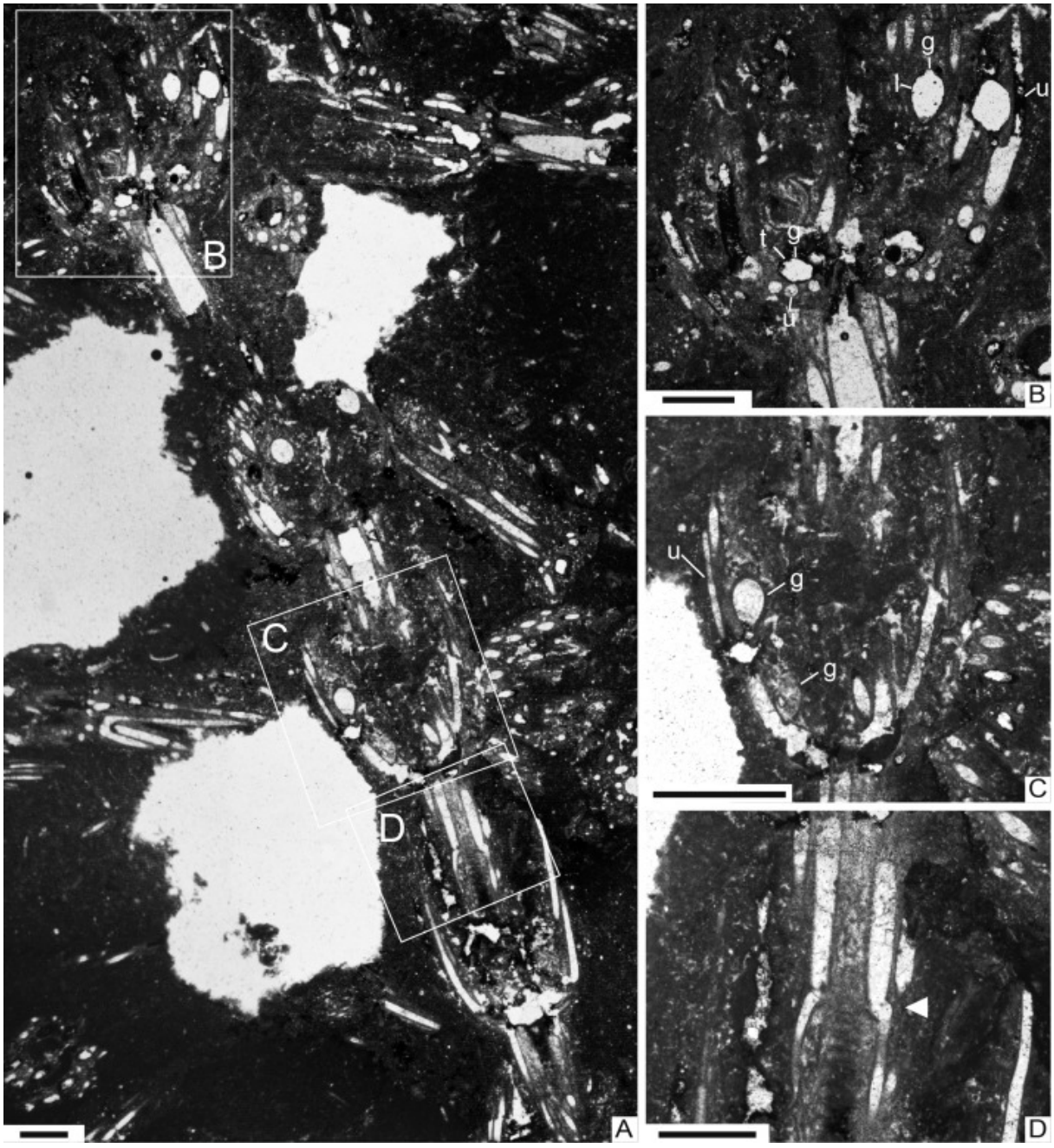
B
C
D
A
g
l
u
t
g
u
B
u
g
g
C
D

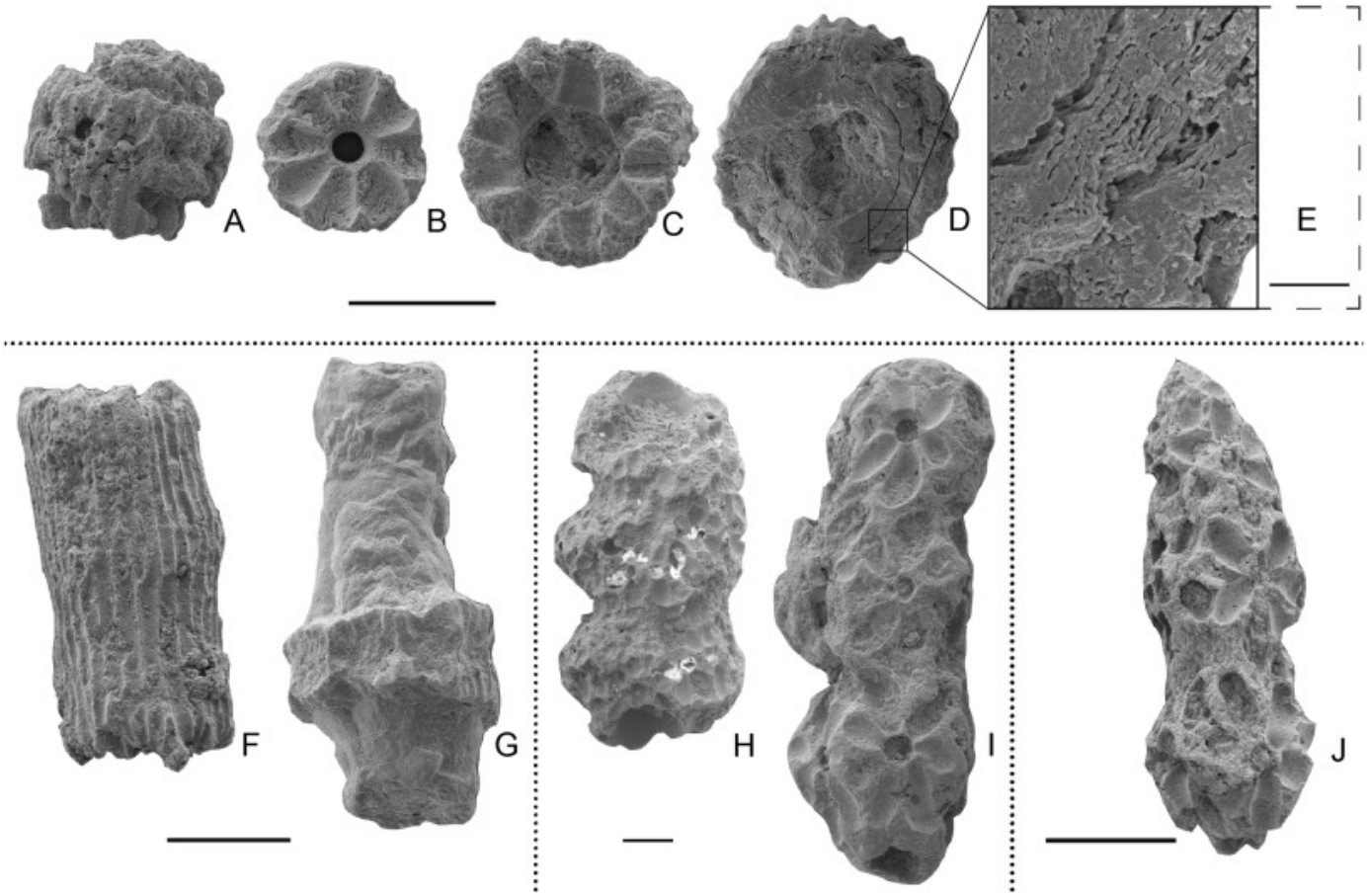
A
B
C
D
E
F
G
H
I
J

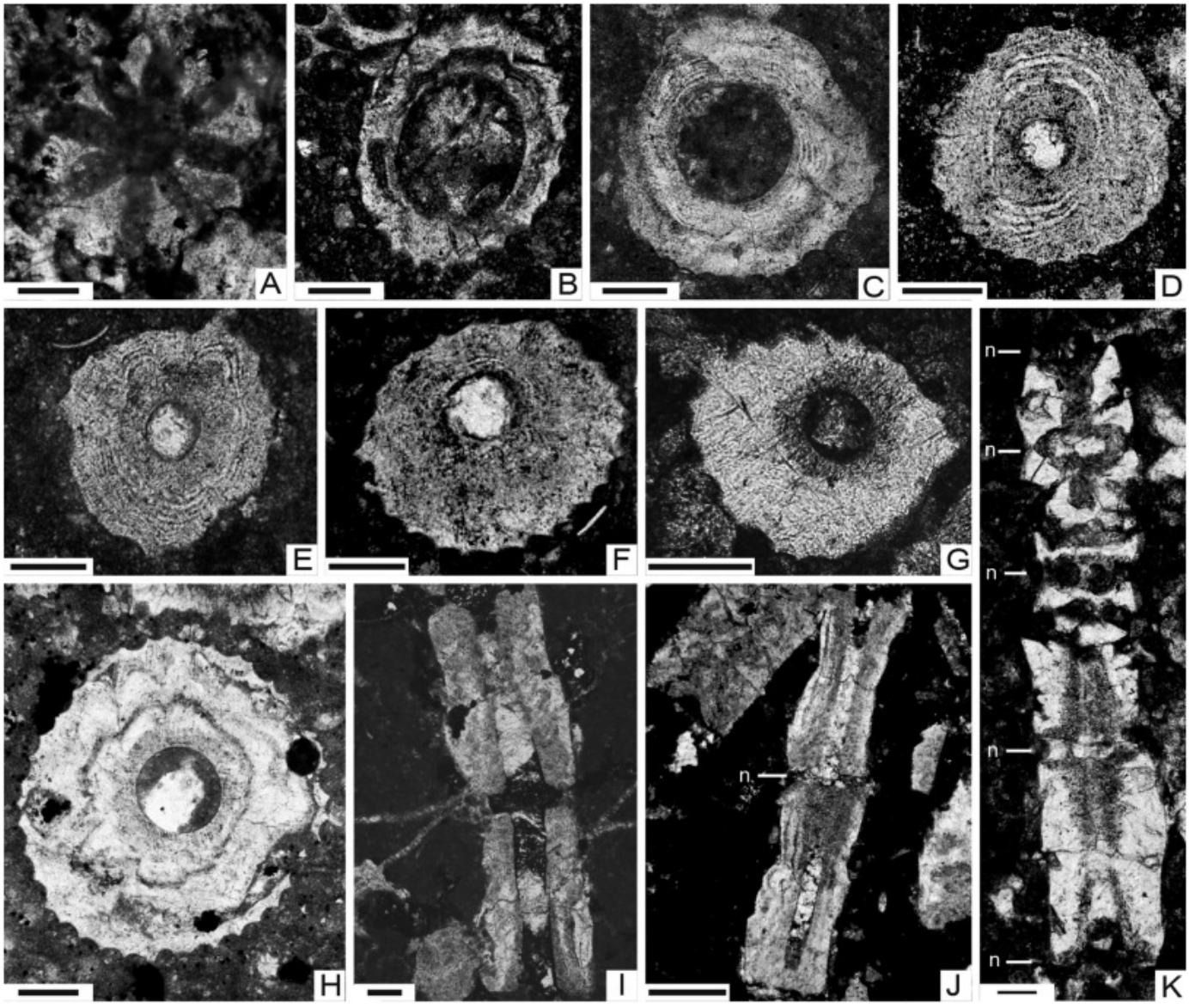
A
B
C
D
E
F
G
n
n
n
n
n
H
I
n
J
K

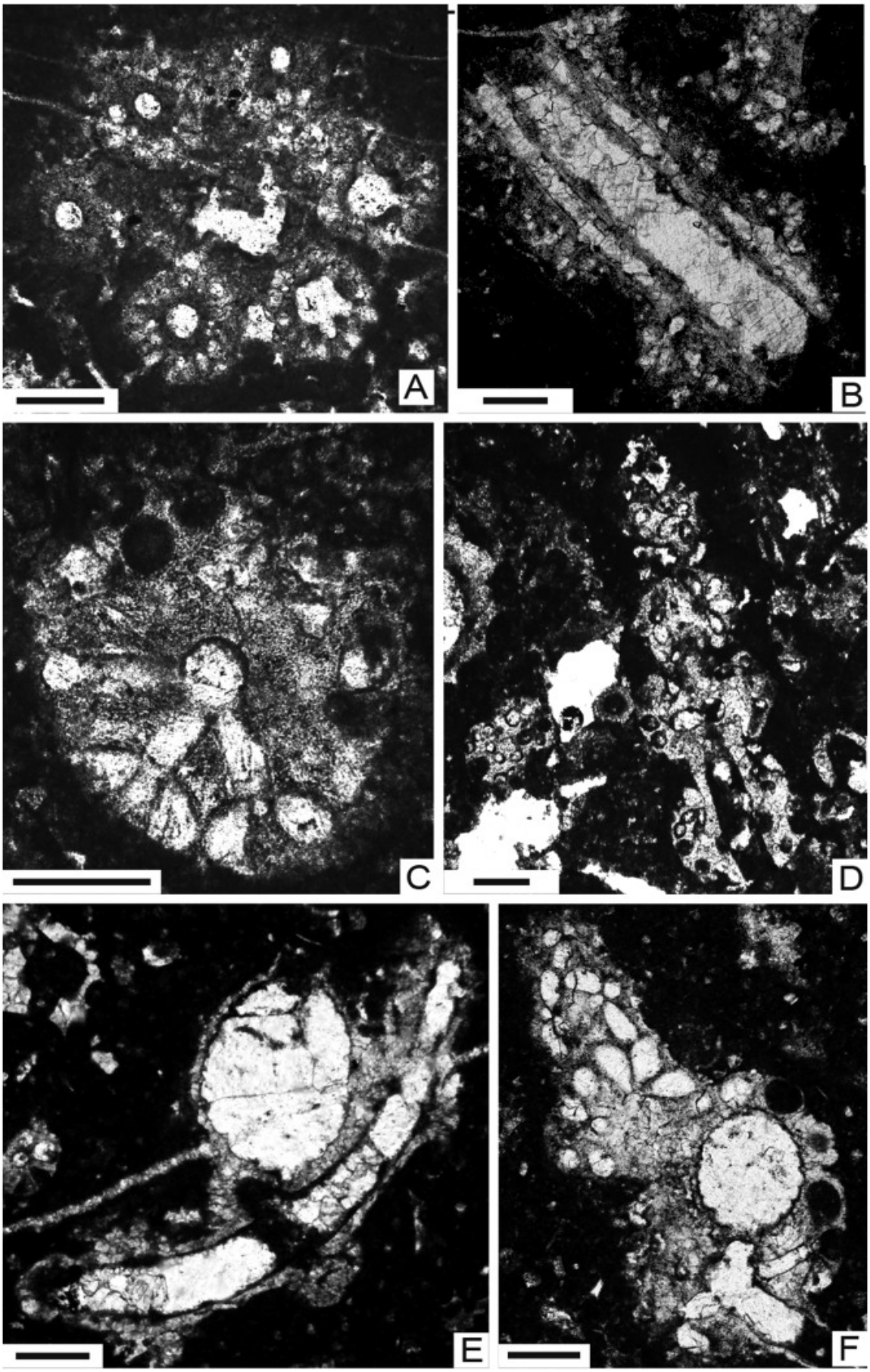
A
B
C
D
E
F

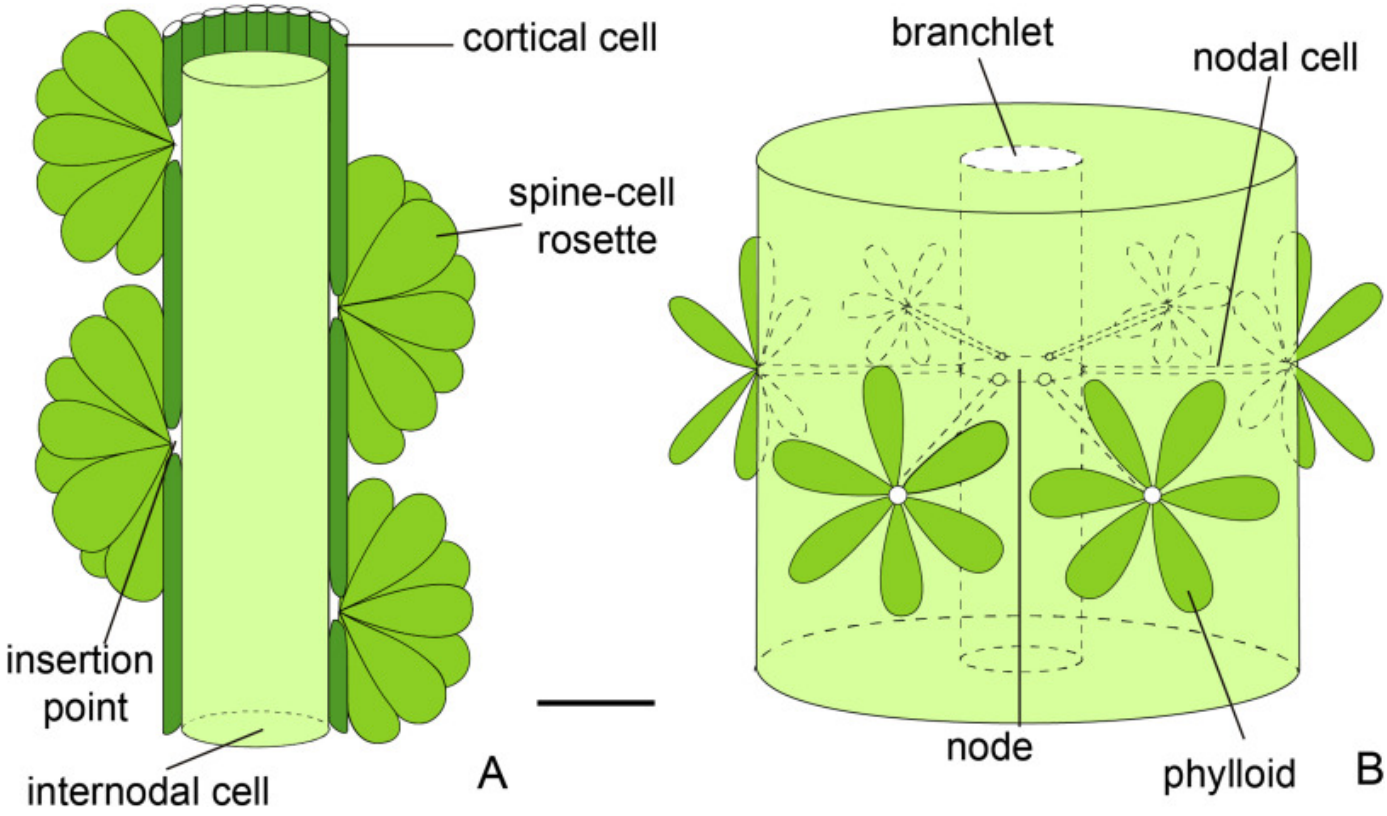
cortical cell
spine-cell rosette
insertion point
internodal cell
A
branchlet
nodal cell
node
phylloid
B

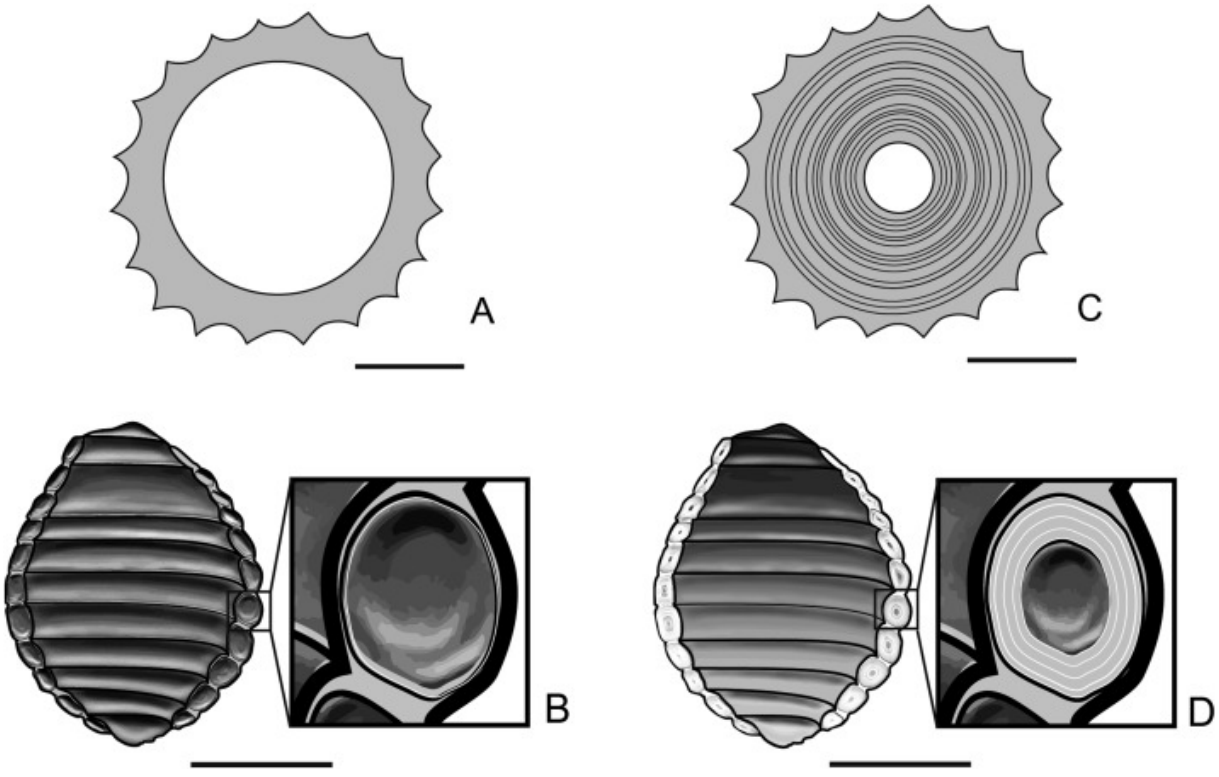
A
C
B
D